

# Harnessing Cell Death Vulnerabilities for the Treatment of Small Cell Lung Cancer

Inaugural Dissertation

zur

Erlangung des Doktorgrades

Dr. nat. med.

der Medizinischen Fakultät

und

der Mathematisch-Naturwissenschaftlichen Fakultät

der Universität zu Köln

vorgelegt von

Lucas Valdez Capuccino

aus Melbourne, Australia

Hundt Druck GmbH,

Köln

2024

# Harnessing Cell Death Vulnerabilities for the Treatment of Small Cell Lung Cancer

Inaugural Dissertation

zur

Erlangung des Doktorgrades

Dr. nat. med.

der Medizinischen Fakultät

und

der Mathematisch-Naturwissenschaftlichen Fakultät

der Universität zu Köln

vorgelegt von

Lucas Valdez Capuccino

aus Melbourne, Australia

Hundt Druck GmbH,

Köln

2024

Betreuer/in: Prof. Dr. Maria de las Nieves Peltzer

Referent/in: Prof. Dr. Silvia von Karstedt

Prof. Dr. Alga Zuccaro

Datum der mündlichen Prüfung: 22.10.2024

To my beloved parents. If I can see far, it is because I am standing  
on their shoulders, the shoulders of giants.

# Abstract

Regulated cell death is an essential process in multicellular organisms, necessary for development and critical for pathogen responses. Apoptosis, justifiably the most studied regulated cell death process, rids the body of old and damaged cells via the ordered activity of caspases. These proteases can activate the pore-forming protein Gasdermin E, which switches the normally immunologically silent apoptosis to pyroptosis. Pyroptosis is a Gasdermin-mediated type of regulated cell death characterised by lytic death of the cell, the release of pro-inflammatory factors and subsequent recruitment of immune cells. Defects in cell death signalling are a common cause of several diseases, leading to exacerbated cell death or nullifying its activation. Resisting cell death is an essential hallmark of Cancer, as regulated cell death prevents tumour formation. Lung cancer is the leading cause of cancer-related deaths worldwide per year with over 1.8 million deaths annually. Small Cell Lung Cancer (SCLC) is a recalcitrant subtype of lung cancer with dismal survival rates of only 7% after 5 years. In this study, we manipulated the apoptotic circuitry by using small molecules to block the Cyclin-dependent Kinase 9 (CDK9) activity, which is necessary for RNA transcription. We showed that the inhibition of CDK9 leads to the decrease of short-lived proteins, particularly of anti-apoptotic proteins, thus triggering apoptosis in SCLC cells. We found that, unlike non-SCLC cells, SCLC cells are unable to adapt their apoptotic signalling upon CDK9 inhibition and are therefore primed to undergo apoptosis. SCLC cells that are resistant to chemotherapy were found to be sensitive to CDK9 inhibition, bypassing their acquired insensitivity. We also found that CDK9 inhibition exerts anti-tumoral effects in autochthonous and syngeneic SCLC mouse models and that the tumour inhibitory effect is dependent on immune cells. We next studied the role of Gasdermin E in the tumour biology of SCLC and found that, although it does not influence tumour initiation and progression, it clearly modulates the sensitivity of SCLC cells to the induction of apoptosis. SCLC cells lacking Gasdermin E were less sensitive to chemotherapy and CDK9 inhibition treatments. Taken together, our study demonstrates that inhibiting CDK9 is a viable treatment option for SCLC. Additionally, we show that the expression of Gasdermin E reduces the threshold necessary for the induction of cell death. In this thesis, we harnessed the vulnerabilities in the apoptotic pathway of cancer cells to treat SCLC.

# Zusammenfassung

Der regulierte Zelltod ist ein wesentlicher Prozess in multizellulären Organismen, der für die Entwicklung notwendig und für die Reaktion auf Krankheitserreger entscheidend ist. Die Apoptose, der zu Recht am meisten untersuchte regulierte Zelltodprozess, befreit den Körper durch die aufeinander abgestimmte Aktivität von Caspasen von alten und geschädigten Zellen. Diese Proteasen können das porenbildende Protein Gasdermin E aktivieren, wodurch die normalerweise immunologisch stille Apoptose in die Pyroptose übergeht. Die Pyroptose ist eine durch Gasdermin vermittelte Form des regulierten Zelltods, die durch den lytischen Tod der Zelle, die Freisetzung entzündungsfördernder Faktoren und die anschließende Rekrutierung von Immunzellen gekennzeichnet ist. Defekte in Zelltod-Signalkaskaden sind eine häufige Ursache für verschiedene Krankheiten, die zu verstärktem Zelltod führen oder dessen Aktivierung aufheben. Der Widerstand gegen den Zelltod ist ein wesentliches Merkmal von Krebs, da ein regulierter Zelltod die Tumorbildung verhindert. Lungenkrebs ist mit über 1,8 Millionen Todesfällen pro Jahr weltweit die häufigste Ursache für krebsbedingte Todesfälle. Das kleinzellige Bronchialkarzinom (Small Cell Lung Cancer, SCLC) ist eine schwer zu behandelnde Unterart von Lungenkrebs mit einer geringen Überlebensrate von nur 7 % nach 5 Jahren. In dieser Studie manipulierten wir den apoptotischen Kreislauf, indem wir kleine Moleküle zur Blockierung der Aktivität der Cyclin-abhängigen Kinase 9 (CDK9) einsetzten, die für die RNA-Transkription notwendig ist. Wir konnten zeigen, dass die Hemmung von CDK9 zu einer Verringerung von kurzlebigen Proteinen, insbesondere von anti-apoptotischen Proteinen, führt und so die Apoptose in SCLC-Zellen auslöst. Wir fanden heraus, dass SCLC-Zellen im Gegensatz zu Nicht-SCLC-Zellen nicht in der Lage sind, ihre apoptotischen Signale nach einer CDK9-Hemmung anzupassen, und daher für die Apoptose gerüstet sind. SCLC-Zellen, die gegen eine Chemotherapie resistent sind, erwiesen sich als empfindlich gegenüber einer CDK9-Hemmung und überwinden so ihre erworbene Unempfindlichkeit. Wir fanden auch heraus, dass die CDK9-Hemmung in autochthonen und syngenischen SCLC-Mausmodellen antitumorale Wirkungen hat und dass die tumorhemmende Wirkung von Immunzellen abhängig ist. Als nächstes untersuchten wir die Rolle von Gasdermin E in der Tumorbilogie von SCLC und fanden heraus, dass das Protein zwar keinen Einfluss auf die

Tumorinitiation und -progression hat, aber eindeutig die Empfindlichkeit von SCLC-Zellen gegenüber der Induktion von Apoptose moduliert. SCLC-Zellen, denen Gasdermin E fehlte, waren weniger empfindlich gegenüber Chemotherapie und CDK9-Hemmungen. Insgesamt zeigt unsere Studie, dass die Hemmung von CDK9 eine praktikable Behandlungsoption für SCLC ist. Darüber hinaus zeigen wir, dass die Expression von Gasdermin E die Schwelle senkt, die für die Auslösung des Zelltods überschritten werden muss. In dieser Arbeit haben wir uns die Schwachstellen im apoptotischen Signalweg von Krebszellen zunutze gemacht, um SCLC zu behandeln.

<b>Abstract</b>	<b>5</b>
<b>Zusammenfassung</b>	<b>6</b>
<b>Abbreviations</b>	<b>i</b>
<b>Unit abbreviations</b>	<b>iii</b>
<b>General Introduction</b>	<b>1</b>
<b>1.1 Regulated cell death</b>	<b>1</b>
1.1.1 Apoptosis	1
1.1.2 Necroptosis	9
1.1.3 Pyroptosis	9
1.1.4 Cancer and resistance to cell death	13
<b>1.2 Lung cancer</b>	<b>15</b>
1.2.1 SCLC	16
<b>Chapter 1 – Inhibiting CDK9 for the Treatment of SCLC</b>	<b>20</b>
<b>1.3 Introduction</b>	<b>20</b>
1.3.1 Cyclin-dependent kinases	20
1.3.2 CDKs and transcriptional homeostasis	21
1.3.3 CDK inhibition in cancer	22
<b>1.4 Aims – Chapter 1</b>	<b>25</b>
<b>1.5 Results</b>	<b>25</b>
1.5.1 CDK9 Inhibition as an effective therapy for small-cell lung cancer	25
1.5.2 CDK9 effectively kills mouse and human SCLC cells while having no significant impact on NSCLC cells	26
1.5.3 Dinaciclib has no additive effect with TRAIL or chemotherapy but potently kills chemotherapy-resistant SCLC cells	32
1.5.4 Evaluating a novel and specific CDK9 inhibitor	38
1.5.5 Inhibition of CDK9 reduced tumour growth and extended survival of mice.	41
1.5.6 The Anti-tumour effect of CDK9 inhibition is dependent on the adaptive immune system.	46
<b>1.6 Discussion</b>	<b>48</b>
1.6.1 CDK9 inhibition in the treatment of SCLC	48
<b>Chapter 2 – The role of Gasdermin E in the biology and drug response of Small Cell Lung Cancer</b>	<b>54</b>



<b>1.7</b>	<b>Introduction</b>	<b>54</b>
1.7.1	Cell Death Proteins in SCLC	54
<b>1.8</b>	<b>Aims – Chapter 2</b>	<b>57</b>
<b>1.9</b>	<b>Results</b>	<b>57</b>
1.9.1	Gasdermin E is activated upon chemotherapy in SCLC cells.	57
1.9.2	Gasdermin E modulates response to treatment <i>in vitro</i>	58
1.9.3	Gasdermin E has no effect on the survival of the autochthonous SCLC model	62
<b>1.10</b>	<b>Discussion</b>	<b>63</b>
1.10.1	The role of Gasdermin E in SCLC	63
<b>Conclusion</b>		<b>69</b>
<b>Materials and Methods</b>		<b>70</b>
1.10.2	Cell Lines and Cell Culture	70
1.10.3	Buffers	70
1.10.4	Drugs	71
1.10.5	Cell viability and cell death assays	72
1.10.6	LDH release assay	73
1.10.7	IL-1 $\beta$ ELISA	73
1.10.8	Dynamic BH3 profiling	74
1.10.9	Cell cycle analysis	75
1.10.10	Western blot analysis	75
1.10.11	siRNA mediated silencing	76
1.10.12	siRNA sequences	76
1.10.13	Plasmid construction for CRISPR gRNA	77
1.10.14	<i>E. coli</i> competence preparation and transformation	77
1.10.15	Transfection of HEK cells for viral production	78
1.10.16	Infection of target cells	78
1.10.17	In vivo toxicity assessment of VC-1	79
1.10.18	In vivo tumour studies	79
1.10.19	Ethical approval	82
1.10.20	Statistical analyses	83
<b>Reference list</b>		<b>84</b>
<b>Acknowledgements</b>		<b>95</b>
<b>Personal thanks</b>		<b>95</b>

# Abbreviations

AIM2 – Interferon-inducible protein

APAF-1 – Apoptotic Peptidase Activating Factor

ASCL1 – Achaete-Scute Family basic Basic Helix-Loop-Helix

BAD – BCL-2 associated Agonist of cell Death

BAK – BCL-2 homologous Antagonist Killer

BAX – BCL-2 Associated X

BCL-2 – B-Cell Lymphoma 2

BCL-xL – B-Cell Lymphoma Extra Large

BFL1/A1 – BCL-2 related protein A1

BH3 – BCL-2 homology Domain 3

BID – BH3 Interacting Domain death agonist

BIK – BCL-2 Interacting Killer

BIM – BCL-2 Interacting Mediator of cell death

BOK – BCL-2 related Ovarian Killer

CARD – Caspase Recruitment Domain

CDK – Cyclin-Dependent Kinase

cFLIP – cellular FLICE-like Inhibitory Protein

clAP – cellular Inhibitor of Apoptosis

CytC – Cytochrome C

DED – Death Effector Domain

DISC – Death Inducing Signalling Complex

DMF – dimethylformamide

DNA - Deoxyribonucleic acid

ER – Endoplasmic reticulum

FADD – FAS-Associated Death Domain protein  
FDA – Food and Drug Administration  
GEP – Gene Expression Profile  
HRK – Harakiri protein  
IC50 – Inhibitory concentration 50  
IRF3 – Interferon regulatory factor 3  
K<sup>+</sup> - Potassium  
KO – Knock Out  
LDH – Lactate Dehydrogenase  
LPS – Lipopolysaccharide  
MCL-1 – Myeloid leukaemia 1  
MDM2 – Mouse Double Minute 2 homolog  
MOMP – mitochondrial outer-membrane permeabilization  
mRNA – Messenger Ribonucleic Acid  
NCAM – Neural Cell Adhesion Molecule  
NEUROD1 – Neuronal Differentiation 1  
NF-κB – Nuclear Factor κB  
NLRC4 – NLR family CARD domain containing 4  
NLRP3 – NLR family pyrin domain containing 3  
NOD-SCID – Non-Obese Diabetic Severe Combined Immunodeficiency  
NOXA – Phorbol-12-myristate-13-acetate-induced protein 1  
NSG – NOD SCID Gamma mouse  
PARP – Poly (ADP-ribose) polymerase  
PJVK – Pejvakin protein  
POU2F3 – POU class 2 homeobox 3  
PUMA – p53 Upregulated Modulator of Apoptosis

RCD – Regulated cell death

RIPK1 – Receptor Interacting Protein Kinase 1

RNA – Ribonucleic Acid

RNA pol II – Ribonucleic Acid polymerase II

TRAIL – TNF-related apoptosis-inducing ligand

TRAILR1/2 – TRAIL Receptor 1/2

YAP1 – Yes-Associated Protein 1

## Unit abbreviations

°C	Degrees Celsius
M, mM, $\mu$ M, nM	Molar, millimolar, micromolar, nanomolar
kDa	kilo Dalton
l, ml, $\mu$ l	litre, millilitre, microlitre

# General Introduction

## 1.1 Regulated cell death

Regulated cell death (RCD) is a fascinating and complex phenomenon that serves many critical roles in multicellular organisms, from development to pathogen containment, including tissue homeostasis and acting as a barrier against cell transformation (1). Our understanding of RCD in mammals has been expanding over the decades, revealing its implication in many physiological and pathological processes (2-4). What was once believed to be only three modes of RCD, has evolved into a myriad of death circuits, each with its unique regulatory mechanisms: apoptosis, autophagy, necroptosis, pyroptosis, anoikis, ferroptosis, cuproptosis, parthanatos, NETosis, oxeiptosis (5-14), all playing a crucial role in regulating cell death. Many of these RCDs are activated as a response to pathogens, underscoring the crucial role of RCD in the defence strategies of multicellular organisms. This variability in RCD activation provides an effective strategy to defend against pathogens. These RCD circuits typically induce the release of pro-inflammatory factors from the dying cells, a signal that recruits the immune system to the tissue affected by the pathogens. Other RCD pathways serve physiological functions, such as retiring old cells during tissue homeostasis, and are therefore immunologically silent.

The factors initiating RCD can be both extrinsic and intrinsic. The best and most studied example of this is apoptosis.

### 1.1.1 Apoptosis

Apoptosis was first described on the basis of morphological features of the cell, where the main observations distinguished a condensation of the nucleus, vacuolisation within the cytoplasm and the formation of small, round, encapsulated cell fragments; a consequence of cell “blebbing” (15). It is justifiably the most studied RCD circuit; apoptosis takes place normally during development and aging, and is the main mechanism for maintaining cell numbers in tissues. Apoptosis is also a defence mechanism against invasive pathogens and is a key component of immune responses

(16). As such, it is tightly regulated, as exacerbated apoptosis can be deadly to the organism, and reduced apoptosis would lead to developmental issues and the emergence of diseases like cancer. The signalling initiating cellular apoptosis can be of extrinsic or intrinsic origin, but both converge on the activation of the executioner proteins Caspase 3 and Caspase 7 by their respective initiator Caspases (Caspase 8 and Caspase 9 for extrinsic and intrinsic apoptosis, respectively). Caspases are a family of signalling cysteine-aspartic proteases with a regulatory N-terminal domain followed by large and small catalytic subunits that together form the protease domain (Fig. 1) (17). The regulatory domain in initiator caspases contains a Caspase Recruitment Domain (CARD) or Death Effector Domain (DED) that promotes and allows their recruitment to multiprotein complexes. Caspases 3 and 7 are activated upon apoptosis and result in the cleavage of hundreds of protein targets (18). These cleavages lead to the dismantling of the cell and prepare it for phagocytic engulfment. For example, the cleavage of the inhibitor of caspase-activated deoxyribonuclease (ICAD) by Caspase 3 or 7 releases the caspase-activated deoxyribonuclease (CAD) to mediate DNA fragmentation (19). This is in concert with the cleavage and inactivation of poly (ADP-ribose) polymerase-1 (PARP), which normally handles the routine repair of DNA (20), enabling CAD to degrade the DNA. Caspase 3 will also cleave the protein Gelsolin, which will, in turn, cleave Actin filaments, disrupting the cytoskeleton, intracellular transport and signal transduction (21, 22). Another example is the proteolytic activation of the scramblase XK-related 8 (XKR8), which leads to the exposure of phosphatidylserine (PS) on the outer side of the cellular membrane, an “eat me” signal for phagocytes (23). Phagocytosis is critical for maintaining the “non-inflammatory” status of apoptosis. In the later stages of apoptosis, the cell turns into “apoptotic bodies” to facilitate phagocytosis. However, if the cells are not “eaten”, they will eventually develop membrane damage, which leads to cell bursting and inflammation. This is also known as secondary necrosis and will be explained in a later section.

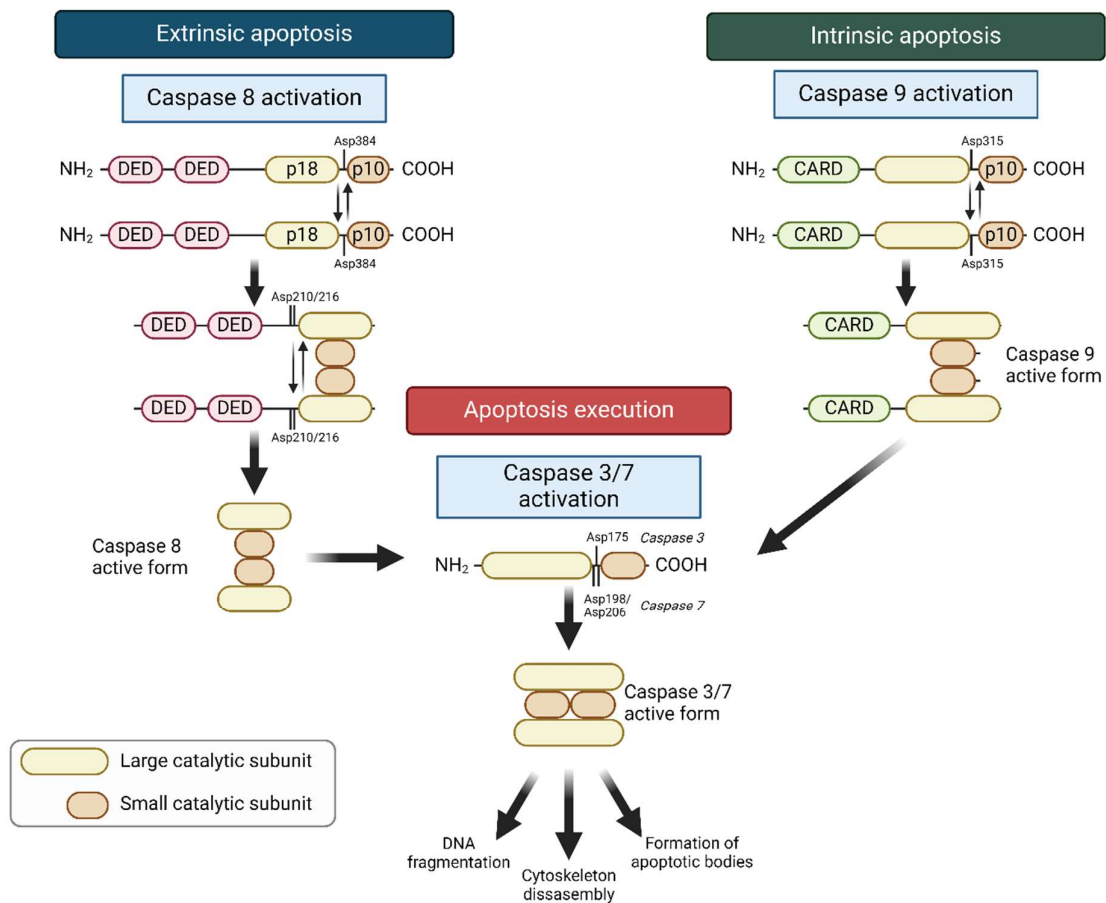


Figure 1. Apoptotic caspase activation. During extrinsic apoptosis, caspase 8 proteins are brought together via their DED domains, generating a proximity-induced cleavage of the proteins at Asp384, releasing the small catalytic subunit. This p10 fragment will bind the large catalytic domain of caspase 8 to prompt cleavages at Asp210 and Asp216, which release the now mature and active Caspase 8 from the DED domains into the cytoplasm (24). Upon extrinsic apoptosis, caspase 9 is concentrated at the apoptosome via its CARD domain, where the caspase undergoes proximity-induced cleavage at Asp315. The released p10 fragment then binds to the large catalytic subunit of Caspase 9, forming the mature and active Caspase 9 (25). When the initiator caspases reach full maturity, they cleave the effector caspases at Asp175 (Caspase 3) or Asp198 and Asp206 (Caspase 7). The resulting catalytic subunits bind at a 2:2 ratio and cleave their downstream targets to execute apoptosis.

As mentioned before, the stimuli that engage apoptosis can be internal or external, thus sub-categorizing apoptosis into two groups: Extrinsic and Intrinsic Apoptosis. However, it is worth noting that their pathways are not fully independent, as there is interconnectivity in their downstream signalling, and both converge on the activation of the effector Caspases 3 and 7.

### 1.1.1.1 Intrinsic apoptosis

Intrinsic apoptosis can be initiated by different stimuli, such as genotoxic stress (e.g DNA damage from chemotherapeutic agents (26)), damage to organelles (ER stress (27)), or lack of pro-survival growth factors, hormones or cytokines. These events directly impact the balance of the BCL-2 family of proteins, which determine the cell's fate by preventing or inducing the permeabilisation of the mitochondrial outer membrane. This permeabilisation results in the loss of mitochondrial potential and allows the release of the mitochondrial proteins Cytochrome C and the second mitochondria-derived activator of caspases (SMAC), among others. Cytochrome C interacts and activates the protein APAF-1 in the cytoplasm, promoting the assembly of the apoptosome complex, which recruits pro-Caspase 9 through homotypic CARD-CARD interactions between APAF-1 and pro-Caspase 9 (28-30). This clustering of the protease induces its self-cleavage at Asp315, converting pro-Caspase 9 into the mature form of Caspase 9 (Fig. 2). Mature Caspase 9 will then trigger the execution phase of apoptosis by cleaving and activating Caspase 3 (21).

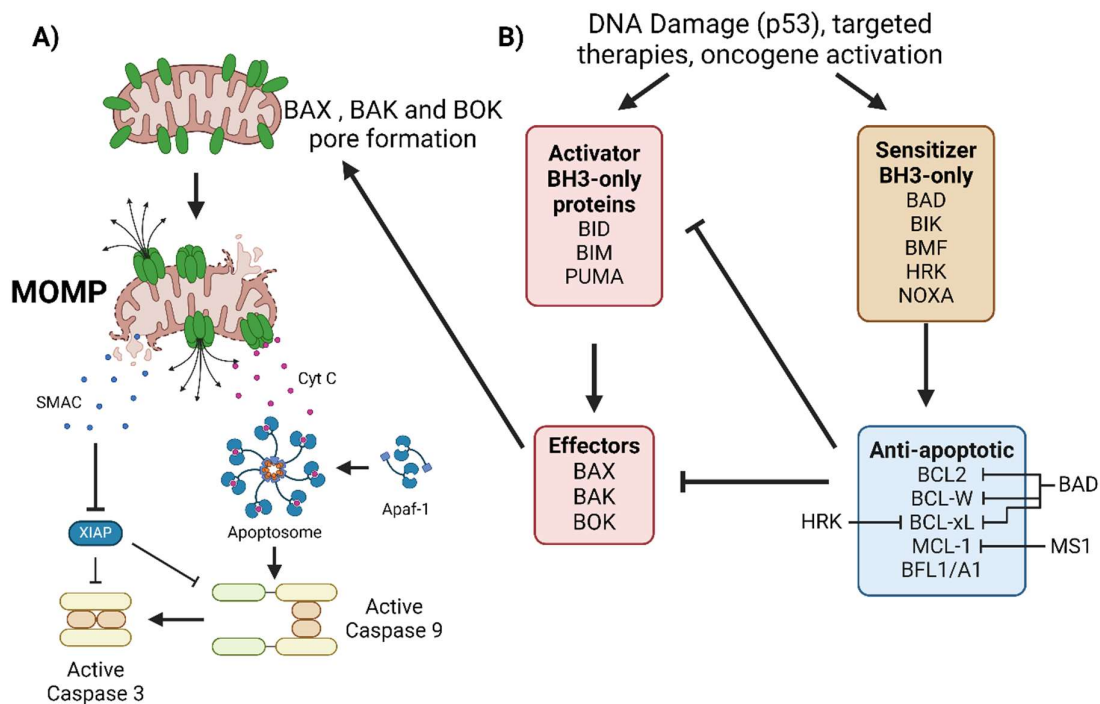


Figure 2. A) BAX and BAK, or BOK, oligomerization in the mitochondria induce Mitochondrial Outer Membrane Permeabilization (MOMP), releasing SMAC and Cytochrome C (Cyt C) into the cytoplasm of the cell. Cyt C binds to Apaf-1, which oligomerises and recruits pro-caspase 9, forming the apoptosome. Here, Caspase 9 becomes



active after undergoing self-cleavage at Asp315. The mature form of Caspase 9 will continue the caspase cascade and cleave and activate Caspase 3, ensuring apoptosis execution. B) The decision to induce MOMP is mediated by BCL-2 protein family members. Activator BH3-only proteins bind to and lead to the oligomerization of the Effector proteins BAX and BAK (31). The anti-apoptotic proteins sequester both Activator and Effector proteins, preventing Effector oligomerisation. Sensitizer BH3-only proteins compete for binding to Anti-apoptotic proteins with Activator and Effector proteins, thus releasing them from their sequestered state and allowing them to interact with each other (32, 33).

The BCL-2 protein family determines the decision to enter apoptosis by mitochondrial outer-membrane permeabilisation (MOMP). The induction of generalised MOMP in a cell is the critical step at which it commits to undergo apoptosis (30, 34). Hence, this process is tightly regulated by a complex system within the BCL-2 protein family. This protein group is divided into four categories: the anti-apoptotic proteins, the BH3-only sensitiser proteins, the BH3-only activator proteins, and the pro-apoptotic effector proteins. The pro-apoptotic effectors are BAX, BAK and BOK, with BOK acting independently from BAX and BAK and being the only one not affected by the pro-survival BCL-2 proteins (35, 36). BOK, in turn, is inhibited by gp78, a ubiquitin ligase that targets it for degradation (37). Details on BOK activation and oligomerization require further research (36). These effector proteins induce MOMP by oligomerising upon activation and forming pores in the mitochondrial outer membrane, thus releasing internal mitochondrial contents (e.g. SMAC and Cytochrome C) (30, 31, 36). BAX and BAK are activated by the BH3-only activator proteins (BID, BIM, PUMA) by binding to them and inducing conformational changes that lead to their oligomerisation (38-40). The anti-apoptotic proteins (BCL-2, BCL-xL, BCL-W, MCL-1 and BFL1/A1) act by directly binding and sequestering the activator proteins and the effectors BAX and BAK, thus preventing apoptosis (41). In fact, neutralising the function of the anti-apoptotic proteins can be enough to trigger this RCD (42). Finally, the BH3-only sensitiser proteins (BAD, HRK, BIK, NOXA and BMF) do not interact directly with BAX and BAK, but exert their pro-apoptotic effect by competing for binding to the anti-apoptotic protein group, releasing the activator and effector proteins (43). The affinity among the proteins in these groups is selective, although sometimes overlapping. For example, HRK selectively binds to BCL-xL (thus releasing BH3-only activator and effector proteins), and BAD inhibits BCL-xL, BCL-2 and BCL-W (44). This allows the system to be regulated through different pathways controlling the expression of one

or more of the BCL-2 protein family members (Fig. 2). One classic example is the induction of MOMP by p53.

Normally, cells induce the proteasomal degradation of P53 by the E3 ligase MDM2 (45, 46). Upon different stress stimuli, such as DNA damage or activation of certain oncogenes, the levels of P53 rise dramatically because these stresses converge on the inhibition of MDM2 (47). P53 will then regulate the expression of ~500 genes (48-52). Among these set of genes, P53 will drive the expression of the effector BAX, the BH3-only activator PUMA, and the BH3-only sensitiser NOXA (53, 54), all of which push the system to induce MOMP and engage in apoptosis. This, of course, makes P53 mutations very frequent in cancer, as its inactivation prevents cell death upon several stresses and promotes the survival of said cells. Interestingly, two members of the p53 protein family share similarities in function with P53: p63 and p73. Both respond to cellular and genomic stresses by promoting the expression of genes involved in DNA repair, cell cycle arrest and apoptosis (55, 56). Moreover, p63 has been shown to induce apoptosis via PUMA and NOXA (57).

Intrinsic apoptosis rids the body of old and damaged cells and prevents the transformation of normal cells guided by internal sensing and signalling. However, external stimuli can also unleash apoptosis, which we call extrinsic or death receptor-mediated apoptosis.

### 1.1.1.2 Extrinsic apoptosis

Extrinsic apoptosis is triggered by extracellular ligands that engage the membrane-bound Death Receptors on the surface. The most studied of these ligand-receptor pairs are Tumour Necrosis Factor (TNF) with TNF receptor 1 (TNFR1), FAS ligand (FASL/CD95L) with FAS/CD95/Apo1, and TNF-related apoptosis-inducing ligand (TRAIL) with TRAILR1 and/or TRAILR2 (in humans) (29, 58, 59). Although it is in their name, Death Receptors do not exclusively signal for cell death. They are also capable of activating the mitogen-activated kinase (MAPK) and the nuclear factor  $\kappa$ B (NF- $\kappa$ B) signalling pathways that induce the expression of pro-survival and pro-inflammatory genes (29). TRAIL and FASL trigger the formation of the Death Inducing Signalling

Complex (DISC) by recruiting FADD and Caspase 8, among other regulatory proteins (59). The formation of the DISC typically results in the induction of apoptosis or another more inflammatory type of RCD named Necroptosis. However, the DISC can release itself from the receptor and promote NF- $\kappa$ B mediated pro-survival and inflammatory gene activation. For example, TRAIL will bind to TRAIL-R1 and/or TRAIL-R2, inducing the recruitment of FADD to the receptor. FADD, in turn, will recruit RIPK1, Caspase 8, Caspase 10, and the Linear Ubiquitin Chain Assembly Complex (LUBAC), among others, forming the DISC (Fig. 3) (59). When Caspase 8 is at high levels in relation to other proteins of the complex, it will rapidly bind to the DEDs of FADD and other Caspase 8 proteins, forming filaments. The proximity between Caspase 8 homodimers, promoted by ubiquitination by Culin 3, induces the cleavage and activation of the protease, which will activate apoptosis via Caspase 3 (59). Cells can be classified depending on their direct response to TRAIL. In type 1 cells, such as thymocytes and mature lymphocytes, Caspase 8 is activated and induces apoptosis via Caspase 3. In type 2 cells, including pancreatic  $\beta$  cells, hepatocytes and most cancer cells, effector Caspase 3 activation is inhibited by X-linked inhibitor of apoptosis (XIAP). Instead, Caspase 8, rather than directly activating Caspase 3, cleaves its substrate BID, which in its truncated form (tBID) binds and activates the pro-apoptotic effectors BAX and BAK. This will release Cytochrome C, activating Caspase 9 as described before, and the protein SMAC, a natural antagonist of XIAP, therefore counteracting Caspase 3 inhibition.

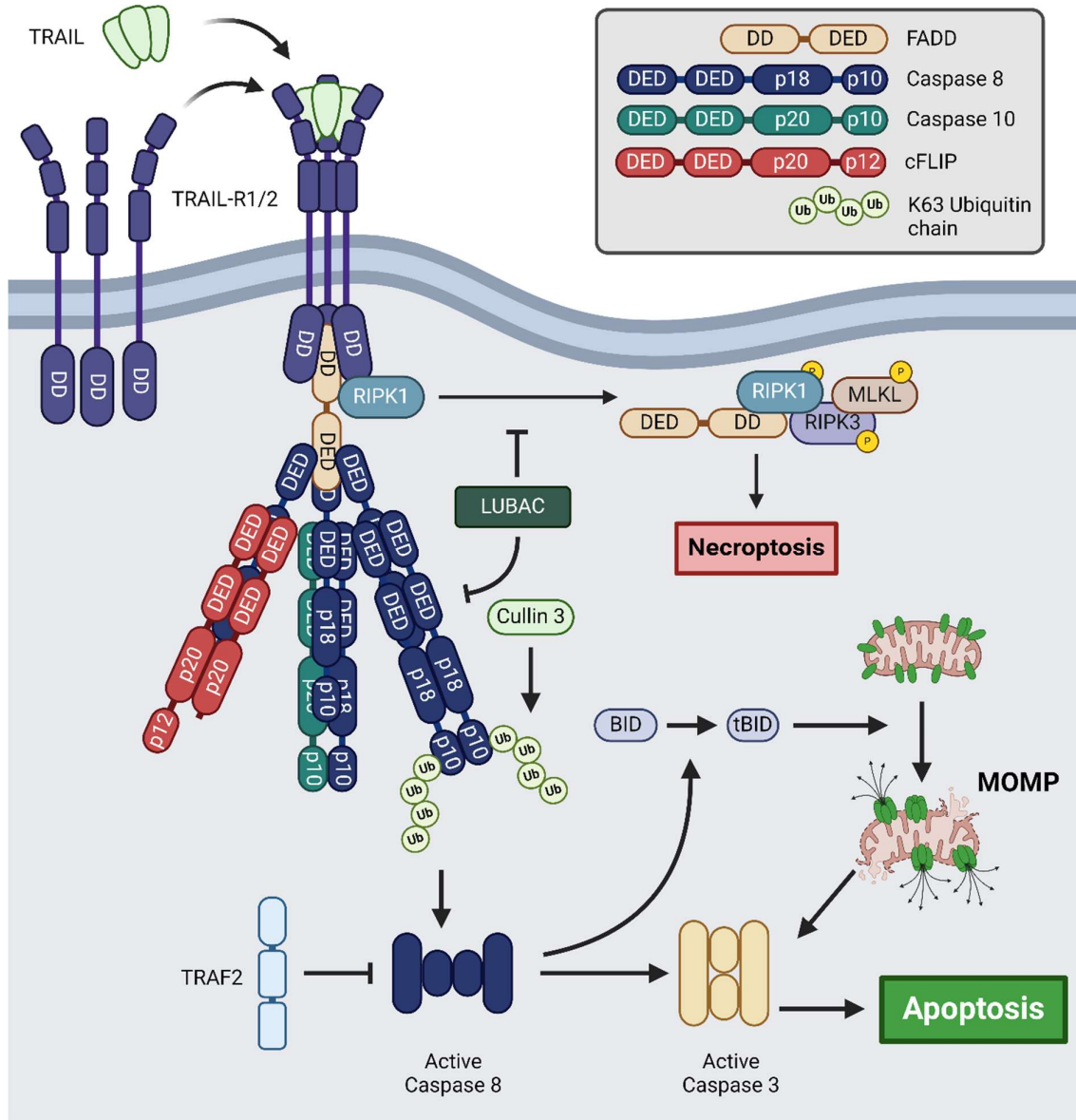


Figure 3. TRAIL signalling and DISC formation. When TRAIL binds to TRAIL receptors 1 or 2 (TRAIL-R1/2), it causes them to trimerize and recruit FADD through their Death Domains (DD). Receptor and downstream proteins follow a 3:1:9 stoichiometry for TRAIL-R1/2:FADD:Caspase 8 (60). When Caspase 8 is in low levels relative to RIPK1, RIPK1 is capable of binding to the DD of FADD, allowing self-phosphorylation by RIPK1, which recruits RIPK3 and MLKL. Phosphorylation of MLKL by RIPK3 then triggers death by Necroptosis. This RCD is inhibited by LUBAC and Caspase 8. When Caspase 8 is expressed in high levels relative to RIPK1, it will bind to the Death Effector Domain (DED) of FADD and other Caspase 8 proteins, where proximity-induced cleavages occur to mature Caspase 8. This maturation can be inhibited by LUBAC, TRAF2 and cFLIP, as cFLIP harbours DED domains, thus competing with other Caspase 8 proteins and preventing their cleavage. However, Cullin 3 promotes Caspase 8 self-cleavage and maturation, releasing the active Caspase 8 to cleave BID into tBID and Caspase 3 into its mature form. tBID binds to BAX and BAK, inducing their oligomerization and MOMP, further activating Caspase 3 and apoptosis (59).

NF- $\kappa$ B can be activated by the receptor-bound, also known as complex I of TNFR1, or the cytoplasmic DISC complex, also known as complex II or FADDosome. The protein complex LUBAC, present in both, is able to restrain Caspase 8 activity and to recruit the I $\kappa$ B kinase (IKK) complex and the TAB/TAK, activating NF- $\kappa$ B and MAPK signalling (61-63).

### 1.1.2 Necroptosis

Apart from activating pro-survival genes and causing apoptotic cell death, TRAIL can also induce the caspase-independent RCD known as necroptosis. Necroptosis is mediated by the previously mentioned RIPK1, RIPK3 (2, 64-67), and the executioner Mixed Linkage Kinase domain-like pseudo-kinase (MLKL) (10, 68, 69), resulting in pore and membrane-disrupting structures, causing cell bursting (70, 71). TRAIL-dependent necroptosis is thought to be triggered by the FADDosome (10, 72, 73), which retains FADD, Caspase 8, LUBAC and RIPK1 (4). Caspase 8 is known to inhibit necroptosis by cleaving RIPK1 and RIPK3, and its absence, or blocked activity, unleashes necroptosis, showing direct regulation of this RCD (4). LUBAC also limits the formation of the necrosome complex (RIPK1 and RIPK3) (63), thus restricting TRAIL-induced necroptosis (62). If necroptosis occurs, intracellular pro-inflammatory Damage-Associated Molecular Patterns (DAMPs) are released from the dying cell, inducing inflammation and immune recruitment (73). DAMPs can also trigger another type of RCD, pyroptosis, hence the need for tight regulation of necroptosis (2).

### 1.1.3 Pyroptosis

Pyroptosis is defined by the formation of gasdermin pores in the plasma membrane and is related to innate immunity (1). Pyroptosis is morphologically characterised by cell swelling and bursting. It generally relies on the activation of the inflammatory Caspases 1, 4, and 5 in humans or 1 and 11 in mice, each causing pyroptosis by cleaving Gasdermin D. The resulting N-terminal fragment of Gasdermin D oligomerises in the cell membrane, promoting cell lysis and allowing the free flow of ions and water (Fig. 4). This inevitably leads to an influx of water to the cell, resulting in swelling (also termed “ballooning”) and culminating in ninjurin 1 (NINJ1)-dependent plasma membrane rupture and the release of intracellular pro-inflammatory DAMPs,

such as High Mobility Group Box 1 (HMGB1) and Lactate Dehydrogenase (LDH). Interestingly, some small DAMPs, such as Interleukin 1 beta (IL-1 $\beta$ ) and interleukin 18 (IL-18), can be released through the Gasdermin D pores. Given the highly pro-inflammatory nature of these two Interleukins, their maturation (cleavage) is restricted to Caspase 1 and partially to Caspase 8.

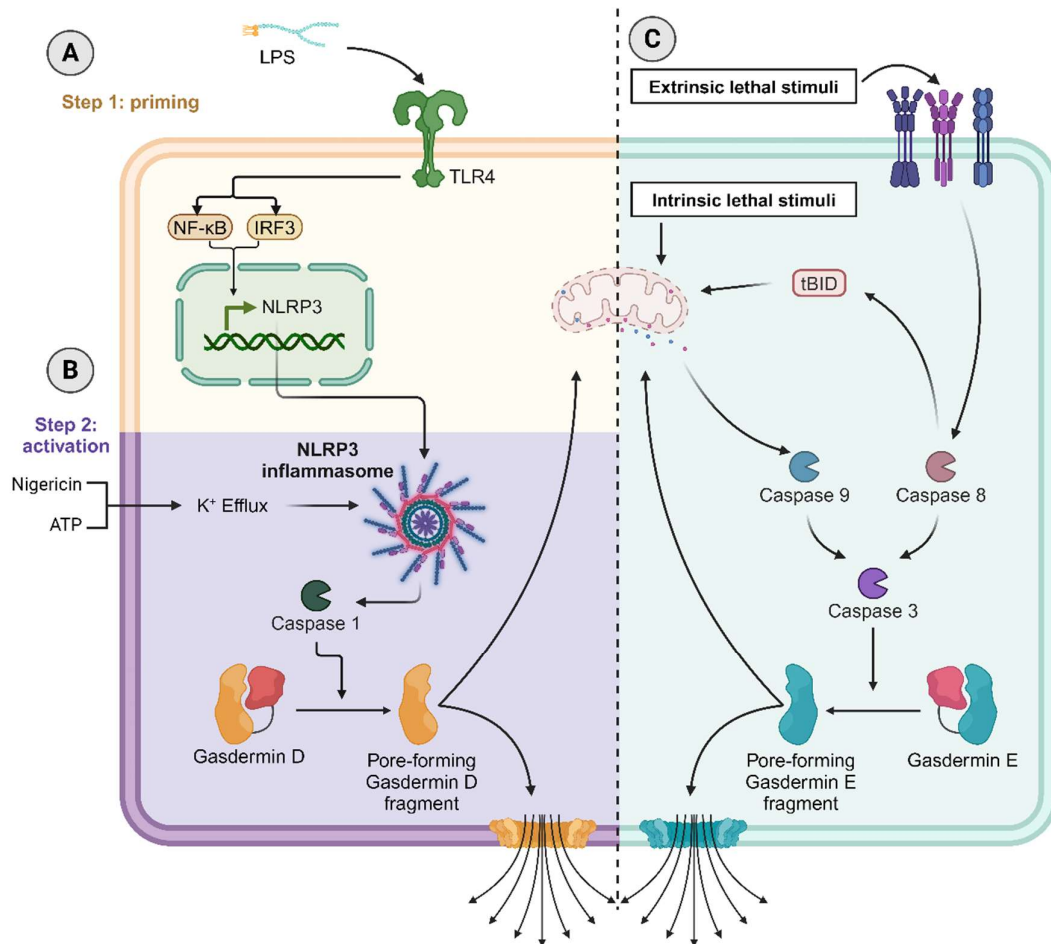


Figure 4. **Canonical NLRP3 mediated pyroptosis.** A) Step 1: priming. LPS sensing by TLR4 receptors leads to the expression of NF- $\kappa$ B and IRF3 target genes. These include NLRP3, among other type 1 Interferon chemokines (IRF3) and pro-inflammatory cytokines (NF- $\kappa$ B). B) Step 2: activation. Different factors can trigger the activation of NLRP3 through potassium (K<sup>+</sup>) efflux, including extracellular ATP, the bacterial toxin Nigericin, and other pore-forming toxins. The K<sup>+</sup> efflux is sensed by NLRP3, triggering the formation of the inflammasome and the activation of Caspase 1. This inflammatory Caspase will cleave Gasdermin D, releasing the pore-forming N terminal domain to form pores in the mitochondria and in the cellular membrane. C) **Apoptotic activation of pyroptosis.** Upon extrinsic lethal stimuli of death ligands (TNF, FASL, TRAIL), Caspase 8 becomes active, cleaving both BID to form tBID and Caspase 3 into its active form. tBID, as do intrinsic lethal stimuli, induce MOMP, thus activating Caspase 9 and, in turn, Caspase 3. The effector Caspase will cleave Gasdermin E at Asp270, releasing the inhibitory C-terminal domain and freeing the pore-forming N-terminal fragment. The N-terminus of Gasdermin E first oligomerises and forms pores in the mitochondria, releasing internal molecules and promoting further Caspase 3 maturation through the CytC-APAF1-Caspase 9 axis. Gasdermin E then permeabilizes the cellular membrane, allowing the free flow of ions and water, which causes cell swelling and NINJ1-mediated bursting.

Caspase 1 is recruited to cytoplasmatic complexes called inflammasomes, where it becomes active by proximity-induced autoproteolytic cleavage (74). Different inflammasomes are formed upon activation of Pattern Recognition Receptors (PRR) engaged directly by DAMPs or Pathogen-Associated Molecular Patterns (PAMPs) or indirectly by detecting perturbations in the cell elicited by DAMPs or PAMPs (75). Cytoplasmatic double-stranded DNA triggers inflammasome formation when detected by AIM2 (76), potassium efflux from the cell triggers the formation of NLRP3 inflammasome (77), NLRC4 inflammasome is activated by bacterial flagellin and type III secretion components (78), NLRP6 inflammasome senses lipoteichoic acid from Gram-positive bacterial cell wall (79), and NLRP7 senses acylated lipopeptides, a bacterial cell wall component (80). By contrast, Caspases 4 and 5 (and Caspase 11 in mice) become active by directly binding to cytosolic bacterial LPS, without the need for intermediary PRRs (81). These non-canonical inflammasome complexes also trigger Gasdermin D-dependent pyroptosis, including mature IL-1 $\beta$  release (11, 82, 83). Cells of the innate immune system are better prepared to trigger pyroptosis.

While the pyroptotic process is essential for host defence, the elicited response must be tightly regulated to prevent collateral damage to the host (75). This control is achieved by PRRs (e.g. Toll-like Receptor proteins), which regulate the expression of the factors needed for inflammasome formation and pyroptosis execution via NF- $\kappa$ B activation. One of the more studied inflammasomes is the NLRP3 inflammasome, which involves a priming and activation step for unleashing pyroptosis. In the first step, inflammatory factors, such as the Toll-like receptor 4 (TLR4) agonist LPS, induce the NF- $\kappa$ B mediated expression of NLRP3, pro-caspase 1 and pro-IL-1 $\beta$  (84). Then, DAMPs such as extracellular ATP, or PAMPs such as the bacterial toxin Nigericin, cause potassium efflux, which triggers NLRP3 phosphorylation and recruitment of Nek7 to the autoinhibitory domain LRR (Leucine-Rich Repeat) of NLRP3 (85). NLRP3 contains 3 main domains: the C-terminal LRR domain, the central NACHT domain (domain present in NAIP, CIITA, HET-E and TP1), and the N-terminal Pyrin domain (PYD). The release of the LRR domain from the NACHT domain by Nek7 allows the self-association of NLRP3 through its NACHT domain (86), and recruitment of the Apoptosis-associated Speck-like (ASC, also known as PYCARD) adaptor protein

through its PYD (Pyrin domain). The NLRP3-ASC filaments coalesce into a single macromolecular structure, known as an ASC speck (85). The ASC protein also contains a CARD domain, which recruits pro-caspase 1 via its own CARD domain and enables proximity-induced Caspase 1 self-cleavage and activation (85).

Gasdermin D is one of six of the Gasdermin family members, along with Gasdermin A, Gasdermin B, Gasdermin C, Gasdermin E, and Gasdermin F (PJVK) (87). Gasdermins owe their nomenclature to their high expression pattern along the gastrointestinal tract and skin (dermis) (88). All gasdermins have a conserved N-terminal pore-forming domain that is held in check by the C terminus, with the exception of Gasdermin F (87). Caspases and Granzymes cleave gasdermins in the linker region (Table 1), releasing the inhibitory C-terminal domain and allowing the N terminus to oligomerise and form pores in the membrane of organelles, plasma membrane, or the outer membrane of bacteria (89-91). Thanks to their pore-forming nature, activated Gasdermins can quickly induce cell bursting and release DAMPs that recruit the immune system and cause inflammation.

**Table 1.** Gasdermin family members and their activator proteins. Gasdermin F is not included as its activator is yet to be identified, and it does not possess pore-forming activity.

<b>Gasdermin</b>	<b>Activator</b>
Gasdermin A	SpeB ( <i>Streptococcus pyogenes</i> (92))
Gasdermin B	Granzyme A (93)
Gasdermin C	Caspase 8, 6 (94)
Gasdermin D	Caspase 1, 4/5, 8, Cathepsin G (87, 95)
Gasdermin E	Caspase 3, Granzyme B (96)

Gasdermin E is typically cleaved and activated during apoptosis by Caspase 3 at Asp270 (96). Like Gasdermin D and the other family members (97), it mediates pore formation in the mitochondria and cellular membrane, leading to inflammatory cell death. Upon cleavage by Caspase 3, the C-terminal inhibitory domain of Gasdermin



E is released from the N-terminal fragment. This pore-forming domain first oligomerises on the outer membrane of the mitochondria, permeabilising it in a BAX- and BAK-independent manner and allowing the release of mitochondrial content such as Cytochrome C (89). At this stage, Gasdermin E promotes further activation of Caspase 3 via the CytC-APAF1-Caspase 9 axis (89). Activated Gasdermin E also forms pores in the cellular membrane, thus leading to cell ballooning, bursting and the release of internal content, including DAMPS (Fig. 4). This phenomenon, termed “secondary necrosis,” occurs via Gasdermin E when cells undergo apoptosis in vitro with no macrophage or phagocytic cells capable of clearing them (96). As secondary necrosis has only been observed in vitro, it is considered a somewhat “artificial” process holding no physiological function. However, taking into consideration the absence of phagocytic cells in the proximity of a dying cell, Gasdermin E activation leads to the release of internal cell content, making the death more inflammatory, recruiting immune cells, such as macrophages, which would clear the remains of the dying cells.

#### 1.1.4 Cancer and resistance to cell death

The accumulation of DNA damage, protein-altering mutations, and hyperactive oncogenes induce apoptosis, which acts as a natural barrier against cancer development and progression. Malignant cell transformation is a multistep process typically initiated by mutational activation of driver oncogenes and/or inhibition of tumour suppressor genes. Normally, cells detecting irreparable DNA damage activate intrinsic apoptosis (e.g. via p53). However, when these mutations interfere with any step of this process, they enable the cell to survive and accumulate more DNA damage. These cells eventually acquire proliferation and survival advantages, for which the different gained phenotypes have been termed the Hallmarks of Cancer: acquired complementary and distinctive capabilities crucial for tumour growth and metastatic dissemination (98, 99). As our understanding of cancer grows, we now have sufficient evidence to classify them into 8 core hallmark capabilities, including “avoiding immune destruction”, “tumour-promoting inflammation”, and “activating invasion and metastasis” (99). It comes as no surprise that one of the Hallmarks is

“resistance to cell death”. Cancers achieve this hallmark by different means, but a common event is the inactivation of *TP53*, the most frequently mutated gene in human cancers (100). Most of the empirically discovered cancer treatments act by blocking DNA synthesis, inhibiting DNA replication, or damaging DNA (101). These treatments select malignant cells that happen to have a higher threshold for activating intrinsic apoptosis (e.g. cells with dysfunctional p53) in a process akin to Darwinian evolution (102).

Malignant cells also influence their protein expression patterns to prevent the induction of intrinsic and extrinsic apoptosis. Overexpression of pro-survival BCL-2 proteins, loss of BH3-only activators (particularly BIM or PUMA), or combined loss of BAX and BAK can render malignant cells resistant to conventional chemotherapeutics (103-106). Moreover, treatment with chemotherapy or radiation selects cancer cells that happen to have a higher threshold for triggering intrinsic cell death. This process of selection can enable the emergence of resistance to treatment in the tumour as the percentage of resistant clones increases (107).

Cancer cells can also be signalled to die via extrinsic apoptosis by the immune system. Upon activation, T-cells and NK cells can kill by death ligands (108, 109) or by secreting perforins, which permeabilise the membrane of the target cells to allow the cytosolic incorporation of granzymes, proteases that activate Caspases and Gasdermins (93, 110-112). Cytotoxic T-cells become activated when they recognise mutated peptides presented by the cancer cell on its Major Histocompatibility Complex Class I (MHC-I) surface protein. Cancer cells can downregulate their expression of MHC-I, but at a risk, as low presence of MHC-I in a cell activates NK cell killing (113). Malignant cells can also avoid death by cytotoxic T-cells by expressing immune checkpoint ligands, such as Programmed cell Death Ligand 1 (PD-L1), which prevent effector functions in the affected T-cell (114).

Even though the body has natural defences against cancer development through apoptosis induction, cancer cells evolve mechanisms to resist this cell death. Understanding these resistance pathways is crucial, as many current cancer therapies work by inducing apoptosis. However, different cancers exhibit varying mutations and,

thus, vulnerabilities. In the next section, we will explore Lung cancer, the main focus of this thesis.

## 1.2 Lung cancer

Lung cancer is the leading cause of cancer-related deaths worldwide, with over 1.8 million deaths per year, as stated by the World Health Organization (115). Based on histopathological and clinical features, two major groups of the disease can be distinguished: Non-Small Cell Lung Cancer (NSCLC), further divided into the sub-groups Lung Adenocarcinoma, Lung Squamous Cell Carcinoma and Large Cell Undifferentiated Carcinoma, and Small Cell Lung Cancer (SCLC). The major differences between SCLC and NSCLC reside in their cell size and appearance, their cells of origin, and driver mutations. SCLC mainly presents loss-of-function mutations in *TP53* and *Retinoblastoma 1 (RB1)* genes (116, 117). RB1 normally prevents cell cycle progression from G1 to S phase until the cell is ready to divide by binding and inactivating the E2F transcription factors responsible for expressing the necessary proteins to progress through the cell cycle (118, 119). The repressor activity of RB1 is reverted by phosphorylation by the Cyclin-Dependent Kinases (CDKs) 2, 4 and 6, thus allowing the expression of the E2F transcription targets (120). RB1 is frequently inactivated by complex genomic translocations that lead to its inactivation (121), which leads to unchecked cell cycle progression. Conversely, NSCLC typically overexpresses the Epithelial Growth Factor Receptor (EGFR) and harbours EGFR-activating mutations (122, 123). EGFR (also known as HER1 or ErbB1) activation leads to the activation of pathways with important roles in proliferation, tumorigenesis and apoptosis (122-124). Kirsten Rat Sarcoma viral oncogene homolog (KRAS) is another frequently mutated protein in NSCLC. These mutations (the majority of which are substitutions in G12, G13 and Q16) result in constitutive KRAS activation and downstream signalling, leading to proliferation, migration and survival (125-127).

These gain of function mutations have positioned EGFR and KRAS as attractive targets for NSCLC treatment, with major breakthroughs achieved in recent years. The

EGFR Tyrosine Kinase Inhibitor (EGFR TKI) osimertinib has already been approved as first-line treatment for patients harbouring the more common mutations in this gene (Ex19del and L858R) in NSCLC (128), and sotorasib and adagrasib are both used in the treatment of G12D KRAS mutant NSCLC tumours (129, 130). All three treatments have prolonged the survival of patients with NSCLC (127). However, SCLC lacks effective targeted therapies with similar clinical efficacy.

## 1.2.1 SCLC

SCLC is a neuroendocrine carcinoma which accounts for 15-18 % of all lung cancer diagnoses. Symptoms include cough, haemoptysis (coughing up blood) and difficulty breathing. Upon diagnosis, two-thirds of patients have metastatic disease. Common metastatic niches include the liver, the brain, adrenal glands, bone and the contralateral lung. It is a disease linked to heavy smoking (defined as at least 30 packs per year). This recurring exposure to mutagens leads to a very high accumulation of mutations in the cells of the lung. This is further reflected in the Tumour Mutational Burden (TMB) of SCLC, placing it as one of the cancers with the highest TMB, second only to Melanoma.

The disease's name comes from its histological features: small cells with scant cytoplasm and an oat-shaped morphology. Other histopathological characteristics include finely granular nuclear chromatin, absent nucleoli, high mitotic rate (average of 60 mitoses per mm<sup>2</sup>), frequent nuclear moulding due to the close proximity of the cells, numerous apoptotic figures and extensive necrosis (117). All these pathological characteristics are used in the diagnosis of SCLC.

As mentioned before, SCLC exhibits loss-of-function mutations in the *TP53* and *RB1* genes. The loss of the activity of these two proteins in neuroendocrine cells of the lung is enough to initiate SCLC tumour formation, as has been proven in genetically modified mouse models (131). SCLC has long been assumed to initiate from neuroendocrine cells from the lung. However, studies in mouse models suggest that other lung epithelial cells may serve as cells of origin for SCLC (132-135).

Neuroendocrine cells are cells found at the intersection between neurons and endocrine cells. Pulmonary Neuroendocrine Cells (PNECs) act as airway sensors, particularly sensitive to changes in oxygen levels. They quickly transmit this information to sensory neurons via serotonin and other signalling molecules when detecting hypoxia. They also regulate the immune response in the lungs and thus play a role in allergies (136). The cell of origin can determine the subtype of the original tumour of SCLC. The subtypes are currently divided into four groups: SCLC-A (ASCL1), SCLC-N (NEUROD1), SCLC-P (POU2F3), and SCLC-Y (YAP1). SCLC-A and SCLC-N are neuroendocrine subtypes, given their upregulation of the neuroendocrine transcription factors ASCL1 and NEUROD1, respectively. SCLC-P and SCLC-Y are considered non-neuroendocrine as they lack typical neuroendocrine markers, such as NCAM (CD56). SCLC-P is thought to originate from the chemosensory Tuft cells of the lung, while the three remaining subtypes are believed to originate from PNECs (137). The malignant transformation of PNECs leads to SCLC-A tumours, which can undergo reprogramming mediated by MYC to switch to SCLC-N and finally lose its neuroendocrine features to transform into SCLC-Y (137). SCLC-Y is also a topic of discussion among researchers as scientists are divided between those who recognise YAP1 expression as a marker for this subtype and those who fail to observe a clear signature of YAP1 expression, focusing instead on the expression of type I IFN response genes, or “triple negative” immunohistochemistry staining of the tumour (tumour tissue negative for ASCL1, NEUROD1 and POU2F3) (138-144). One recent study went as far as stating that YAP1 cell lines with mutated SMARCA4 are actually not SCLC, as xenograft tumours from said cell lines resemble Thoracic SMARCA4-deficient Undifferentiated Tumours in terms of transcriptional expression and pathological characteristics (144). While the classification of the fourth subtype is still in debate, we will refer to this subtype as SCLC-Y for simplicity.

### 1.2.1.1 The standard of care in SCLC

SCLC is treated as soon as a positive diagnosis is confirmed. The stage of SCLC is typically divided into Limited Stage (LS), where the tumour is not detectable outside of the lungs, and Extensive Stage (ES), where the tumour has metastasised outside the

lungs. However, it is worth noting that around 70% of patients have metastasis at the time of diagnosis (145). First-line treatment for LS consists of surgery and chemotherapy (platinum-based compounds such as cisplatin or carboplatin, and etoposide) in combination with radiation (117). First-line treatment for ES-SCLC maintains the chemotherapy and radiation treatment with the addition of anti-PD1 (atezolizumab) (117). First-line treatment has a success rate of 70%, as assessed by complete or partial response and stable disease rates (145). However, tumour recurrence with acquired resistance is the norm, reflected in its decrease in success rate among patients upon second-line treatment to only 22% (145). There is no established second-line treatment (146), but the majority include a combination of topotecan with a second agent, the choice of which depends on the sensitivity of the patient to the first-line treatment (145-147).

Chemotherapy and radiotherapy both induce DNA damage, which proves more lethal in cancer cells due to their rapid proliferation rates. Cisplatin acts by crosslinking the DNA, preventing DNA replication and activating DNA repair signalling pathways. If the damage persists, the cell will induce the activation of intrinsic apoptosis. Etoposide is an inhibitor of topoisomerase II, a protein responsible for releasing the torque tension accumulated in the DNA strands during the unravelling of the DNA upon replication. The resulting increased tension leads to double-strand breaks. Radiotherapy makes use of ionising radiation to generate DNA damage in the location of the cancer cells. These genotoxic agents would typically induce intrinsic apoptosis mediated by p53. However, in the case of SCLC, p53 is universally mutated, preventing it from increasing the expression of BAX, PUMA and NOXA, which would induce MOMP (121). This comes in contrast to the good response SCLC patients have to first-line chemotherapy. As previously mentioned, p63 and p73 can also induce intrinsic apoptosis upon DNA damage, albeit not as efficiently as p53. A recent study also found that DNA damage in cancer cells triggers p53-independent intrinsic apoptosis by ribosomal stalling, although the specific activator BCL-2 proteins engaged remain unclear (148).

Atezolizumab is a Programmed cell Death 1 (PD1) inhibitor and does not directly target the cancer cells. PD1 is primarily expressed by T-cells and can inhibit the cytotoxic activity of T-cells. Cancer cells can evolve the capacity to overexpress the ligand for

PD1, PD-L1, thus inactivating cytotoxic T-cells and avoiding the induction of extrinsic apoptosis. Blocking PD1 prevents the inhibition of the killing activity of T-cells, therefore enhancing the tumour clearance by the immune system. Nonetheless, despite these treatments, SCLC cells can evolve and bypass these mechanisms of action. This acquired resistance, on top of the rapid metastatic capacity of SCLC, all add up to a dismal outlook of 5-year survival of only 7% (149), urgently calling for therapies capable of overcoming this acquired resistance.

# Chapter 1 – Inhibiting CDK9 for the Treatment of SCLC

## 1.3 Introduction

### 1.3.1 Cyclin-dependent kinases

In the search for novel treatments to target cancer cells, Cyclin-Dependent Kinases (CDKs) have emerged as interesting candidates with great therapeutic potential. CDKs can only exert their function in the presence of their Cyclin counterparts and can be divided into two groups: those involved in cell cycle regulation (e.g. CDKs 1, 2, 4 and 6) and those in charge of transcriptional homeostasis (e.g. CDKs 7 and 9) (150). CDKs regulate the cell cycle by controlling the passage to and progress of the different stages. They are regulated by phosphorylation and CDK Inhibitor (CDKI) proteins.

During Mitosis, progression through the four phases (G<sub>0</sub>/G<sub>1</sub>, S, G<sub>2</sub>, and M) is mediated by CDKs to ensure faithful DNA replication and prevent chromosomal instability (151). As normal cells exit cellular division, they enter the reversible (or permanent) quiescent state (G<sub>0</sub> phase) regulated by CDK3/cyclin C. Different extracellular signals lead to the synthesis of Cyclin D, which stimulates CDKs 4 and 6, promoting entry into the cell cycle (151). Active CDK4/6 complexes phosphorylate the RB protein, removing its repression of the E2F transcription factors, and allowing the expression of Cyclins E, A and B, and many other genes required for the S phase. Cyclin E binds to CDK2, further phosphorylating RB, inducing the start of the S phase and initiating DNA synthesis. Nearing the end of the S phase, Cyclin A replaces Cyclin E within CDK2, forming a new complex which terminates the S phase and drives the cell into the G<sub>2</sub> phase (151). This complex also activates CDK1 by Cyclin A, transitioning the cell to the M phase (Mitosis). Upon Mitosis, Cyclin A is replaced by Cyclin B within CDK1, maintaining the CDK activity. The controlled degradation of Cyclin B and CDK1 enables chromosomal separation and the completion of Mitosis (151).



Cell cycle progression and regulation by CDKs and Cyclins ensures cells can fulfil all the requirements necessary to progress to the next cell cycle stage. CDKs not only regulate this essential process but also play a critical role in transcription.

### 1.3.2 CDKs and transcriptional homeostasis

CDKs regulate transcription initiation and elongation. CDK7 is a key component in the Transcription Factor II H (TFIIH), while CDK9 is part of the Positive Transcription Elongation Factor b (P-TEFb) complex (152-154). This complex allows the elongation of mRNA transcripts. Transcription is a multi-step process consisting of initiation, promoter clearance, elongation, processing of nascent transcripts, termination, mRNA cleavage, and polyadenylation (pA) (152).

Transcription is initiated when the RNA pol II pre-initiation complex (PIC) is recruited by transcription factors and the Mediator Complex (co-activator that links transcription factors with the RNA pol II) at the promoter to the transcription starting site (TSS). RNA pol II requires phosphorylation at Ser5 of its C-terminal tail by CDK7 (from the TFIIH) for clearance from the promoter (152, 153). Next, the capping enzyme (CE) adds a 7-methylguanosine “cap” to the 5' end of the nascent transcript, protecting it from nuclease digestion. After copying 20-100 nucleotides, the RNA pol II becomes arrested and remains attached to the DNA template because of negative transcription elongation factors (NTEFs) (153). These include 5,6-dichloro-1-β-D-ribofuranosylbenzimidazole sensitivity-inducing factor (DSIF) and the negative elongation factor (NELF) (155). The release of RNA pol II is mediated by P-TEFb, which contains cyclins T1, T2 and CDK9 (154). When recruited to the paused RNA pol II, CDK9 phosphorylates the C-terminal tail of RNA pol II at Ser2 and the NTEFs NELF and DSIF (Fig. 5). NELF dissociates after phosphorylation, and DSIF is converted to a positive elongation factor, remaining with RNA pol II. The protein phosphatase 2A (PP2A) and PP4 antagonize the P-TEFb-dependent release of RNA pol II (156). When released, the phosphorylated C-terminal tail serves as a docking site for splicing

regulators (SR) and poly-A machineries. As such, P-TEFb is the critical factor that releases the arrest of RNA pol II and promotes transcription elongation (152).

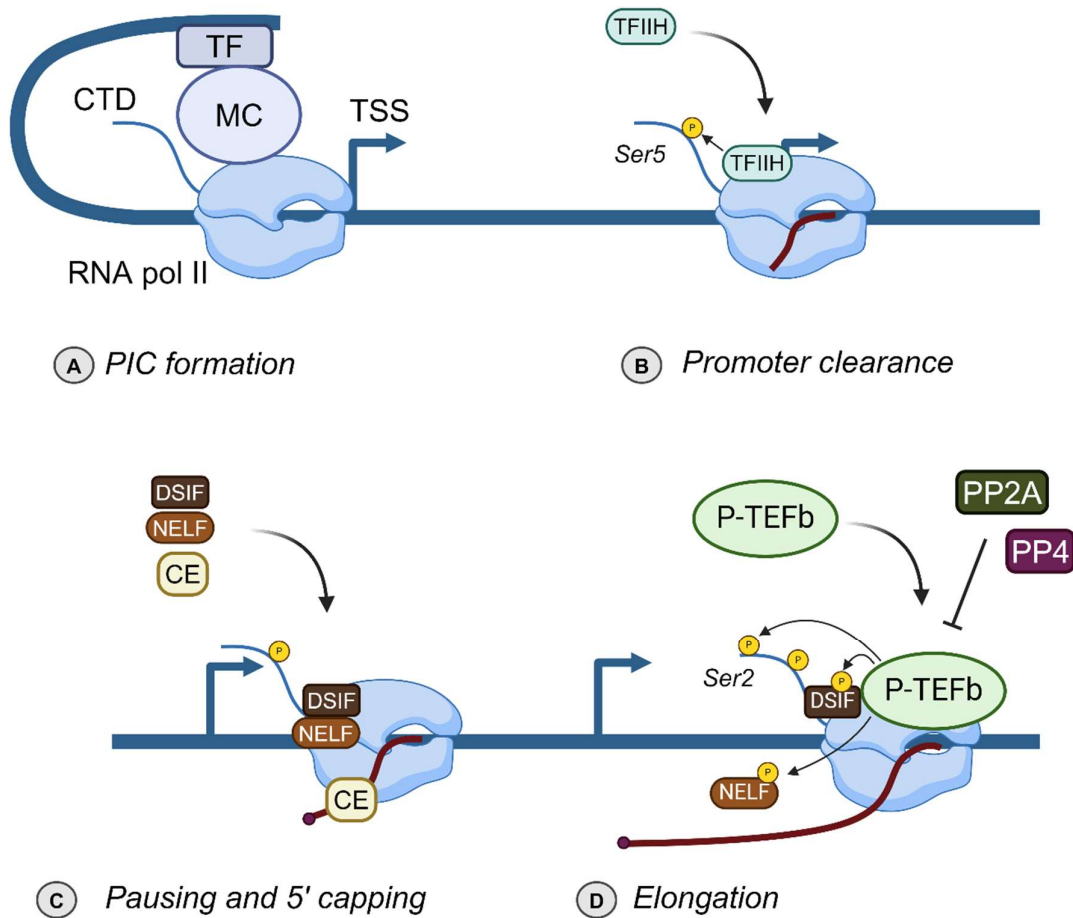


Figure 5. Transcription initiation. A) Formation of the Pre-initiation Complex (PIC). Transcription factors (TF) recruit RNA pol II via the Mediator complex (MC) to the Transcription Starting Site (TSS). B) TFIID is recruited to RNA pol II and phosphorylates the Ser2 of the C-Terminal Domain (CTD), releasing the protein from the promoter. C) the negative transcription elongation factors (NTEFs) DSIF and NELF arrest the polymerase after 20-100 nucleotides from the TSS. This allows for the Capping Enzyme to add a 7-methylguanosine "cap" to the 5' end of the RNA transcript. The release from this arrested state is mediated by P-TEFb (D), where the complex phosphorylates the CTD at Ser2 and the NTEFs, dissociating NELF from the polymerase and turning DSIF into a positive transcription elongation factor. The phosphatases PP2A and PP4 antagonize the activity of P-TEFb, preventing the release of P-TEFb (152).

### 1.3.3 CDK inhibition in cancer

While CDKs are rarely mutated, cancer cells can enhance their activities by overexpressing Cyclins and losing CDKI expression. As such, CDKs are attractive

targets for hampering cancer cell proliferation. While essential for mRNA transcription, P-TEFb is known to bind to different transcription factors, such as NF- $\kappa$ B (157) and cMYC (158, 159). Cancer cells depend on continuously activated gene expression for survival. This, in combination with the fact that CDKs are rarely mutated, has made CDK9 a therapeutic target for cancer treatment.

Since the development of the drug Flavopiridol (Alvociclib), originally designed to target CDK4 and 6 (160), it has been used as a standard for the development of new CDK9 inhibitors, as it was found to have stronger CDK9 inhibition than CDKs 4 or 6 (160). Since then, many CDK9 inhibitors have been developed, of which are worth mentioning: SNS-032, dinaciclib and NVP-2. SNS-032 inhibits CDKs 2, 7 and 9, and it has been shown that inhibition of CDK9, combined with the death ligand TRAIL, proved deadly in a broad range of cancers, including NSCLC and Colorectal cancer (161). Dinaciclib, an inhibitor of CDKs 1, 2, 5 and 9, was also shown to have a synergistic effect on a broad range of cancers upon combination with TRAIL (162). Dinaciclib has also advanced clinically onto several clinical trials, including a phase III trial in refractory Chronic Lymphocytic Leukaemia (CLL) (163). NVP-2 on the other hand, specifically inhibits CDK9 (164). All these drugs target the hinge region of CDK9, the binding pocket of ATP, thus competing with the molecule, preventing the phosphorylation of the Ser2 of RNA pol II and inhibiting the formation of new mRNA transcripts. Studies with SNS-032 and dinaciclib showed that CDK9 inhibition, indeed, the lack of mRNA production, leads to the decrease of short-lived proteins, particularly the anti-apoptotic proteins cFLIP, MCL-1 and cIAP1/2 (162, 163). This shift in the levels of anti-apoptotic proteins sensitised the cells to the death ligand TRAIL, facilitating the induction of cell death by the DISC. However, the inhibition of CDK9 alone was not enough to induce extensive cell death in the different cancer cell lines tested.

One study focused on the combination of dinaciclib with Immune Checkpoint Inhibitors (ICI), targeting PD1 in colorectal and bladder cancer (165). Their results showed an improved overall quality of the immune response generated, with increased Dendritic Cell activation and CD8 T cell recruitment in the tumours (165). Since one of the main issues with SCLC is the acquired resistance to treatment, targeting different pathways can bypass the resistance mechanism. In the case of CDK9 inhibition, since it decreases short-lived anti-apoptotic proteins, we could also think of a re-sensitisation

to chemotherapy. In line with this, some preliminary experiments have been conducted in SCLC, only showing synergy with dinaciclib and the BCL-2 inhibitor navitoclax in SCLC cell lines (166). However, this study was not as extensive as we show in this chapter. Here, we will test and characterise the use of CDK9 inhibitors, both known (dinaciclib and NVP-2) and novel (VC-1), for the treatment of SCLC. We will delve into their mechanism of action and their activity against SCLC cell lines both *in vitro* and *in vivo*. Finally, we will combine our results with the current literature to set the stage for the future steps needed to tackle SCLC effectively and, hopefully, help the lives of patients.

## 1.4 Aims – Chapter 1

SCLC is an aggressive disease with dismal survival rates. Patients generally respond positively to first-line treatment. However, they invariably relapse with acquired resistance to treatment, highlighting the need for novel and alternative therapies (117). In this Chapter, we aim to address this gap in treatment by the:

1. Assessment of the effectiveness of CDK9 inhibition for the induction of cell death in SCLC as compared to NSCLC cells.
2. Identification of the molecular cell death pathways engaged upon CDK9 inhibition.
3. Characterisation of the effect of CDK9 inhibition in subcutaneous and autochthonous *in vivo* models of SCLC.

## 1.5 Results

### 1.5.1 CDK9 Inhibition as an effective therapy for small-cell lung cancer

With the known literature as a foundation and our understanding of cell death mechanisms, we extensively investigated CDK9 inhibition in SCLC to provide more effective options to patients with this disease. Here, we report our findings and observations, showing the potential of CDK9 inhibition for reducing the aggressiveness of this cancer.

The majority of the results presented in this section are part of a recently published publication in the Cell Death and Disease journal. This study was accomplished thanks to the collaboration of Vichem Chemie Ltd., the creators of VC-1; AG Lindermann and AG Sos, who provided insight and scientific contribution; AG Tovari, who performed *in vivo* inoculations of VC-1; AG Montero, who performed and provided insight into the Dynamic BH3 profiling experiments; and AG Walczak, who provided material resources.

## 1.5.2 CDK9 effectively kills mouse and human SCLC cells while having no significant impact on NSCLC cells

To evaluate the effect of dinaciclib on SCLC, we employed a range of human cell lines and mouse cells derived from the autochthonous mouse model of SCLC (RP). This model features lung-specific mutations in *Rb1* and *Trp53* (131). Treatment with dinaciclib significantly reduced viability and induced cell death in a dose-dependent manner across SCLC cell lines (Fig. 6a-c), with IC<sub>50</sub> values spanning from 44 to 124 nM for mouse cell lines and 5 to 20 nM for human cell lines (Fig. 6d, e).

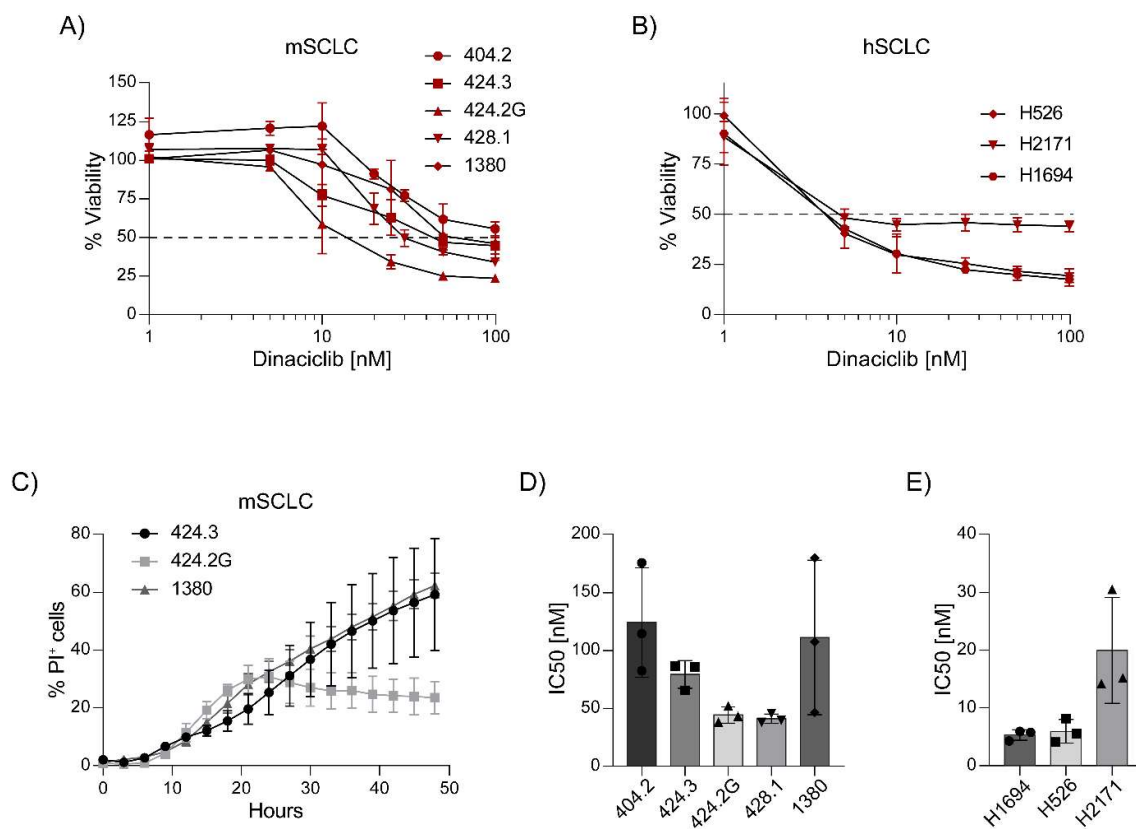


**Figure 6.** A) Viability of mouse SCLC cell lines as measured with Cell TiterGlow (CTG, Promega) expressed as % of the untreated control (100%) after a 30-hour treatment with different concentrations of dinaciclib: 1, 5, 10, 20, 25, 30, 50 and 100 nM. Mean + SD, n=3. B) Viability of human SCLC cell lines after 30-hour treatments of 1, 5, 10, 30, 50 and 100 nM of dinaciclib. Mean + SD, n=3. C) Percentage of PI<sup>+</sup> cells after treatment with 50 nM dinaciclib as measured by Incucyte with Cell-by-cell analysis. Mean + SD, n=3. D) IC<sub>50</sub> (nM) of mouse SCLC. Mean + SD, n=3. E) and human SCLC cell lines. Mean + SD, n=3. Adapted from Valdez Capuccino et al. *CDDis*, 2024.

We corroborated the inhibition of CDK9 by dinaciclib in murine SCLC cells by checking the decrease of phosphorylated RNA pol II through immunoblotting. Moreover, a reduction in the expression of the reported targets anti-apoptotic proteins MCL-1 and cFLIP, alongside an induction of caspase-3 cleavage, was observed in the three cell lines examined at 18-, 24- and 30 hours post-treatment (Fig. 7a). Notably, dinaciclib treatment led to changes in c-Myc expression, showing an increase in the longer isoform. Similar changes in protein expression were observed in human SCLC cells treated with dinaciclib, which also showed abrogation of c-MYC, downregulation of BCL-xL and increased levels of cleaved Caspase-3 and PARP, indicative of apoptosis activation upon treatment (Fig. 7b). Indeed, caspase inhibition completely abrogated cell death induced by dinaciclib (Fig. 7c), while minimal changes in cell cycle progression were observed after 24 hours of treatment (Fig. 7d). Thus, dinaciclib induces caspase-dependent cell death in SCLC cells at nanomolar concentrations.

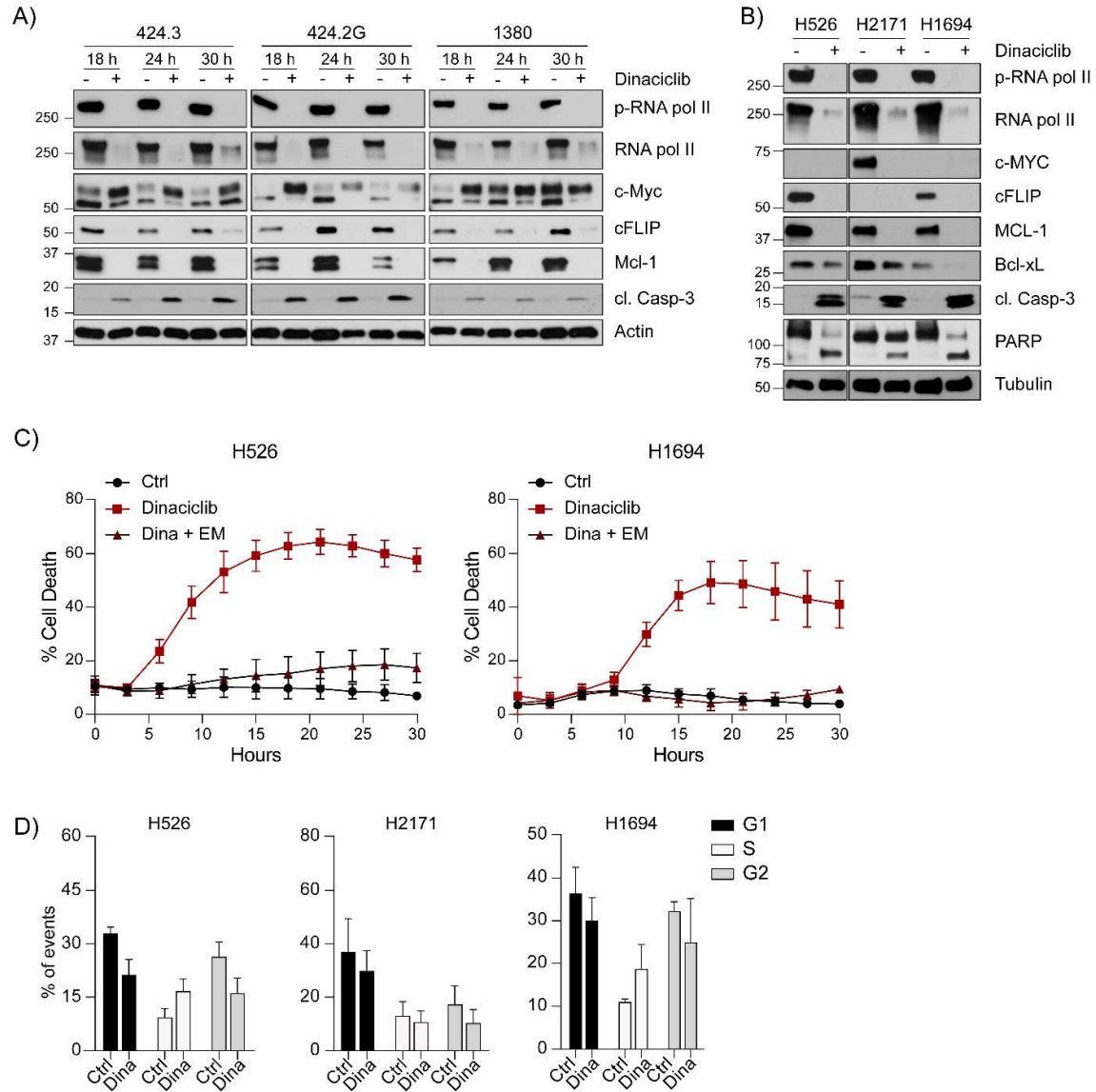
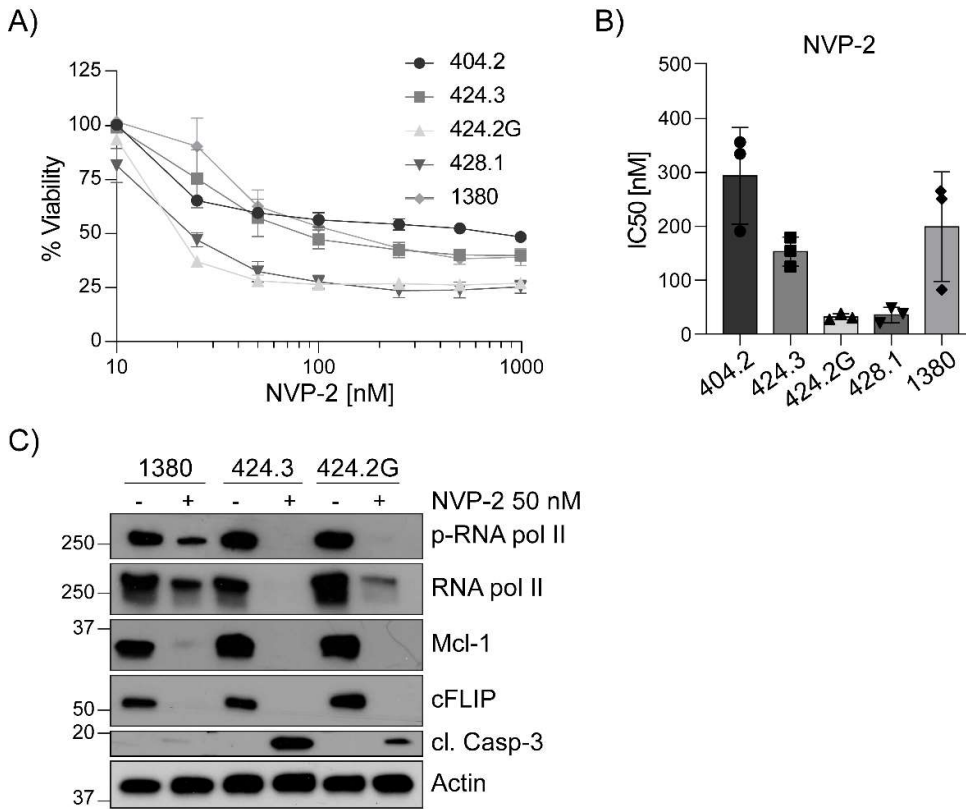


Figure 7. A) Mouse SCLC cells were lysed with RIPA buffer after 18, 24 and 30 hours of treatment with dinaciclib (50 nM) or vehicle. Representative blots of 3 independent experiments. B) Human SCLC cells were lysed with RIPA buffer after 18 hours of treatment with dinaciclib (50 nM) or vehicle. Representative blots of 3 independent experiments. p- = phospho-; cl. = cleaved. C) Percentage of PI-positive cells after treatment with 50 nM dinaciclib and 5  $\mu$ M emricasan (EM) as measured by Incucyte. Mean + SD, n=3. D) Cell cycle distribution was assessed by permeabilising the cells and staining with PI after 24 hours of treatment with 50 nM of dinaciclib. Mean +SD, n=3. Adapted from Valdez Capuccino et al. *CDDis*, 2024.

Next, we investigated whether a more specific CDK9 inhibitor would yield analogous cytotoxic effects in SCLC. We used NVP-2, a compound known to selectively target CDK9 without affecting the other CDKs targeted by dinaciclib (167). Treatment of mouse SCLC cells with NVP-2 resulted in cell death akin to that observed with dinaciclib (Fig. 8a) with IC<sub>50</sub>s in the nanomolar scale (Fig. 8b). Concurrently, we



observed suppression of RNA pol II phosphorylation, leading to reduced levels of MCL-1 and cFLIP, as well as an increase in cleaved caspase 3 (Fig. 8c).



**Figure 8.** A) Viability, as measured by CTG, expressed as percentage of the untreated control (100%) after a 30-hour treatment with different concentrations of NVP-2 (10, 25, 50, 100, 250, 500 and 1 000 nM). Mean + SD, n=3. B) IC50 of NVP-2 for each cell line. Mean + SD, n=3. C) Cells were lysed with RIPA buffer after 30 hours of treatment with NVP-2 (50 nM) or vehicle. Representative blots of 3 independent experiments. p- = phospho; cl. = cleaved. Adapted from Valdez Capuccino et al. *CDDis*, 2024.

Previous reports have highlighted the downregulation of pro-apoptotic proteins by dinaciclib in NSCLC. However, dinaciclib monotherapy does not induce significant cytotoxicity in NSCLC cells (161, 162). This prompted us to conduct a direct comparative analysis of the cytotoxic potential of dinaciclib in SCLC versus NSCLC. To this end, we employed human and mouse cells derived from the *Kras* and *Trp53* (KP) model for NSCLC (168). Compared to SCLC, dinaciclib had a modest impact on the viability of NSCLC cells (Fig. 9a, b). Notably, the higher sensitivity of SCLC cells to dinaciclib was more pronounced in the panel of human SCLC cells than in human NSCLC cell lines (Fig. 9c).

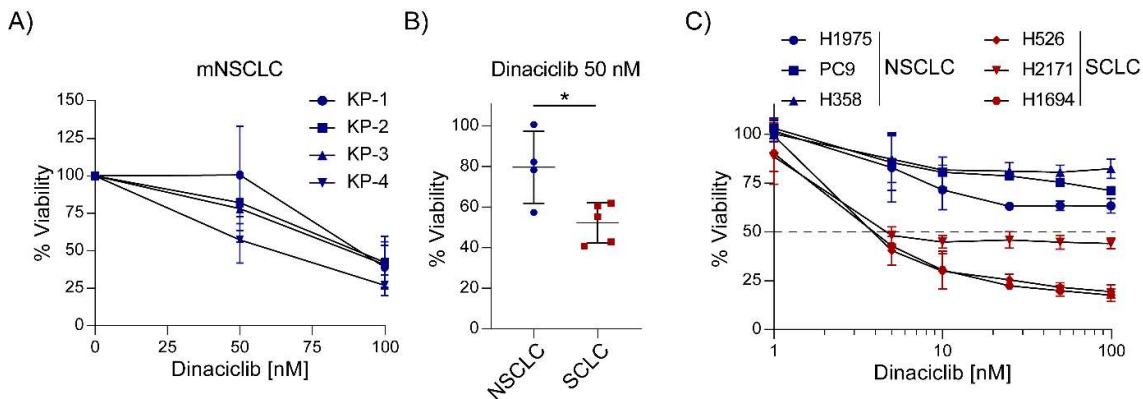


**Figure 9.** A) Viability of mouse NSCLC cell lines after a 30-hour treatment at 50 nM and 100 nM of dinaciclib. Mean + SD, n=3. B) Viability of human SCLC and NSCLC cell lines after 30-hour treatments of 1, 5, 10, 30, 50 and 100 nM of dinaciclib. Mean + SD, n=3. C) Viability of mouse SCLC compared to NSCLC after a 30-hour treatment with 50 nM of dinaciclib. Mean + SD, n=3. Adapted from Valdez Capuccino et al. *CDDis*, 2024.

To further elucidate the underlying difference in sensitivities between SCLC and NSCLC to dinaciclib, we conducted dynamic BH3 profiling (DBP). DBP relies on the assessment of Cytochrome C release following 16-hour incubation with the drug of interest (in this case, dinaciclib) and one additional hour with either sensitizing peptides, BAD, HRK and MS1, or the activating peptide BIM (169). BIM binds directly to Bax and Bak, thereby allowing their oligomerization and inducing mitochondrial outer membrane permeabilization (MOMP) and Cytochrome C release, making it the perfect positive control (170). After the incubation with the peptides, Cytochrome C is measured by Flow Cytometry, which indicates the levels of MOMP reached. We use alamethicin to measure the total release of Cytochrome C and report the measured release on the other conditions as the percentage of priming (% Priming). We compare the % Priming for each peptide with or without the dinaciclib pre-treatment and show the difference between these percentages as delta % Priming ( $\Delta\%$  Priming).

NSCLC cells treated with BIM and BIM + dinaciclib showed no statistically significant difference in their mitochondrial membrane permeabilization (Fig. 10a), thus indicating no contribution from dinaciclib to prime NSCLC cells to death. Moreover, the addition of dinaciclib to the sensitizer peptides BAD, HRK and MS1 showed a high  $\Delta\%$  Priming, demonstrating that NSCLC cells don't become more primed to death by dinaciclib but are able to adapt to the treatment by increasing their dependency to anti-apoptotic proteins. BAD targets both Bcl-2 and Bcl-xL; HRK targets Bcl-xL; and MS1 targets Mcl-1. By knowing this, we can understand that H1975 most likely becomes dependent

on Bcl-xL. The cell line PC9, however, had relatively high  $\Delta\%$  priming with all three peptides, suggesting that it becomes reliant on Mcl1 and Bcl-xL to prevent cell death by dinaciclib. SCLC cells, on the other hand, had significantly higher  $\Delta\%$  priming with the BIM peptide, meaning that SCLC cells are primed to death upon treatment with dinaciclib. Interestingly, dinaciclib had a low (H526) or no statistically significant impact (H2171) on the % priming of the sensitiser peptides. This indicates that, contrary to NSCLC, SCLC cells become primed to death when treated with dinaciclib. Altogether, we are able to show that the difference in the response to dinaciclib is due to the inability of the drug to prime NSCLC cells to death, and the inherent capacity of these cells to undergo an “apoptotic adaptation” upon treatment.

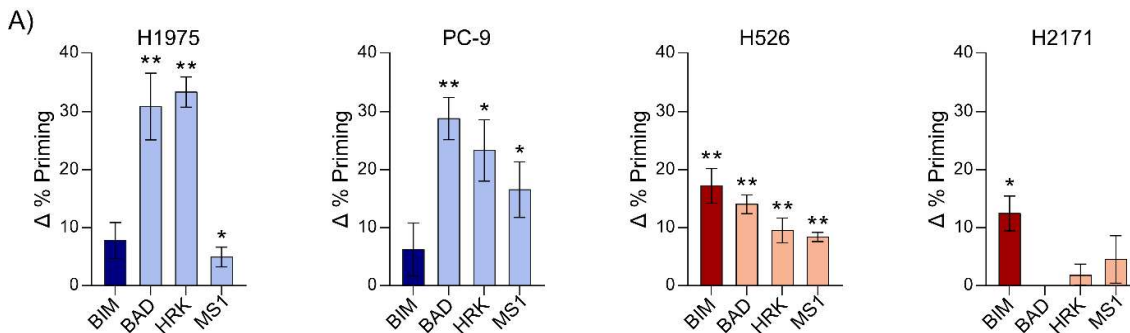


**Figure 10.** A) Dynamic BH3 profiling after 96 h incubation with 25 nM dinaciclib with the indicated peptides BIM, BAD (BCL-2, BCL-xL, BCL-W dependence), HRK (BCL-xL dependence) and MS1 (MCL-1 dependence). Results expressed as  $\Delta\%$  priming, representing the increase in priming compared to non-treated cells. Values indicate mean  $\pm$  SEM from at least three independent experiments. Paired t- test of dinaciclib treated vs. ctrl in each condition, \*\* $p < 0.01$  and \* $p < 0.05$ . Experiments performed by collaborator AG Montero. Adapted from Valdez Capuccino et al. *CDDis*, 2024.

Thus, while NSCLC cells demonstrate pro-survival adaptations, SCLC cells appear less proficient in doing so. Consequently, whereas CDK9 inhibition by dinaciclib is enough to induce apoptosis in SCLC cells, NSCLC cells exhibit greater resistance due to lower overall apoptotic priming and greater plasticity for rapid adaptation through anti-apoptotic proteins to promote survival. Consequently, SCLC cells exhibit a lesser capability to counteract the cytotoxic activity of dinaciclib, resulting in a robust apoptotic induction.

### 1.5.3 Dinaciclib has no additive effect with TRAIL or chemotherapy but potently kills chemotherapy-resistant SCLC cells

As dinaciclib treatment led to the reduction of anti-apoptotic proteins MCL-1, BCL-xL, and cFLIP, we next aimed to assess its potential synergy with therapies targeting either intrinsic or extrinsic cell death pathways. Previous studies have reported the high efficacy of combining CDK9 inhibition with TRAIL treatment across various tumour types, including NSCLC and pancreatic cancer (161, 162, 171). Consequently, we hypothesised that the combination of dinaciclib and TRAIL treatment would have similar efficacy in SCLC. However, contrary to NSCLC cells, the combined therapy of dinaciclib and TRAIL failed to exhibit a synergistic or additive effect in SCLC cells (Fig. 11a). Consistent with this finding, the combination treatment was unable to induce caspase-8 cleavage in H1694 SCLC cells, while it successfully did so in NSCLC cell lines (Fig. 11b). Notably, the expression of caspase-8 in H2171 SCLC cells was considerably lower compared to NSCLC, consistent with prior reports indicating a generally reduced expression of caspase-8 in SCLC (121, 172, 173).

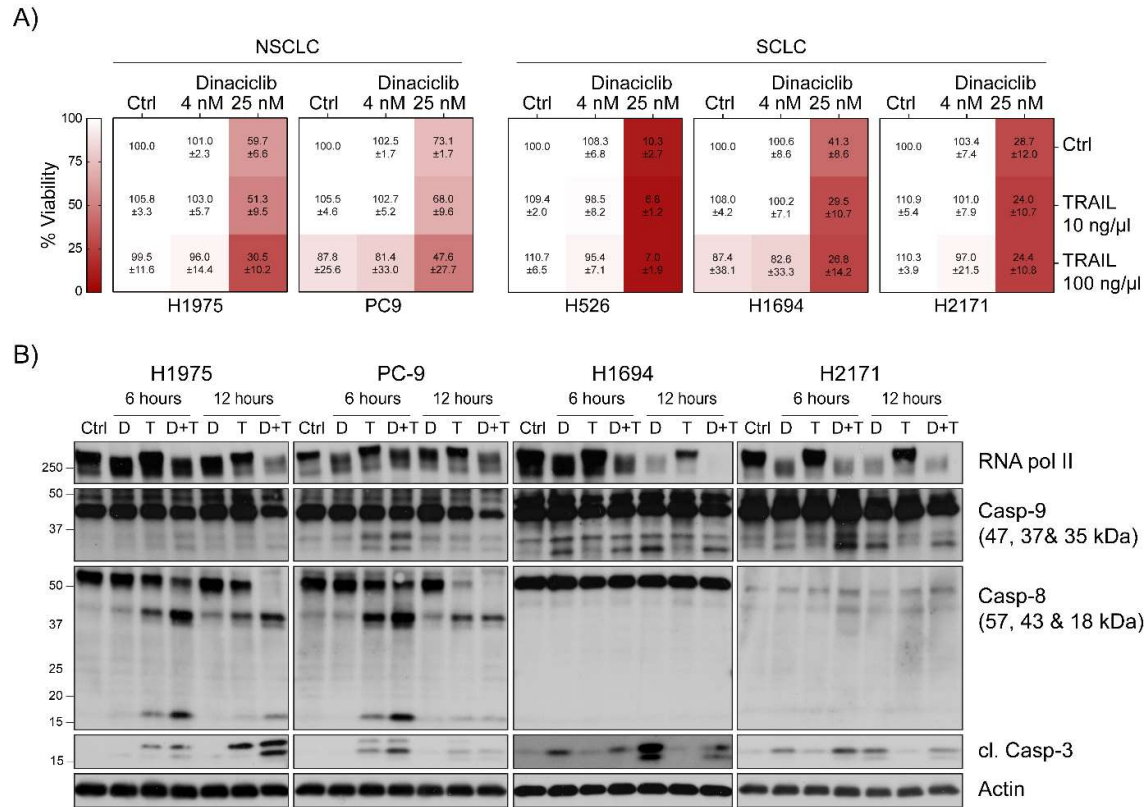


Figure 11. A) Viability, as measured by CTG, expressed as a percentage of the untreated control (100%) after a 30-hour treatment with dinaciclib (4 nM, 20 nM) and TRAIL (10 ng/μl, 100 ng/μl). Mean + SD of at least 3 independent experiments. B) Cells were lysed with RIPA buffer after 6 and 12 hours of treatment with 50 nM dinaciclib and/or 100 ng/μl of TRAIL. Representative blots of 3 independent experiments. *Adapted from Valdez Capuccino et al. CDDis, 2024.*

To evaluate the potential synergy between dinaciclib and standard-of-care chemotherapy, we treated SCLC cells with dinaciclib in combination with cisplatin and etoposide. Co-treatment at a fixed concentration of cisplatin and etoposide with varying doses of dinaciclib, and vice versa, revealed no synergistic or additive effect within the tested concentration range (Fig. 12a-d). Among the human cell lines tested, H2171 exhibited increased tolerance to cisplatin and etoposide, requiring higher doses of chemotherapeutic agents to achieve reductions in viability comparable to the other cell lines tested. However, its response to dinaciclib was consistent with other SCLC cell lines (Fig. 6b).

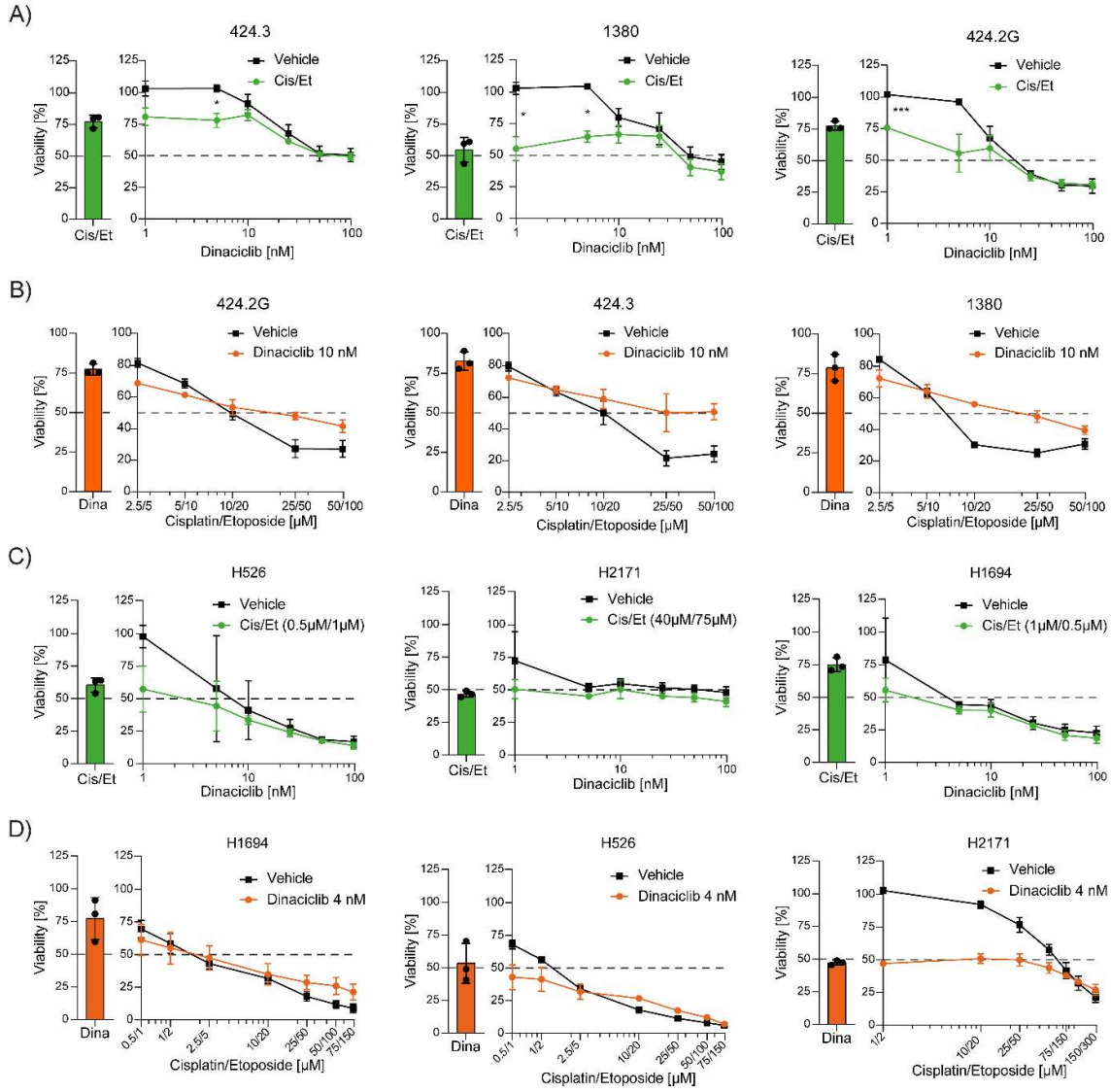


Figure 12. A) Mouse SCLC cells were treated with increasing doses of dinaciclib (1, 5, 10, 25, 50 and 100 nM) for 30 hours in the presence or absence of a combination of cisplatin (5  $\mu$ M) and etoposide (10  $\mu$ M). Mean + SD, n=3. B) Mouse SCLC cells were treated with increasing doses of cisplatin and etoposide for 30 hours in the presence or absence of 10 nM dinaciclib. Mean + SD, n=3. C) Human cell lines were treated with increasing doses of dinaciclib (1, 5, 10, 25, 50 and 100 nM) for 30 hours in the presence or absence of a combination of cisplatin and etoposide. H526: Cis 0.5  $\mu$ M, Et 1  $\mu$ M. H1694: Cis 1  $\mu$ M, Et 0.5  $\mu$ M. H2171: Cis 40  $\mu$ M, Et 75  $\mu$ M. Mean + SD, n=3. Viability was measured by CTG and expressed as a percentage of the viability of control. D) Human cell lines were treated with increasing doses of cisplatin and etoposide for 30 hours in the presence or absence of 4 nM dinaciclib. Mean + SD, n=3. Adapted from Valdez Capuccino et al. *CDDs*, 2024.

Next, we assessed the kinetics of caspase cascade kinetics downstream of mitochondrial damage following dinaciclib alone or in combination with chemotherapy (cisplatin and etoposide). Immunoblotting showed enhanced activation of caspase-9 and caspase-3 as early as 6 hours of dinaciclib treatment, albeit with lower activation in chemotherapy treatment alone (Fig. 13a). Interestingly, the combination of dinaciclib

and chemotherapy increased the activation of these caspases at 6 hours. However, this increase in caspase cleavage was no longer observed at later time points. Additionally, although the triple combination showed higher caspase activity at 6 hours than that of the single agents, there was no accelerated kinetics of cell death compared to dinaciclib alone (Fig. 13b). This was consistent with comparable levels of PARP cleavage between cells treated with dinaciclib or the triple combination at early and late time points (Fig. 13a). Further investigation into the potential additive effect of the CDK9 specific inhibitor NVP-2 and chemotherapy yielded no further decrease in viability upon combination in SCLC cells (Fig. 13c), as observed with dinaciclib.

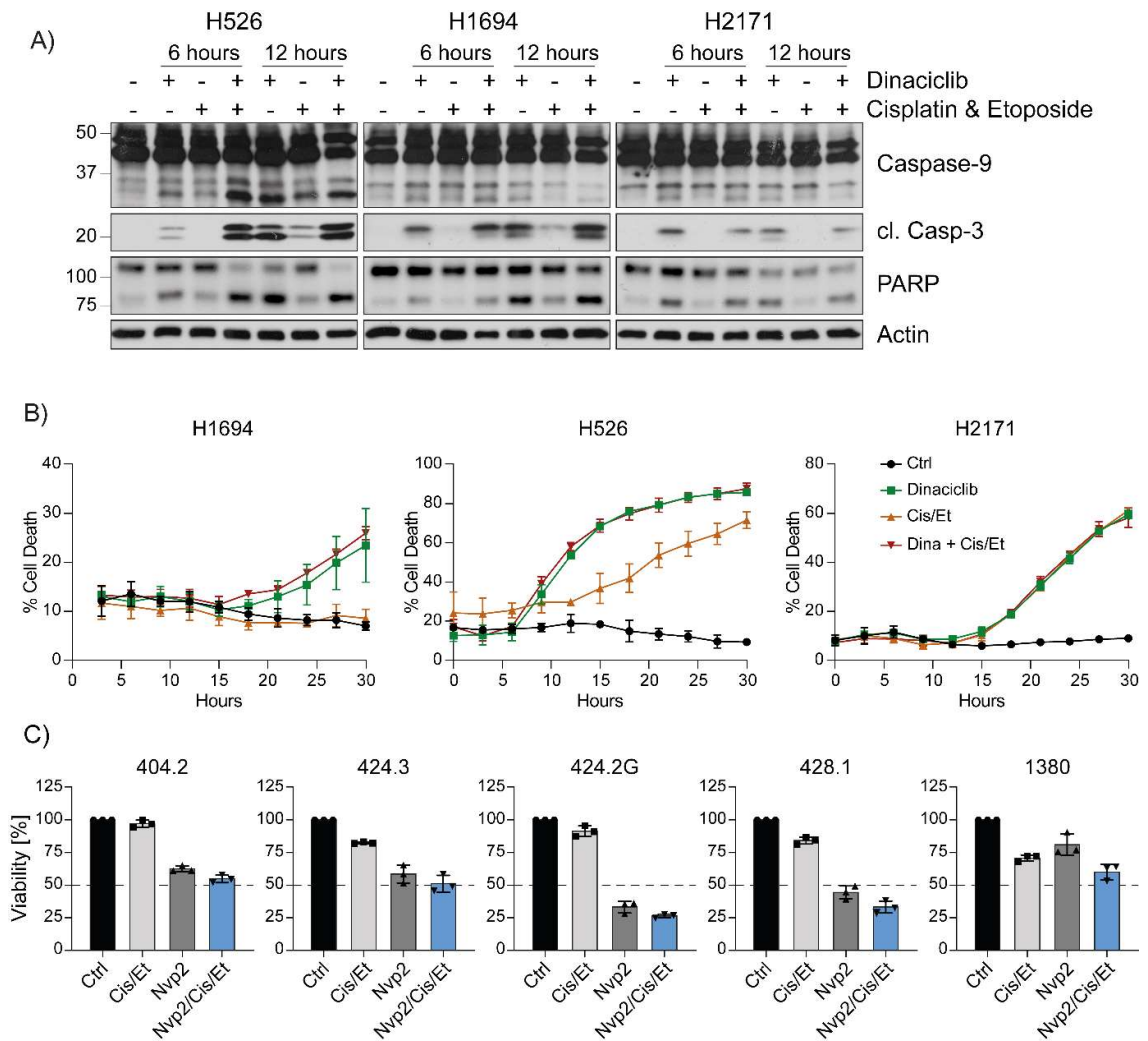


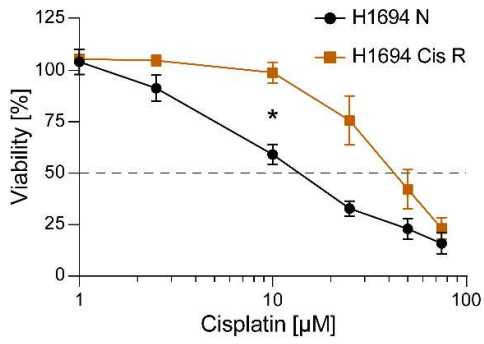
Figure 13. A) SCLC cells were lysed with RIPA buffer after 6 and 12 hours of treatment with either 25 nM dinaciclib and/or cisplatin and etoposide. H526 & H1694: Cis 20  $\mu$ M, Et 50  $\mu$ M. H2171: Cis 40  $\mu$ M, Et 100  $\mu$ M. Representative blots of 3 independent experiments. Cis = cisplatin, Et = etoposide. cl. = cleaved. B) Percentage of PI-positive cells as measured by Incucyte after treatment with 25 nM dinaciclib and/or cisplatin & etoposide. H526 & H1694: Cis

1.25  $\mu$ M, Et 3.125  $\mu$ M. H2171: Cis 40  $\mu$ M, Et 100  $\mu$ M. Mean + SD. Representative graphs of 3 independent experiments. C) Mouse SCLC cells were treated with 25 nM NVP-2, 5  $\mu$ M cisplatin and/or 10  $\mu$ M etoposide for 30 hours. Viability was measured by CTG and expressed as a percentage of the viability of control. Mean + SD, n=3. Adapted from Valdez Capuccino et al. *CDDis*, 2024.

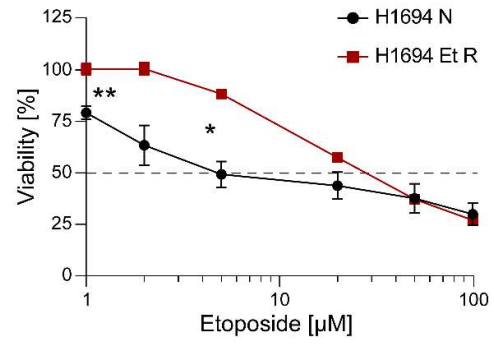
Given the high killing activity of dinaciclib alone, we assessed its efficacy in cells rendered resistant to chemotherapy through chronic exposure. H1694 cells cultured with increasing doses of cisplatin or etoposide over time developed tolerance to 4 and 3  $\mu$ M of the drug, respectively. We corroborated this acquired resistance by treating the cells with different doses of the chemotherapy agents (Fig. 14a,b). Exposing the resistant cells to dinaciclib showed comparable sensitivity to the inhibitor as the naïve parental cell line (Fig. 14c). Furthermore, there was no synergism observed between dinaciclib and cisplatin or etoposide in the corresponding resistant cells (Fig. 14d-g).



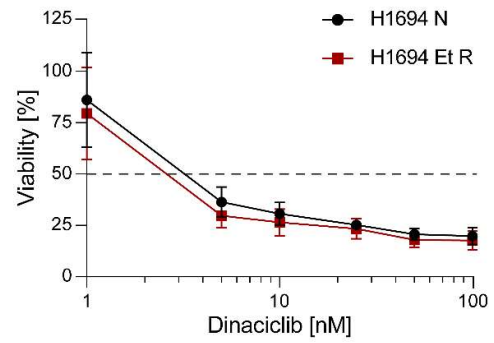
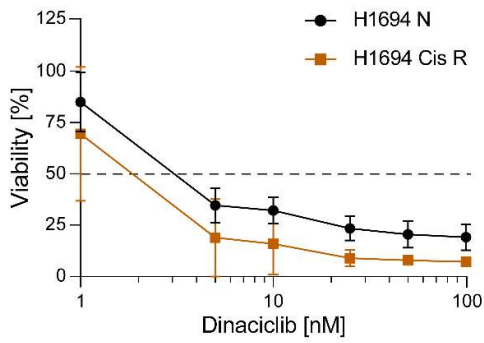
A)



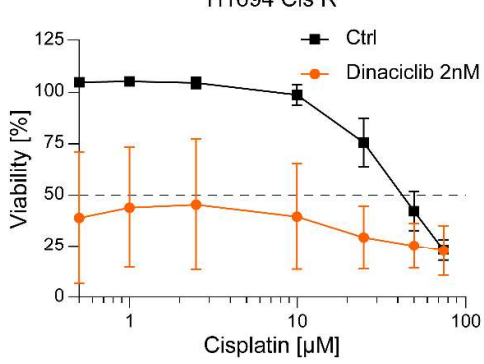
B)



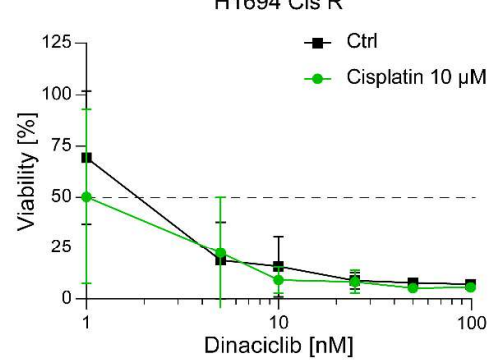
C)



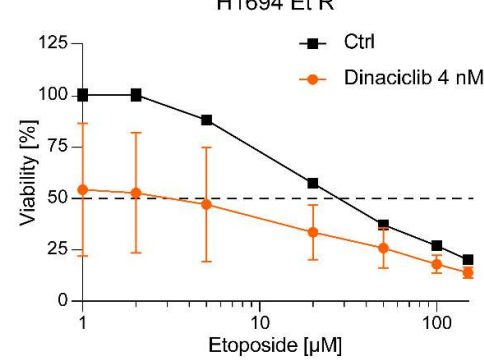
D)



E)



F)



G)

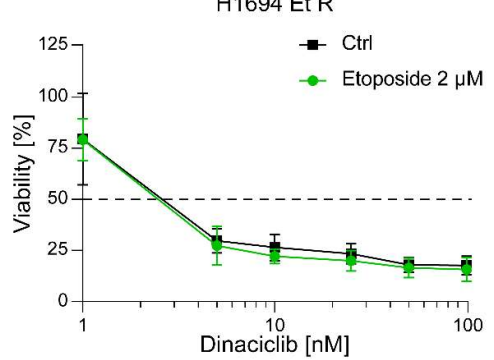


Figure 14. A) SCLC cells with acquired resistance to cisplatin (Cis R) and the naïve parental cell line (N) were treated with increasing doses of cisplatin (0.5, 1, 2.5, 10, 25, 50 and 75  $\mu$ M) for 30 hours. Mean + SD, n=3. B) SCLC cells with acquired resistance to etoposide (Et R) and the naïve parental cell line (N) were treated with increasing doses of etoposide (1, 2, 5, 20, 50 and 100  $\mu$ M) for 30 hours. C) Resistant and naïve cell lines were treated for 30 hours with increasing doses of dinaciclib (1, 5, 10, 25, 50 and 100). Mean + SD, n=3. Viability was measured by CTG and expressed as a percentage of the viability of control. Two-way ANOVA with Geisser-Greenhouse correction. \* = p-adj<0.05, \*\* = p-adj<0.01. D) and E) SCLC cells with acquired resistance to cisplatin (Cis R) were treated with increasing doses of cisplatin (0.5, 1, 2.5, 10, 25, 50 and 75  $\mu$ M) for 30 hours with or without dinaciclib 2nM (D), or increasing doses of dinaciclib (1, 5, 10, 25, 50, and 100 nM) with or without cisplatin 10  $\mu$ M (E). F) and G) SCLC cells with acquired resistance to etoposide (Et R) were treated with increasing doses of etoposide (1, 2, 5, 20, 50 and 100  $\mu$ M) for 30 hours with or without dinaciclib 4nM (F), or increasing doses of dinaciclib (1, 5, 10, 25, 50, and 100 nM) with or without etoposide 2  $\mu$ M (G). Viability was measured by CTG and expressed as a percentage of the viability of control. Mean + SD, n=3. Adapted from Valdez Capuccino et al. *CDDis*, 2024.

In summary, while dinaciclib treatment did not synergise with TRAIL or chemotherapy, it effectively targeted chemo-resistant cells, potentially offering an alternative therapeutic approach in cases where this resistance arises.

## 1.5.4 Evaluating a novel and specific CDK9 inhibitor

To understand if CDK9 inhibition is responsible for the killing capacity of dinaciclib, we used a novel inhibitor, VC-1, that specifically inhibits CDK9 but not other CDKs (Fig. 15a). This molecule was designed to target the hinge region of the kinase, which is responsible for binding to ATP. The affinity and specificity of VC-1 to CDK9 were determined by the collaborators that generated the compound as follows: VC-1 binding affinity to CDK9 was assessed using a competitive fluorescence polarization assay, which showed an IC<sub>50</sub> of 7 nM (174). To further evaluate the selectivity of VC-1, they utilized a radiometric profiling assay against a panel of 16 CDK/Cyclin pairs. This analysis revealed high specificity, with only the CDK9/CyclinT1 complex demonstrating significant inhibition and a high affinity compared to 15 other CDK-cyclin pairs (174).

We then evaluated the cytotoxic effects of VC-1 in both mouse and human SCLC cells. Consistent with our observations with dinaciclib, VC-1 induced a dose-dependent reduction in viability in both normal SCLC cells and chemotherapy-resistant cell lines (Fig. 15b, c). Furthermore, VC-1-induced cell death was prevented by caspase inhibition (Fig. 15d) and had no effect on the cell cycle of the cells (Fig. 10e). Immunoblotting revealed that VC-1 treatment led to a marked decrease in both total and phosphorylated RNA pol II, alongside reductions in cFLIP, MCL-1, and BCL-xL levels (Fig. 15e). Moreover, increased cleavage of caspase-3 and PARP was observed

in all cell lines except for H2171, which exhibited only a slight increase in active caspase 3 and cleaved PARP. This goes in line with the viability results from Fig. 15c, where we observe H2171 maintained higher viability compared to other cell lines at the tested concentration (1  $\mu$ M of VC-1).

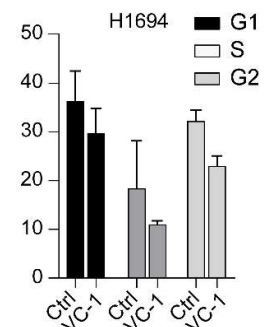
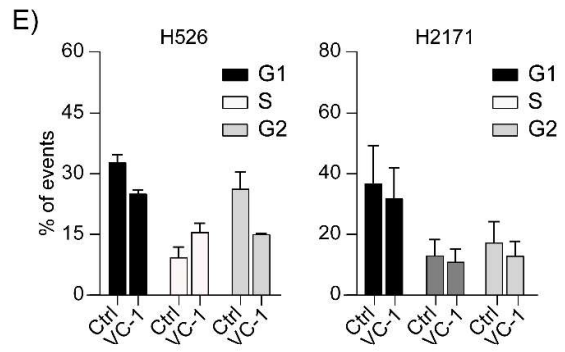
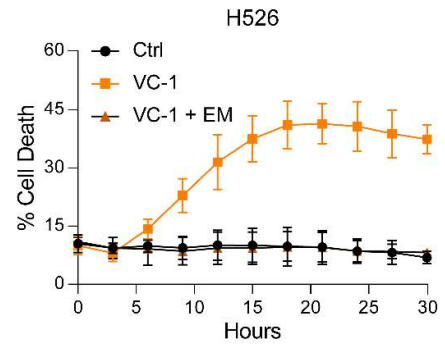
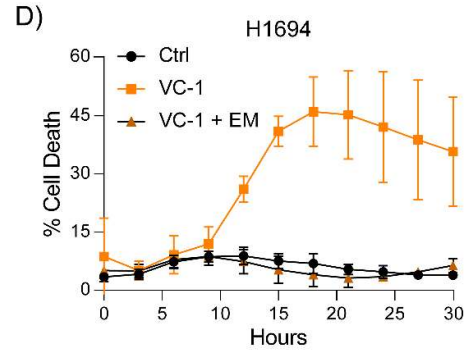
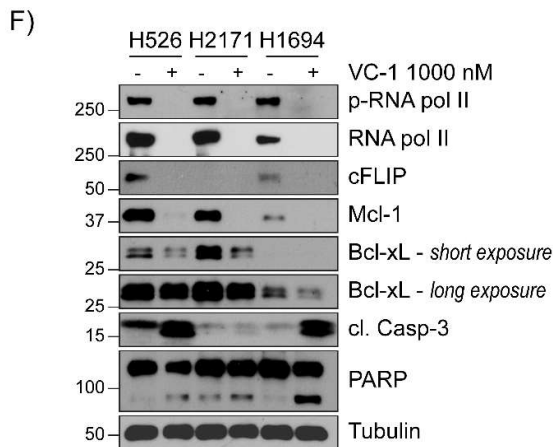
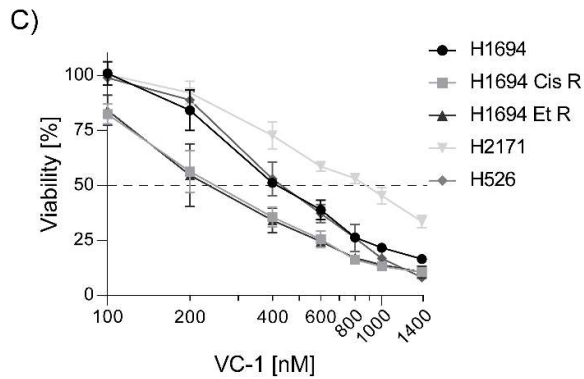
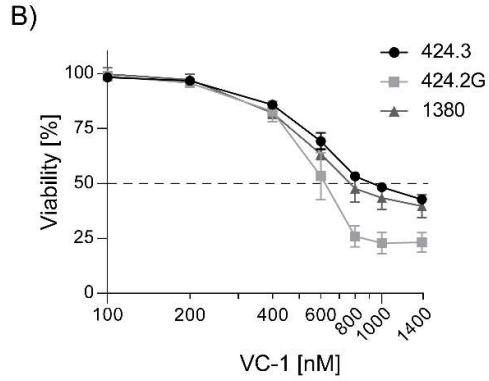
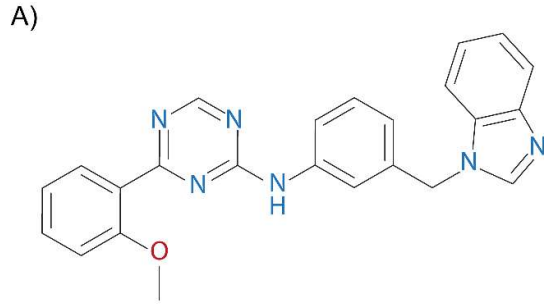


Figure 15. A) Chemical structure of the compound VC-1. B) and C) Viability was measured by CTG and expressed as a percentage of the viability of Control after a 30-hour treatment with different concentrations of VC-1 (100, 200, 400, 600, 800, 1 000 and 1 400 nM) Mean + SD, n=3. D) Percentage of PI-positive cells after treatment with 1 000 nM VC-1 and 5  $\mu$ M emricasan (EM) as measured by Incucyte. Mean + SD, n=3. E) Cell cycle distribution was assessed by permeabilising the cells and staining with PI after 24 hours of treatment with 1  $\mu$ M of VC-1. Mean +SD, n=3 F) Human SCLC cells were lysed with RIPA buffer after 18 hours of treatment with 1 000 nM VC-1 or vehicle. Representative blots of 2 independent experiments. *Adapted from Valdez Capuccino et al. CDDis, 2024.*

Notably, SCLC cell lines displayed greater sensitivity to VC-1 treatment compared to NSCLC cells (Fig. 16a), mirroring our findings with dinaciclib. This remained true when expanding the panel of SCLC and NSCLC cell lines, as evidenced by their lower IC50 values (Fig. 16b). These results show that VC-1 efficiently inhibits CDK9 and triggers apoptosis in SCLC cells.

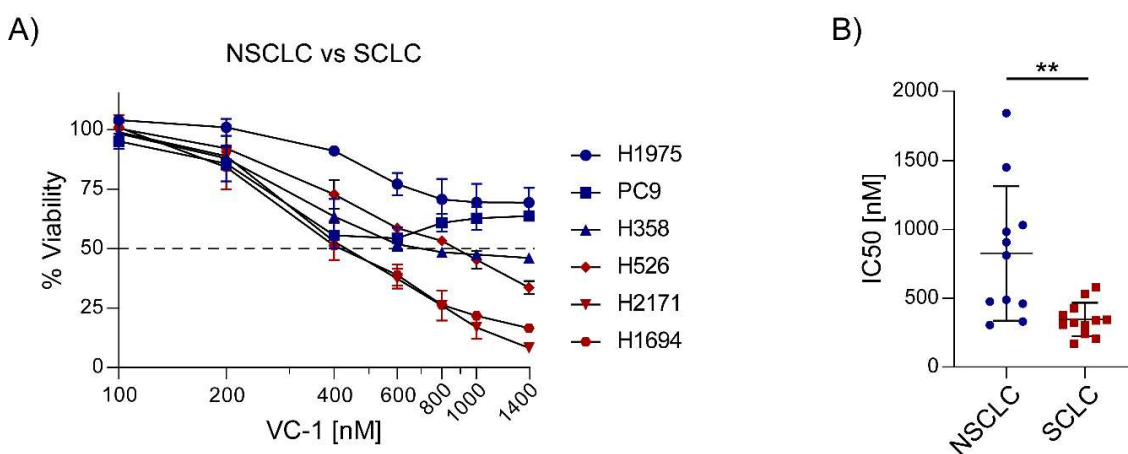


Figure 16. A) Viability was measured by CTG and expressed as a percentage of the viability of Control after a 30-hour treatment with different concentrations of VC-1 (100, 200, 400, 600, 800, 1 000 and 1 400 nM). Mean + SD, n=3. B) IC50 [ $\mu$ M] of twelve SCLC and eleven NSCLC human cell lines after 72 hours of treatment with VC-1. Unpaired t-test NSCLC vs. SCLC  $**p=0.0034$ . *Adapted from Valdez Capuccino et al. CDDis, 2024.*

## 1.5.5 Inhibition of CDK9 reduced tumour growth and extended survival of mice.

Next, we sought to assess the effectiveness of CDK9 inhibition in vivo using a syngeneic subcutaneous model. We chose dinaciclib, as it has been extensively evaluated in clinical trials and is closer to clinical application than other counterparts (175-178), including VC-1. Given the comparable efficacy of CDK9 inhibition with and without chemotherapy observed earlier, we evaluated dinaciclib as a potential single treatment. To this end, we subcutaneously injected mouse-derived SCLC cells in the

flank of C57BL/6 and initiated treatment once palpable tumours were detected until reaching the defined endpoint size. This experimental setup would allow us to determine whether dinaciclib treatment impacts the survival of mice. We tested two cell lines, 1380 and 424.3, and found that dinaciclib treatment led to delayed tumour growth (Fig. 17a, c) and improved survival (Fig. 17b, d) compared to vehicle controls. Of note, mice injected with cell line 424.3 exhibited ulcerations, prompting the premature termination of the experiment (Fig. 17a, b). Importantly, no significant changes in body weight were observed between vehicle and dinaciclib-injected mice (Fig. 17e, f).

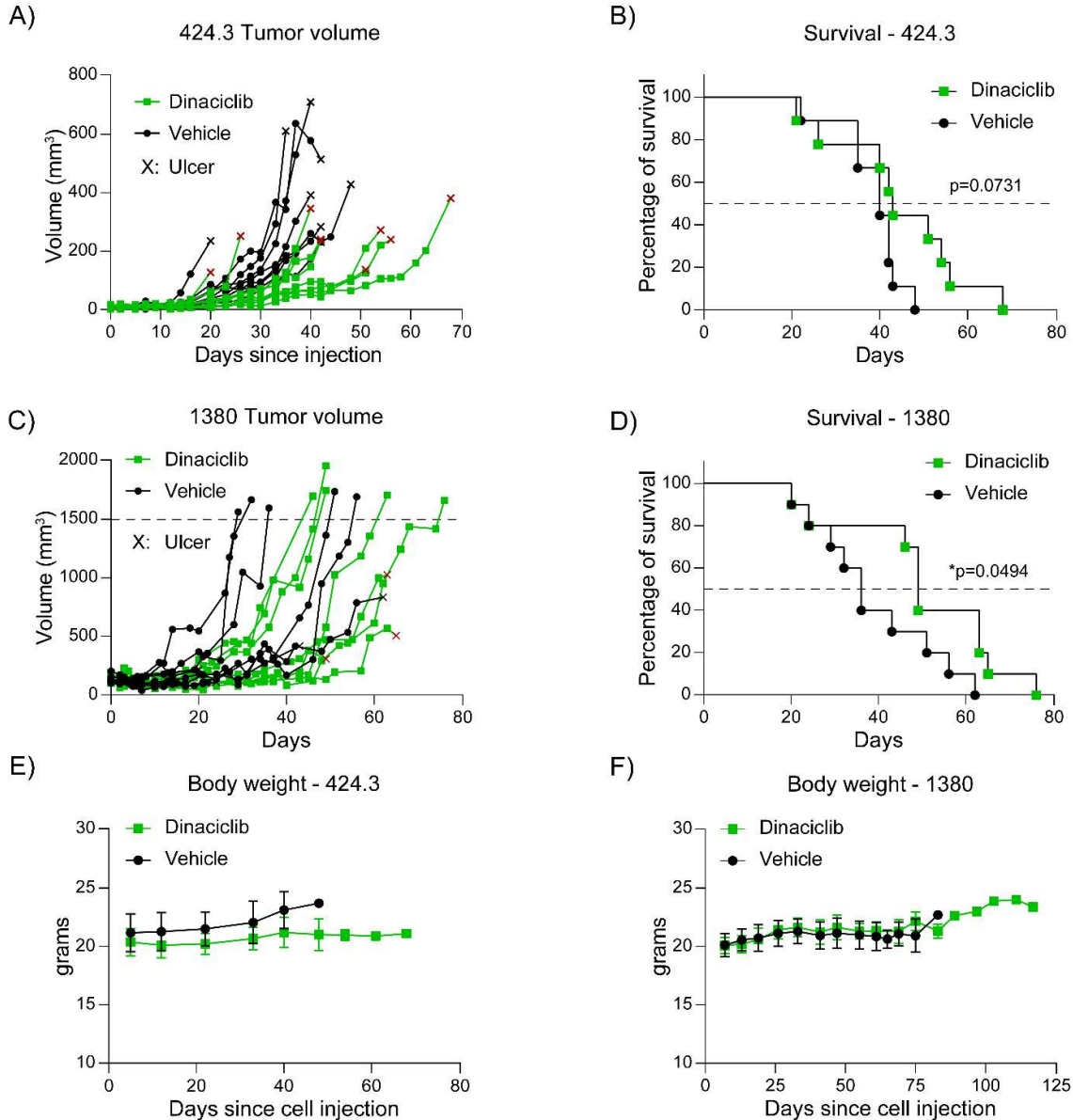


Figure 17. A) 424.3 mouse cells were injected subcutaneously on the flank of C57BL/6 mice. Treatment began 16 days after injection with either dinaciclib (20mg/kg) or vehicle (10% Hydroxypropyl Beta Cyclodextrin) twice per week, followed by a week of drug holiday. Tumours were measured three times a week. N=9 per group. B) Survival curve of mice from (A). Log-rank (Mantel-Cox) test. C) 1380 mouse cells were injected subcutaneously on the flank of C57BL/6 mice. Treatment began upon tumour establishment with either dinaciclib (30mg/kg) or vehicle. Tumours were measured two times a week. N=10 per group. D) Survival curve of mice from (C). Log-rank (Mantel-Cox) test. \*p = 0.0494. E) Weight of mice from (A & B). Mean + SD. E) Weight of mice from (C & D) since injection with 1380 cells. Mean + SD. Adapted from Valdez Capuccino et al. *CDDis*, 2024.

To further bolster the preclinical rationale for the efficacy of dinaciclib treatment, we evaluated its anti-tumour properties in the well-established autochthonous RP-SCLC model. Briefly, genetically modified RP mice (Rb1<sup>fllox/fllox</sup>; Trp53<sup>fllox/fllox</sup>) were subjected to inhalation of non-replicative Cre-expressing Adenovirus, which induces the deletion of

Rb1 and Trp53 and the formation of SCLC as a consequence (131). Encouragingly, dinaciclib treatment significantly prolonged survival and reduced tumour burden, as confirmed by MRI scan assessment (Fig. 18a-c).

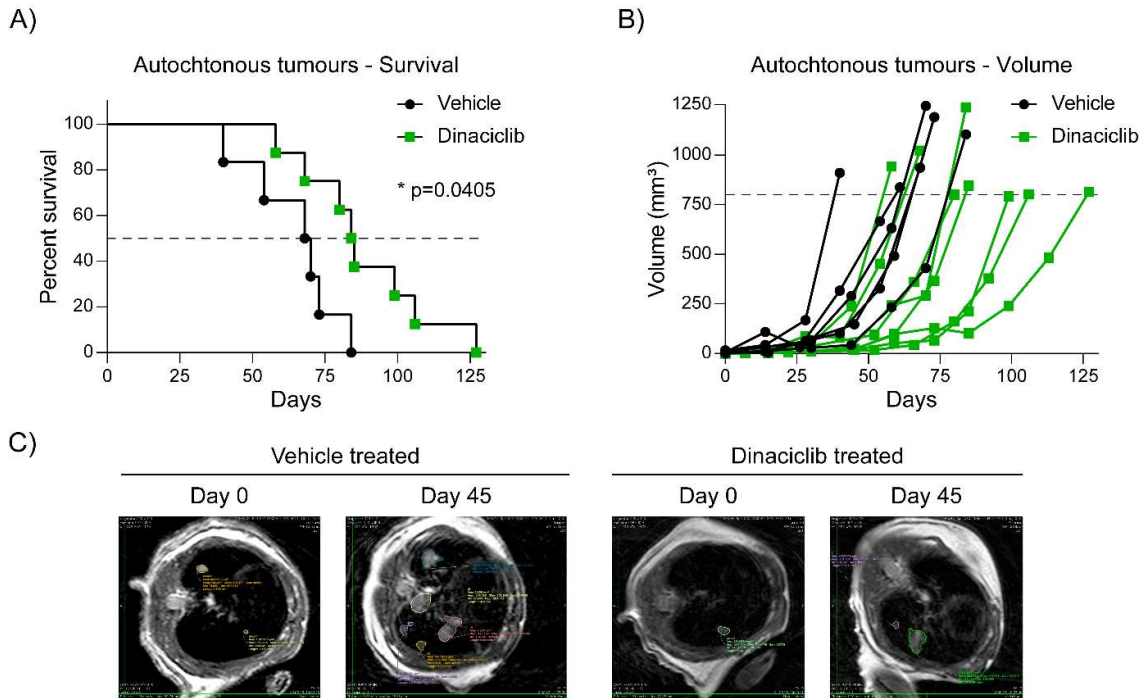


Figure 18. A) Survival curve for tumour-bearing mice treated with dinaciclib. Log-rank (Mantel-Cox) test.  $*p = 0.0405$ . Treatment began upon tumour establishment with either dinaciclib (30mg/kg) or vehicle (10% Hydroxypropyl Beta Cyclodextrin) twice per week, followed by a week of drug holiday until endpoint criteria were met (tumour volume  $>800\text{mm}^3$ ). Tumours were measured every 14 days. Vehicle treated  $N=6$ , dinaciclib treated  $N=8$ . B) Volume of autochthonous SCLC tumours as measured by MRI and the Horus software. C) Representative images of MRI scans of vehicle and dinaciclib-treated mice since tumour volume reached  $>1\text{mm}^3$  and 45 days after. Adapted from Valdez Capuccino et al. *CDDis*, 2024.

We next investigated the potential of the VC-1 inhibitor as an anti-tumour agent *in vivo* as a proof of concept for its potential clinical application. Firstly, we assessed the toxicity of the drug upon chronic or acute administration. Encouragingly, our findings revealed that VC-1 exhibited no adverse effects in mice, as evidenced by its negligible impact on liver or body weight (Fig. 19a, b). With the safety of VC-1 confirmed, we proceeded to evaluate its anti-tumour efficacy in a syngeneic subcutaneous model, this time for a defined time period. This particular set-up, now optimized for tumour engraftment, allowed us to assess whether VC-1 has a similar anti-tumour activity as dinaciclib. Remarkably, three weeks of VC-1 treatment led to a significant reduction in tumour growth, comparable to the anti-tumour effect observed with dinaciclib (Fig. 19c,



d). Throughout the experiment, there were no differences in body weight among the different treatment groups (Fig. 19e). Therefore, our findings suggest that CDK9 inhibition, by treatment with either dinaciclib or VC-1, reduces SCLC tumour growth and improves survival of tumour-bearing mice. Furthermore, both drugs, particularly VC-1, are well tolerated *in vivo*.

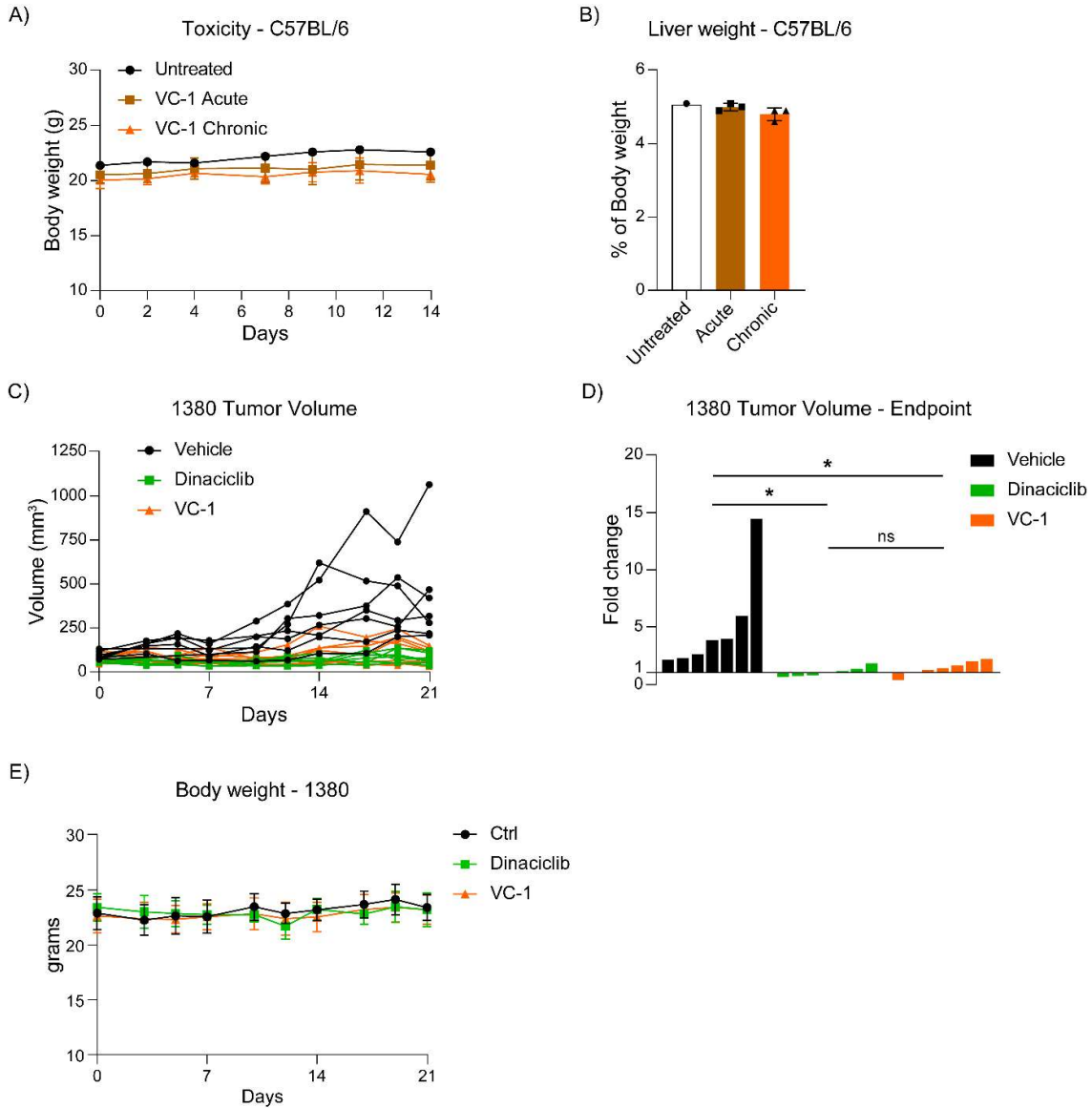


Figure 19. A) Weight of C57BL/6 mice treated with a single i.p. injection of 40mg/kg of VC-1 (Acute) or three injections per week of 20mg/kg (Chronic). B) Percentage of liver weight with respect to the body weight of each mouse on day 14 of (A). C) 1380 cells were injected subcutaneously on the flank of C57BL/6 mice. Treatment consisted of either VC-1 (20mg/kg), dinaciclib (30mg/kg) or vehicle (10% Hydroxypropyl Beta Cyclodextrin) three times per week (VC-1) or twice per week, followed by a week of drug holiday (dinaciclib). Tumours were measured three times per week. N=7 for each group. D) Individual tumour volumes of (C) at day 21 expressed as fold change from day 0. One-way ANOVA, Dunnet's multiple comparison test. \*p-adj. < 0.05. E) Body weight of mice from (C)

since the first day of treatment. Mean + SD. Experiments conducted by collaborator AG Tovari. *Adapted from Valdez Capuccino et al. CDDis, 2024.*

## 1.5.6 The Anti-tumour effect of CDK9 inhibition is dependent on the adaptive immune system.

In Figure 19, we clearly observe the anti-tumour effect of CDK9 inhibition in a syngeneic subcutaneous mouse model. We conducted another *in vivo* subcutaneous experiment using human SCLC cell lines to investigate further whether dinaciclib also reduces tumour growth in a human setting. For this experiment, we utilized NOD-SCID mice, whose mutational background prevents the development of NK, B, and T cells (179). The immunocompromised mice also allow us to understand whether the *in vivo* anti-tumour effect of CDK9 inhibition requires the immune compartment. Human cells were injected into the flanks of the mice, and upon tumour establishment (volume 50-100 mm<sup>3</sup>), treatment commenced and concluded as described in the previous experiment.

Interestingly, no tumour growth inhibition was observed in these immunocompromised mice (Fig. 20a, b). Treatment with either dinaciclib or VC-1 did not affect the weight of NOD-SCID mice (Fig. 20c). The lack of difference between the vehicle and treated tumours suggests a significant contribution of the immune system to the *in vivo* anti-tumoral effect of CDK9 inhibition and warrants further investigation.

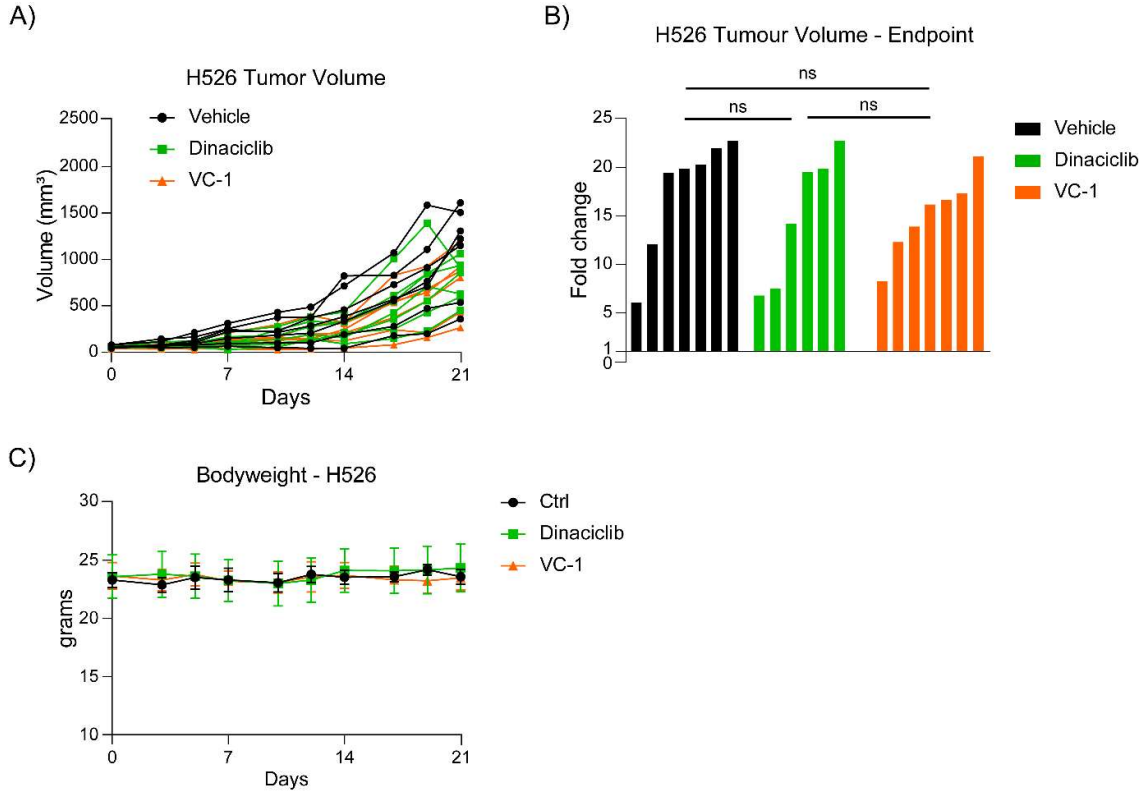


Figure 20. A) H526 cells were injected subcutaneously on the flank of NOD-SCID mice. Treatment consisted of either VC-1 (20mg/kg), dinaciclib (30mg/kg) or vehicle (10% Hydroxypropyl Beta Cyclodextrin) three times per week (VC-1) or twice per week, followed by a week of drug holiday (dinaciclib). Tumours were measured three times per week. N=7 for each group. B) Individual tumour volumes of (A) at day 21 expressed as fold change from day 0. One-way ANOVA, Dunnet's multiple comparison test. \*p-adj. < 0.05. C) Body weight of mice from (A) since the first day of treatment. Mean + SD.

Overall, our results clearly show that CDK9 inhibition is a valid approach to kill SCLC cells. The inhibitor dinaciclib primes SCLC cells to death while also inducing caspase-dependent cell death in SCLC cells *in vitro*. CDK9 inhibition also reduced tumour growth and improved the survival of tumour-bearing mice, with strong evidence for a critical role for the immune system in this anti-tumour activity.

## 1.6 Discussion

### 1.6.1 CDK9 inhibition in the treatment of SCLC

In an effort to offer alternative treatments, we assessed the efficacy of dinaciclib and VC-1 as promising anti-tumour agents. The results align with multiple studies reporting that the cell death induced by dinaciclib is mainly due to the decrease of antiapoptotic proteins in malignant cells (166, 180-182). Here, we show that CDK9 inhibition is very effective against SCLC. We also demonstrated that the cell death induced by dinaciclib and VC-1 is caspase-dependent, and dinaciclib does so by inducing caspase 9 activation. It is a valid concern whether the readout we observe is due to an inhibition of cell growth, as the Celltiter Glo kit estimates viability as a direct measure of the ATP present in the cells, meaning that what we read as a reduction in viability can be due to cell death or cell cycle arrest. However, our results did not show any significant alterations to the cell cycle upon the treatments (Fig. 7d, Fig. 15e). Moreover, the increase in Caspase 9 and 3 cleavage are a clear indication that the treatments are activating the mitochondrial apoptotic pathway. These results clearly indicate that CDK9 inhibition efficiently kills SCLC cells without major changes in the cell cycle.

We consistently observed a lower sensitivity to CDK9 inhibition from NSCLC when comparing them to SCLC cells. To understand this difference, we analysed the activation of caspases after dinaciclib treatment by immunoblotting the protein content of both SCLC and NSCLC cells. We used a combination of TRAIL + dinaciclib as a positive control of caspase 8 cleavage, as the co-treatment has been shown to activate extrinsic apoptosis consistently (161, 162, 171). In NSCLC cells, the positive control worked as expected. Strikingly, our results showed no activation of the extrinsic pathway in SCLC cells. In contrast, dinaciclib alone did not engage in apoptosis in the first 12 hours of treatment in NSCLC cells, contrary to what we have seen with SCLC cells. This differential pathway activation drove us to look deeper into the possible cause, for which we turned to dynamic BH3 profiling (DBP). The results showed us that the difference in the response to dinaciclib is due to the inability of the drug to prime NSCLC cells to death, and the inherent capacity of these tumour cells to undergo an “apoptotic adaptation” upon treatment. This adaptation prevents dinaciclib

from activating the intrinsic apoptotic pathway, likely by overexpressing Bcl-2 family proteins, but the inhibition of CDK9 sensitises NSCLC to the death receptor pathway by reducing the levels of FLIP (161, 162, 171). This explains why dinaciclib treatment alone is not as efficient in NSCLC as in SCLC, but the combination with TRAIL is effective. We also show that SCLC cells do become primed for cell death upon dinaciclib treatment and are unable to adapt to it. The lack of response to TRAIL and its combination with dinaciclib can be explained by the basally low expression of Caspase 8, although other death-receptor agonists could be tested. It has been shown that TRAIL doesn't activate cell death in SCLC cells and, on the contrary, induces cell proliferation (183). This was shown to be dependent on the Death receptor 5 (DR5), also known as TRAIL Receptor 2 (TRAIL-R2), and the low expression of caspase 8. Interestingly, IFN-gamma treatment induced the expression of caspase 8 and led to apoptosis upon TRAIL. One could think of a possible treatment where IFN-gamma is given prior to a CDK9 inhibitor and TRAIL, maximizing the killing potential of these agents. Altogether, we now understand more in terms of the different responses of NSCLC and SCLC cells to CDK9 inhibition, although the root of the difference is yet unclear.

We present dinaciclib as a possible alternative to the standard of care treatment when resistance arises. The first-line treatment for SCLC has changed little in the past 30 years, with the FDA approving the PD-L1 inhibitor atezolizumab 6 years ago. However, clinical trials with this Immune Checkpoint Inhibitor (ICI) along with standard-of-care chemotherapy only led to an increase in overall survival of 2 months (149, 184). We tested the combination of dinaciclib with the first-line chemotherapy agents, finding no interaction between the drugs *in vitro*. Delving deeper, we saw that the kinetics of caspase 9 cleavage was faster in the triple combination in one of the cell lines, but the activity of caspase 3 (assessed by PARP cleavage) becomes equivalent as time progresses. Nonetheless, we believe that the complete first-line treatment of chemotherapy and ICI in combination with CDK9 inhibition is worth researching. We propose that by combining it with dinaciclib, SCLC patients could benefit from this multi-component treatment regimen. The suggestion stems from the different results observed in Figures 19 and 20, where SCLC cells injected in C57BL/6 mice showed a good response to CDK9 inhibition, whereas SCLC cells injected in

immunocompromised mice had no response at all. This is a strong indicator of the important role played by the immune system in CDK9 treatment. One obvious question would be why the killing effect we observe *in vitro*, with absent immune cells, does not translate *in vivo*. We must look at dinaciclib pharmacokinetics studies to answer this. The work performed by Nemunaitis et al. shows that the concentrations of dinaciclib in the plasma of patients after a 2-hour intravenous (IV) administration of the drug at a 14 mg/m<sup>2</sup> dose decrease rapidly from ~2000, 200 and 100 nM at 2, 4 and 6 hours, respectively, since starting the infusion (185). By comparison, the work performed by Booher et al. in mice shows that after a 40 mg/kg i.p. injection of dinaciclib, plasma levels in mice are ~330, 65 and 30 nM at 2, 4 and 6 hours, respectively (166). As seen in Figure 13, 6 hours only begins to activate caspase 3 in human SCLC cells, not reaching full-fledged activation until at least 12 hours. Not only that but in Figure 13, no cell line shows advanced cell death at 6 hours. These results suggest that while dinaciclib does not massively activate cell death in SCLC tumours, it is both killing enough cancer cells to recruit immune cells and priming the cancer cells to die by the hand of the immune system. This conclusion goes in line with previous studies showing that dinaciclib treatment induces the expression of type I interferon (IFN) response genes and the release of damage-associated molecular patterns (DAMPs) from tumour cells (165, 186). These events play a crucial role in immune recruitment and recognition. Indeed, *in vivo* studies with combined dinaciclib/PD-1 therapy in triple-negative breast and colorectal cancers have shown increased infiltration and activation of CD8+ T and dendritic cells (165, 186). Therefore, it would be exciting to investigate the possible synergy between CDK9 inhibition and ICI in SCLC.

The concept of combining dinaciclib with specific inhibitors has been proposed before, also in SCLC cells, where co-treatment of dinaciclib with the BCL-2, BCL-xL, and BCL-w inhibitor Navitoclax was found to exhibit synergistic effects (166). The combined impact of reducing MCL-1 levels by dinaciclib alongside the inhibition of the remaining members of the BCL-2 family by Navitoclax has proven highly effective in SCLC. This efficacy stems from the known dependence of SCLC cell lines on BCL-2, BCL-xL, or MCL-1 for survival (181). However, our observations indicate a lack of synergism with drugs that induce DNA damage (e.g., cisplatin, etoposide) and activate apoptosis through BCL-2 family members. This discrepancy may be attributed to the loss of P53

in SCLC, which alters the cellular response to DNA damage. Furthermore, the absence of synergy can also be explained by the fact that both therapies exclusively activate mitochondrial apoptosis in SCLC, characterized by robust early cleavage of caspase-9 and -3, with no activation of caspase-8. The elevated apoptosis priming observed in SCLC cells upon dinaciclib treatment alone might further contribute to the lack of synergy with chemotherapy, as both treatments fully engage apoptosis in these cells. Consequently, it is conceivable that dinaciclib treatment saturates the apoptotic response, and based on inefficient apoptotic adaptation in certain SCLC cell lines, there is no additional sensitization upon treatment with agents targeting mitochondrial cell death. However, this conclusion does not go in line with studies demonstrating a synergistic effect between dinaciclib and Navitoclax, as discussed earlier. The variability in response observed between different SCLC cell lines could indeed be attributed to the diverse characteristics of these cell lines. It is evident from our findings, and that of others (166), that not all SCLC cell lines exhibit equivalent responses to dinaciclib or show similar apoptotic adaptation. Specifically, our results indicate that while SCLC cells generally display lower overall adaptation compared to NSCLC, H526 SCLC cells exhibit slight yet statistically significant sensitivity to BH3 peptides, whereas H2171 cells do not. This underscores the necessity for personalized medicine approaches and emphasizes the importance of profiling tumour-derived cells for treatment stratification. Moreover, the study highlights a significant finding: dinaciclib demonstrates efficacy not only in eradicating treatment-naïve SCLC cells but also in targeting cells with intrinsic and acquired resistance to chemotherapy. This discovery holds particular significance because resistance to chemotherapy upon relapse represents a major challenge in SCLC treatment (121, 187). Studies suggest that transcriptional inhibitors can suppress the emergence of resistant cells when in combination with other therapeutic agents (188, 189). Therefore, our findings highlight the potential of dinaciclib as a promising therapeutic option for overcoming and possibly preventing chemotherapy resistance in SCLC patients.

Further acquired resistance to dinaciclib is a valid concern, and c-Myc overexpression has been proposed as a resistance mechanism to sustained CDK9 inhibition in different cancer cell lines, however, not including SCLC (190). Moreover, what the

authors refer to as “sustained” is a single 8-hour treatment with a CDK9 inhibitor, not a regimen where resistance to the treatment can properly arise. Furthermore, our results show changes in c-Myc at 18 hours of treatment in the mouse cell lines. C-Myc has 2 main isoforms, c-Myc1 (long isoform) and c-Myc2 (shorter isoform) (191). There is a decrease in the shorter isoform c-Myc2 and an increase in the long isoform c-Myc1 upon dinaciclib treatment in the mouse-derived SCLC cells (Fig. 7a). c-Myc2 promotes cell proliferation and colony formation and is thought to promote tumour growth through the activation of oncogenic pathways (192). In comparison, the longer isoform c-Myc1 inhibits cell growth when in high levels, and its loss is beneficial for tumour growth (192-194). We also analysed the levels of c-Myc in the human SCLC cell lines. However, only H2171 exhibited expression of c-MYC, which was lost entirely upon dinaciclib treatment (Fig. 7b). This last result goes in line with a previous study where dinaciclib treatment reduced c-MYC levels in aggressive MYC-driven lymphomas (180). Aberrant Myc expression is present in >70% of cancers and has been related to poor prognosis and aggressive tumour phenotypes (195-198). In SCLC, MYC family genes have been found to be amplified (121) and play a major role in driving tumour plasticity and evolution (137, 199, 200). A recent comprehensive whole-exome, genome and transcriptome sequencing study on patients at different time points before and after treatment revealed that first-line treatment clears the main, rapidly growing population of cancer cells that dominates the tumour prior to treatment and induces the expansion of a multitude of subclones with increased acquired mutations (138). This heterogeneity induced by first-line treatment shapes clinical relapse (138). Our data only brushes upon c-MYC changes upon dinaciclib treatment. However, knowing that dinaciclib abolishes c-MYC expression in SCLC cells, it would be extremely interesting to investigate whether MYC family proteins play a role in the post-treatment tumoral diversification observed by George et al. (138) and whether it can be prevented by CDK9 inhibition.

CDK7 is worth mentioning as it is required for the release of RNA pol II from the promoter during transcription, similar to CDK9 function within the P-TEFb (153). The CDK7/Cyclin H pair is part of the TFIIH complex, which phosphorylates Ser5 of the CTD of RNA pol II, releasing it from the Transcription Starting Site (TSS) (152). CDK7 inhibition has been tested in SCLC, where it showed potent killing activity both *in vitro*



and *in vivo* (201-203). Inhibition of CDK7 in combination with anti-PD-1 proved synergistic in SCLC, supporting the hypothesis that ICI therapies benefit from transcriptional initiation inhibition in this cancer.

In this study, we also characterise the anti-tumour activity of VC-1, a novel and highly specific CDK9 inhibitor. VC-1 demonstrated potent inhibition of SCLC cell viability, with IC<sub>50</sub> values in the nanomolar range. With an IC<sub>50</sub> against CDK9 of 7nM (174), VC-1 represents an effective and alternative tool to NVP-2 for investigating CDK9 inhibition. Moreover, its demonstrated anti-cancer activity *in vivo* positions VC-1 as an exciting candidate for SCLC treatment along with dinaciclib. We anticipate that the use of CDK9-specific inhibitors such as VC-1 may lead to fewer adverse effects resulting from the inhibition of other CDKs, such as is the case with dinaciclib and CDK1, 2, and 5 (175, 176, 204-207). However, it is necessary to acknowledge that while VC-1 may offer advantages in terms of specificity, it may not necessarily address the issue of resistance development to CDK9 inhibition, as the target region of CDK9 by VC-1 and dinaciclib is equivalent, meaning their main interactions with CDK9 are hydrogen bonds to the same amino acid (174).

The work conducted in this thesis sets the ground for the use of dinaciclib and CDK9 inhibitors in the treatment of SCLC, hopefully prolonging patients' survival. Follow-up studies should focus on finding successful combinations of CDK9 inhibition with ICI and first-line treatment, maximizing antitumour effects while minimizing toxicity. Nonetheless, this work not only focused on the treatment of SCLC but also on its biology. More particularly, the relationship between Gasdermin E and the response to treatment and tumourigenesis of SCLC.

# Chapter 2 – The role of Gasdermin E in the biology and drug response of Small Cell Lung Cancer

## 1.7 Introduction

### 1.7.1 Cell Death Proteins in SCLC

Cancer cells modify their expression of cell death-related proteins as this enhances their chances of survival. A clear example is the overexpression of BCL-2, which owes its name to B-cell lymphomas, where it was first identified thanks to its high levels in the tumour cells, SCLC is no exception. Analysis from patient samples comparing bulk tumour vs normal tissue show a strong downregulation of extrinsic apoptotic and necroptosis transcripts. TRAIL, FASL and Caspase 8 were all downregulated when compared to normal lung, suggesting a shut-down of this pathway (172). Caspase 8 downregulation can lead to the induction of necroptosis by leaving RIPK1 unchecked. However, the necroptotic effector protein MLKL is also downregulated in the tumour tissue, likely preventing the induction of necroptosis (172). Among the proteins assessed, Gasdermin E also showed a decrease in expression in tumour cells (172).

Gasdermin E clearly plays an important role in apoptotic activation. Its forward-activating loop lowers the threshold of initially active Caspase 3 needed to commit the cell to apoptosis. Gasdermin E levels also determine whether active Caspase 3 will trigger the immunologically silent apoptosis or the inflammatory pyroptosis (112, 208). Upregulation of Gasdermin E in cancer cells inhibits cell proliferation and tumour growth while sensitising the cancer cells to treatment (209, 210). As such, it is no surprise that its expression is decreased in SCLC and other cancers. However, studies have also found cancers with increased Gasdermin E (211, 212). This suggests that the protein holds cell-death-independent functions that have yet to be unravelled. There has been progress in this regard, with studies finding interactions between

Gasdermin E and mTOR signalling (213) and EGFR signalling (214) in different cancers. This indicates that Gasdermin E has biological roles capable of influencing tumour growth.

During tumour evolution, cells which evade inflammatory cell death are selected and survive to promote tumour growth. Because of the resulting inflammatory nature of the cell death unleashed by Gasdermin E pores, this gasdermin is typically found downregulated by, for example, promoter methylation (215-218). However, this is not always the case, as it has been shown that some cancers actually upregulate their expression of Gasdermin E (219). In NSCLC, Gasdermin E upregulation has been shown to promote cell proliferation and NSCLC development by interacting with the Epithelial Growth Factor Receptor (EGFR) and facilitating its activation (214). Furthermore, a pan-cancer study revealed the pro- and anti-tumoral roles of Gasdermin E across several cancer types, and this was confirmed for all Gasdermin family proteins (219). Expression of Gasdermin E in particular, was found to be decreased in 4 different cancers and increased in 7 cancers in this study (Table 2) (219). When assessing the overall survival of patients, Gasdermin E expression is a risk factor for Kidney renal clear cell carcinoma (KIRC), Liver hepatocellular carcinoma (LIHC) and Stomach adenocarcinoma (STAD), while it plays a protective role in Adrenocortical carcinoma (ACC) (219). Unfortunately, the study did not evaluate Gasdermin E's effect on SCLC. Its role in this disease remains an open question and warrants further investigation.

Table 2. Gasdermin E expression in different cancers as compared to normal tissue. Adapted from *Huo et al. Sci Rep 2022. (219)*

<b>Cancer</b>	<b>Gasdermin E expression compared to normal tissue</b>
Breast invasive carcinoma (BRCA)	Decreased
Kidney cancer (KICH)	Decreased
Prostate adenocarcinoma (PRAD)	Decreased
Uterine corpus endometrial carcinoma (UCEC)	Decreased

Cholangiocarcinoma (CHOL)	Increased
Glioblastoma multiforme (GBM)	Increased
Head and neck squamous cell carcinoma (HNSC)	Increased
Kidney renal papillary cell carcinoma (KIRP)	Increased
Liver hepatocellular carcinoma (LIHC)	Increased
Lung adenocarcinoma (LUAD)	Increased
Lung squamous cell carcinoma (LUSC)	Increased

Without an established role in SCLC, we aimed to determine its impact on the biology of this disease. We compared the response to different treatments between cell lines with relatively high and low Gasdermin E expression. We assessed the susceptibility to cell death in Gasdermin E knockout cells in comparison to their wild-type parental counterparts. Finally, we investigated changes in tumorigenesis and tumour growth in vivo using an autochthonous mouse model of SCLC.

## 1.8 Aims – Chapter 2

Gasdermin E's modulation of the apoptotic to pyroptotic cell death switch makes it an interesting study focus in the cancer context. SCLC was found to downregulate this protein, suggesting a role for Gasdermin E in this disease. In this chapter, we aim to:

1. Determine the role of Gasdermin E in the susceptibility of SCLC cells to cell death.
2. Assess the impact of Gasdermin E loss in the tumorigenesis of SCLC.

## 1.9 Results

### 1.9.1 Gasdermin E is activated upon chemotherapy in SCLC cells.

As described in the introduction, Gasdermin E levels are decreased in naïve SCLC when compared to normal lung (172). To confirm this observation, we used a panel of SCLC cell lines. For this, we examined the levels of Gasdermin E in mouse and human SCLC cell lines by immunoblotting. We found that Gasdermin E expression was quite heterogeneous among the cell lines (Fig. 21a). We then studied whether Gasdermin E could play a role in response to chemotherapy agents used in first-line treatment and dinaciclib in mouse SCLC cells, given that they induce apoptosis in these cells. Indeed, Gasdermin E is cleaved upon treatment of SCLC cells with cisplatin or etoposide, but less so with dinaciclib (Fig. 21b). We also observed that Gasdermin E cleavage can be prevented by the addition of the pan-caspase inhibitor Z-VAD-FMK (zVAD) (Fig. 21c). This blocking of caspases hindered Gasdermin E cleavage and, interestingly, led to phosphorylation of MLKL, a hallmark of necroptosis.

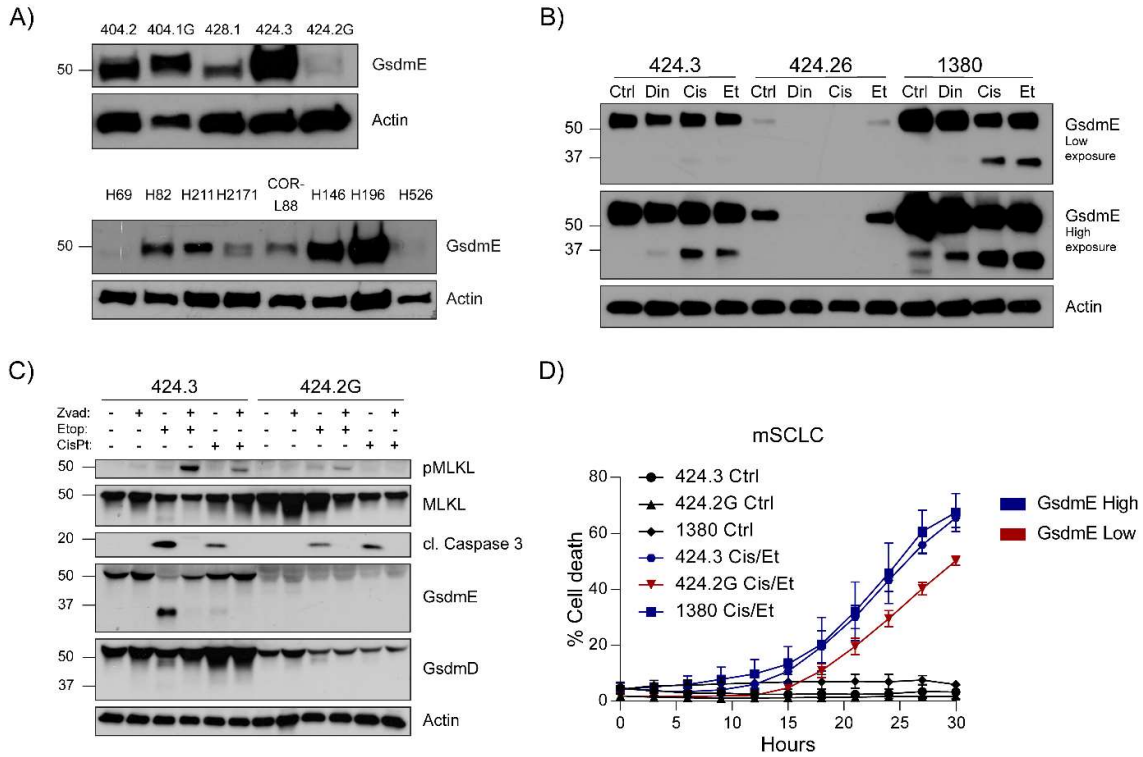


Figure 21. A) Mouse and human SCLC cell lines were lysed in RIPA buffer under normal conditions. B) Mouse SCLC cell lines were lysed with RIPA buffer after a 30-hour treatment of dinaciclib (50 nM), cisplatin (20  $\mu$ M) or etoposide (50  $\mu$ M). Representative blots of 3 independent experiments. C) Cells were treated with zVAD (150  $\mu$ M) and/or etoposide (100  $\mu$ M) and cisplatin (20  $\mu$ M) and lysed with RIPA buffer after 30 hours of treatment. D) Percentage of PI-positive cells after treatment with 10  $\mu$ M cisplatin and 30  $\mu$ M etoposide as measured by Incucyte with Cell-by-cell analysis. Treatments are grouped by expression levels as observed in (A). Mean + SD, n=3.

Next, we compared the cell death kinetics of these cell lines, grouping them by Gasdermin E expression levels. The results showed that the cell line with the lowest expression of Gasdermin E also responded the least to the cisplatin & etoposide treatment (Fig. 21d). This is indicative that Gasdermin E may play a role in the extent by which cells respond to chemotherapy. Altogether, these results suggest that Gasdermin E is potentially involved in tumour response to treatment.

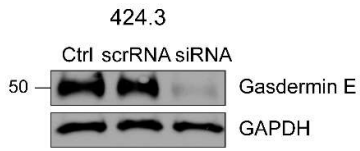
## 1.9.2 Gasdermin E modulates response to treatment

### *in vitro*

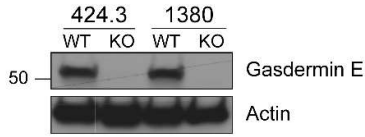
To investigate whether Gasdermin E plays a role in therapy response, we silenced Gasdermin E with siRNA transfection in the mouse cell line 424.3, which expresses the protein, and assessed its response to treatment. We observed that the Knock

Down (KD) of the protein was efficient but not complete (Fig. 22a). When comparing the percentages of cell death, we observed that there was a slight difference between the scramble-RNA (scrRNA) and the Gasdermin E small interfering RNA (siRNA) transfected cells when treated with etoposide (Fig. 22b). Since we could still observe Gasdermin E in the KD cells, we proceeded to knock out the protein by CRISPR cas9, this time in two different cell lines. The cells were infected with non-replicative lentiviral particles to express a Cas9 protein fused to GFP along with a guide RNA (gRNA) directed to Gasdermin E or no gRNA. We sorted infected cells using the GFP-tagged Cas9 and confirmed the loss of Gasdermin E expression by immunoblotting (Fig. 22c), and we proceeded to treat the cells with the etoposide and dinaciclib. This time, the difference between Gasdermin E expressing and KO cells became more evident than in the silencing experiment, showing a slower cell death kinetic and reduced overall cell death upon treatment with dinaciclib (Fig. 22d) and etoposide (Fig. 22e) upon Gasdermin E loss. We also observed that the proliferation of the cells was not significantly affected by Gasdermin E loss (Fig. 22f), ruling out a potential role of this gasdermin in SCLC proliferation.

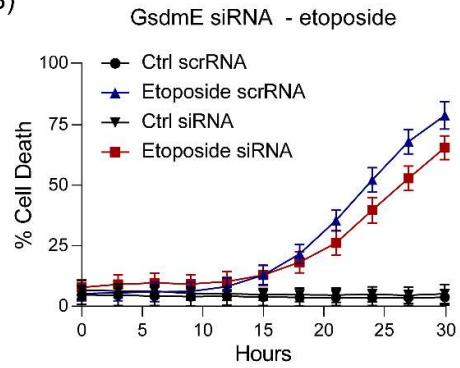
A)



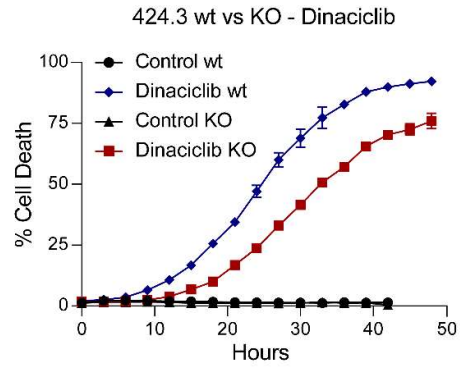
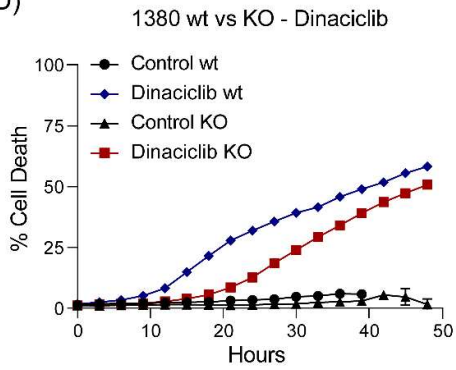
C)



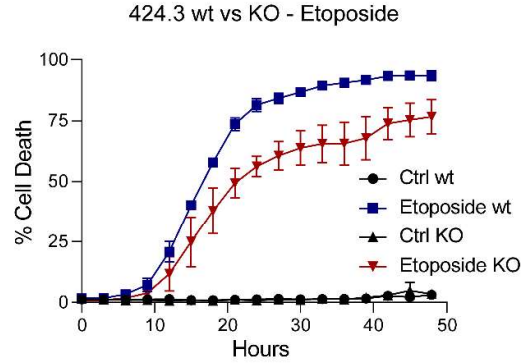
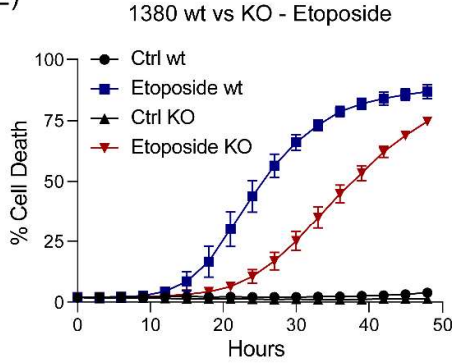
B)



D)



E)



F)

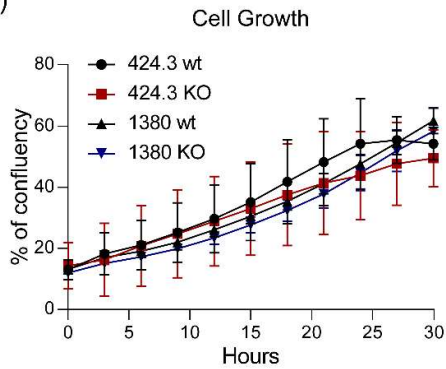




Figure 22. A) Mouse SCLC cells were lysed with RIPA buffer 48 hours after transfection with either scramble (scrRNA) or Gasdermin E targeted small interfering RNA (siRNA). B) Percentage of PI-positive cells after treatment with 100  $\mu$ M etoposide as measured by Incucyte with Cell-by-cell analysis. Mean + SD, n=3. C) CRISPR-expressing mouse SCLC cells were lysed with RIPA buffer to corroborate the efficiency of KO. Percentage of PI-positive cells after treatment with 100 nM of dinaciclib (D) or 100  $\mu$ M etoposide (E) as measured by Incucyte with Cell-by-cell analysis. Representative graphs of 3 independent experiments. F) Cell Growth measured across time as confluency percentage. Mean + SD, n=3.

Since Gasdermin E activation leads to pore formation in the cellular membrane and a pyroptotic death largely associated with LDH release upon cell bursting, we assessed the release of LDH from the cells with and without Gasdermin E. As expected, Gasdermin E KO cells released less LDH when treated with dinaciclib or etoposide (Fig. 23a). Cell bursting is known to release several intracellular pro-inflammatory factors, and Gasdermin E is known for allowing the release of the highly inflammatory interleukin IL-1 $\beta$  (220). Therefore, we decided to test whether cytotoxic treatment would induce the release of IL-1 $\beta$  among these pro-inflammatory factors, and if this is affected by the loss of Gasdermin E. To this end, we performed an ELISA with the supernatant of etoposide- and dinaciclib-treated Gasdermin E wt and KO cells. As a positive control, we used supernatant from mouse bone-derived macrophages (BMDMs) exposed to inactivated *mycobacterium tuberculosis* to trigger pyroptosis and, therefore, the release of IL-1 $\beta$  to the supernatant. The ELISA results with our treated cells show that there is no release of IL-1 $\beta$  upon dinaciclib or etoposide in any of the cell lines tested (Fig. 23b). This means SCLC cells do not engage pyroptosis upon the treatments, independently of Gasdermin E.

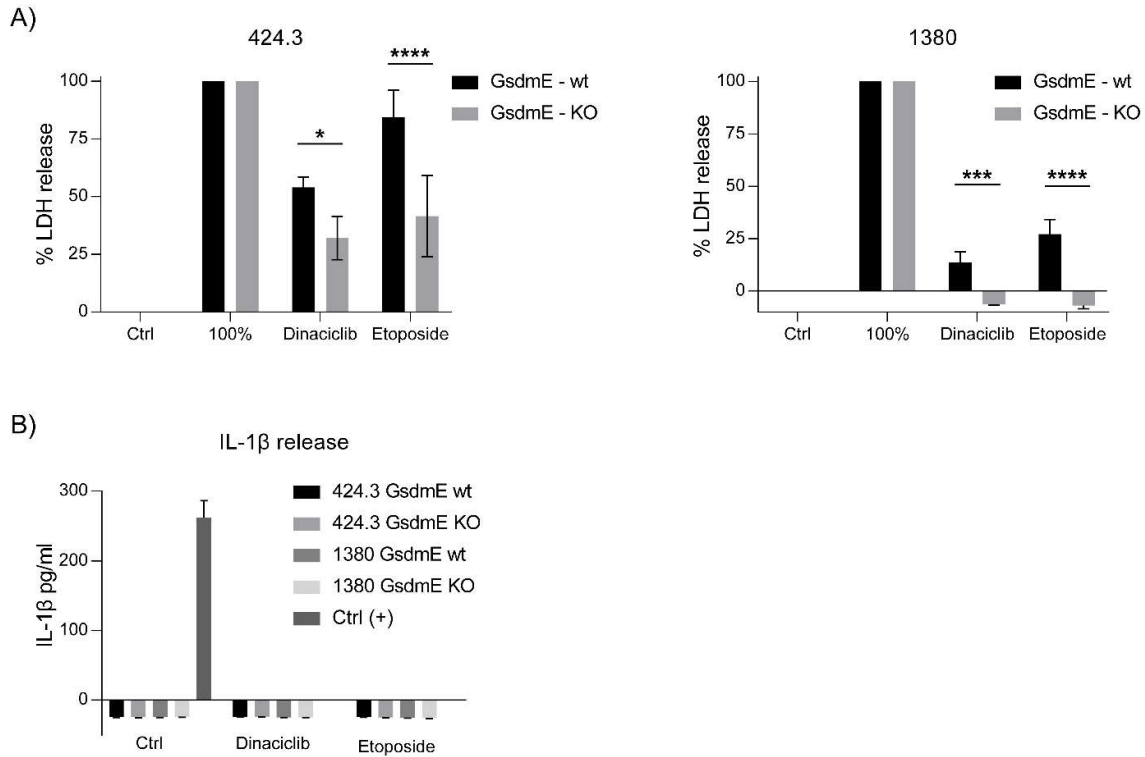


Figure 23. A) Percentage of LDH release from Gasdermin E wt and KO cells after a 24-hour treatment of 50 nM dinaciliclib or 100  $\mu$ M etoposide. Mean + SD, n=3 (424.3), n=2 (1380). B) Concentration of IL-1 $\beta$  from the supernatant of vehicle, 50nM dinaciliclib, or 100  $\mu$ M etoposide. Mean + SD, n=3.

These results show that Gasdermin E modulates treatment response *in vitro*, and its absence proves beneficial for tumour cells in this context.

### 1.9.3 Gasdermin E has no effect on the survival of the autochthonous SCLC model

Finally, following our results where Gasdermin E promotes the release of LDH from the cells, we studied whether the loss of Gasdermin E would confer an advantage to tumour growth *in vivo*. To this end, we made use of the autochthonous RP mouse model described in section 2.1.4, which we crossed with mice bearing Gasdermin E KO alleles to generate SCLC tumours in mice lacking Gasdermin E expression. We inhaled the mice with a non-replicative Cre-expressing Adenovirus to induce tumour formation in the lung. Due to changing animal regulations, tumour volume assessment could only be carried out 7 months after the viral inhalation. This led to an incomplete

assessment of tumour initiation and growth (Fig. 24a). In spite of the setback, we can safely say that, from the day of inhalation, there is no difference between the survival of Gasdermin E KO and wt mice (Fig. 24b). However, with the available data, it is still unclear if tumour latency and tumour development is affected by the absence of Gasdermin E.

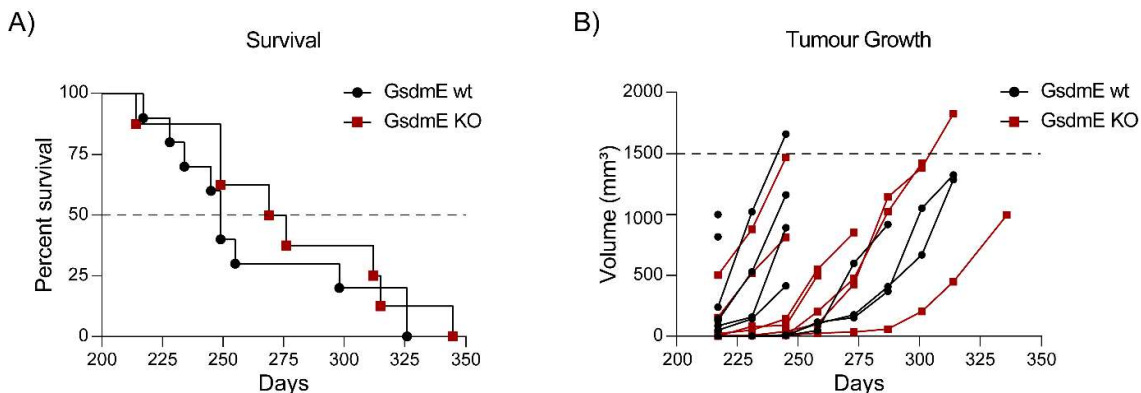


Figure 24. A) Survival curve of Gasdermin E wt and KO counting from the day of inhalation. B) Tumour volume of mice since inhalation day, starting from the first possible MRI scan. Volume calculated from MRI images using the Horos software. Wt N = 10, KO N = 7.

Overall, our data suggests that Gasdermin E does not, in principle, affect tumour development and progression of the untreated disease in the autochthonous mouse mode. Yet, it could play a role in the cells' response to therapy. Further research into this relationship would be of great benefit to patient treatments.

## 1.10 Discussion

### 1.10.1 The role of Gasdermin E in SCLC

It is established by now that Gasdermin E is implicated in cell death as a Caspase 3 substrate (221). Its cleavage by this caspase leads to the release of the auto-inhibitory C-terminal domain, allowing the pore-forming fragment to permeabilize the mitochondria and the cellular membrane (89). The pores in the mitochondria allow the release of Cytochrome C, enhancing the apoptotic signalling, whereas the pores in the cellular membrane lead to cell bursting and the release of inflammatory DAMPS.

Our expression assessment in SCLC cell lines proved similar to the results seen in the pan-cancer analysis, with heterogeneous expression across the different cell lines (219). Focusing on the role of Gasdermin E in cell death, we Knocked Out the protein, finding differences in the death induced in response to treatment, but no changes to the cell growth of the cells. Complete loss of Gasdermin E rendered the cells more resistant to drug treatments. Hence, treatments that induce or boost the expression of Gasdermin E could benefit SCLC, in particular in combination with chemotherapy. Xuzhang et al. focused on this idea and explored it in a recent study where they collected samples from patients with metastatic SCLC. First, they showed that in the patient cohort of their study, SCLC patients with high Gasdermin E expression had improved progression-free survival (PFS), both with chemotherapy alone or with immunochemotherapy (222). Next, they proceeded to Knock Out and overexpress Gasdermin E in SCLC cells, where they observed, in congruency with our results, that loss of Gasdermin E leads to a decreased sensitivity to cisplatin (222). As we hypothesised, overexpression of Gasdermin E leads to increased cell death induced by cisplatin (222). Moreover, they go on to show that activation of Gasdermin E by cisplatin treatment leads to more immunologically active tumours by increasing the number of infiltrating CD4 effector memory T cells. When treating with chemoimmunotherapy (atezolizumab plus cisplatin and etoposide), IL-12 was found as the intermediary protein linking Gasdermin E and the anti-tumour effect of the treatment (222). IL-12 is an interleukin mainly secreted by dendritic cells (DC), macrophages and monocytes (223-225). It is required for Th1 cell differentiation from naïve T cells (226), and it stimulates the production of INF- $\gamma$  and TNF from T cells and NK cells (225-227). Therefore, their study indicates that SCLC cells dying by Gasdermin E activation stimulate the production of IL-12 from the already infiltrated immune cells, and this, in turn, stimulates the production of IFN- $\gamma$  and TNF that further induces the production of IL-12 from DC (by IFN- $\gamma$ ), and favours immune cell recruitment and a pro-inflammatory tumour-microenvironment (TME) (222). Importantly, they showed that this improves the efficacy of anti-PD-L1 treatment *in vivo* (222).

The previous study is a really encouraging one, identifying a vulnerability in SCLC for therapies already active in the clinic. This also further emphasizes the need for a more

personalised approach in the treatment of this disease (139, 228-234); in Xuzhang's et al. case in particular, treating Gasdermin E high patients with chemotherapy and anti-PDL1. One problem raised by Xuzhang et al. is defining what is considered a "high" expressing tumour; which the authors defined as the top 50% expressing tumours as "high".

The drawback of the approach of using "high" Gasdermin E as a vulnerability marker is that it does not offer new treatment options for "low" expressing tumours. As mentioned before, cancers with decreased Gasdermin E achieve this by methylating its promoter and preventing its transcription (215-218). One interesting research path would be to investigate if this methylation can be reversed with epigenetic drugs to restore the expression of Gasdermin E in SCLC. With this in mind, our group conducted a preliminary experiment which showed an increase of Gasdermin E mRNA upon 72-hour treatments with the methyl-transferase inhibitor decitabine, thus providing encouraging evidence to pursue this epigenetic approach for increasing Gasdermin E levels.

Epigenetic drugs have been approved for haematological malignancies as early as 2004 (235). Their effectiveness as monotherapy in solid tumours, however, has been less successful, mainly due to excessive toxicity and low antitumour activity (236, 237). Nonetheless, combination therapies reduced the onset of adverse effects and proved more beneficial in clinical trials (238). This same approach could be undertaken in SCLC tumours with low Gasdermin E in an attempt to re-express the protein so the tumours respond better to the first-line chemoimmunotherapy.

Another approach would be to target proteins modulating Gasdermin E expression levels. Reported up-regulators of this gasdermin are Specificity protein 1 (Sp1), Signal transducer and activator of transcription 3 (STAT3) and Zinc finger E-box binding homeobox 1/2 (ZEB1/2) (239-241). However, available small molecules capable of targeting these proteins act as inhibitors of their activity (e.g. Napabucasin for STAT3), thus decreasing Gasdermin E levels. Targeting proteins responsible for reducing Gasdermin E expression is, therefore, a more practical approach. Interestingly, a study in SCLC from Wu et al. claims that Gasdermin E expression is decreased by the expression of a constitutively active YAP1 (242, 243). This is most intriguing given

YAP1s proposed role as a SCLC subtype marker (228, 234, 244). Wu et al go on to suggest that acquired chemoresistance is a result of a YAP1 increase leading to a reduction of Gasdermin E expression, which induces a switch from pyroptosis-like cell death to apoptosis upon chemotherapy (242). Indeed, Gasdermin E has been defined as the executor protein responsible for inducing pyroptosis upon chemotherapy treatment (96, 221, 242). This positions YAP1 as a possible target for the re-expression of Gasdermin E to increase the benefit from the first-line treatment. Agreeing on targeting YAP1, *in vitro* assays by Chen et al. demonstrated that YAP1 activity induces PD-L1 expression in SCLC cells (245). PBMC co-culture with SCLC cell lines showed that YAP1 also suppresses the cytotoxic activity of CD8 + T cells and the activation of immune cells, and the authors claim the protein induces apoptosis of T cells by increasing the levels of FAS in the immune cells (245). The inhibition of YAP1 led to a reversion of such immunosuppression. Moreover, YAP1 inhibition combined with first-line chemoimmunotherapy led to a significant increase in the efficacy of the treatment (245). Thus, Chen et al. conclude that high YAP1 expression is linked to an immunosuppressed TME and a worse prognosis for patients with SCLC (245). However, another study by Owonikoko et al. is partially in discordance with the conclusions from Chen et al.

Owonikoko et al. observed that SCLC-Y patients correlated with a high T-cell Inflamed Gene Expression Profile (GEP) and with prolonged survival (244). GEP is a biomarker for anti-PD1 immunotherapy response (246-248). While Chen et al. report that YAP1 suppresses CD8+ T cells (245), Owonikoko et al. link YAP1 to a higher T-cell Inflamed gene expression profile (244). Chen's conclusions came from using PBMC co-culture *in vitro*, while Owonikoko et al. retrospectively analysed patient samples (only treated with chemotherapy), so while both studies have their downsides, we could consider Owonikoko's observation as more valid as it is taken directly from patients. The studies also disagree on another important aspect. Chen et al. also analysed the survival of a group of patients with SCLC, and a worse survival was attributed to SCLC-Y tumours, while Owonikoko et al. showed the contrary with the patients they studied, albeit not statistically significant. These differences could be attributed to the low number of patient samples in each study, which translates to even lower YAP1 high tumours and low power to make statistical conclusions. Still, Chen et al. point to YAP1 as the

inducer of PD-L1 expression and T-cell dysfunction, while Owonikoko et al. correlate YAP1 to an inflammatory TME. Nonetheless, both studies agree that patients with SCLC-Y tumours are the most likely to benefit from immunotherapies.

One interesting observation from Owonikoko et al. was that the long survival outlier patients (top decile of survivors) consistently upregulated IFN- $\gamma$  response genes, some of which are part of the T-cell Inflamed GEP (244). This brings us back to the observations from Xuzhang et al. As mentioned before, in their study they link Gasdermin E to the release of IL-12, which in turn induces the production of IFN- $\gamma$  by DCs, promoting the tumours' response to chemoimmunotherapy. They also found that Gasdermin E high tumours also had a high T-cell Inflamed GEP (222). Taking this into consideration, one could look at Owonikoko et al.'s and Xuzhang et al.'s work side by side and suggest that YAP1 tumours upregulate Gasdermin E by as of yet unknown factors; in dying cells, Gasdermin E leads to the release of IL-12, which induces the production of IFN- $\gamma$ , increasing the T-cell Inflamed GEP in the TME, and the response of the tumours to chemoimmunotherapy. Contrarily, the previously discussed work of Wu et al. goes against this affirmation, as they observed that using a constitutively active mutant of YAP1 led to a decrease in Gasdermin E and an increase in chemotherapy resistance. They did not assess changes in gene expression, so it remains unclear how this affected IFN- $\gamma$  response genes and how it relates to the observations of Xuzhang et al. and Owonikoko et al. regarding the T-cell Inflamed GEP. It is still likely that the effects on the T-cell Inflamed GEP are not dependent on Gasdermin E in some cases, and this would require further research. While each study provides insight into the roles of these proteins from their respective models, a unifying view of their functions becomes hard to achieve.

To unravel the specific relationship between Gasdermin E and YAP1, one could use Gasdermin E-low and YAP1-high cells and inhibit YAP1 to corroborate the re-expression of Gasdermin. Since Xuzhang et al. showed Gasdermin E needs to be activated by chemotherapy treatment to induce IL-12 production and the expression of inflammatory genes, testing the inhibition of YAP1 in combination with chemoimmunotherapy in relevant models (co-culture with PBMCs, humanized NSG mice) would show if it leads to an increase in activation of Gasdermin E. Changes in the T-cell Inflamed GEP with and without YAP1 inhibition should also be assessed.

Lastly, to properly confirm that Gasdermin E is key in determining an inflammatory signature in the TME, the previous experiment should also be performed with Gasdermin E-deficient cells and compare them to Gasdermin E-proficient cells. Finding the intermediary protein responsible for the downregulation of Gasdermin E by YAP1 would also provide us with a new target to attempt a re-expression of this gasdermin, and a re-sensitization to chemoimmunotherapy. This could be achieved by inducing YAP1 overexpression in cell lines, expecting it to lead to a downregulation of Gasdermin E, as Wu et al. showed and performing RNA-seq to determine upregulated proteins that could be potential targets. These proteins could then be validated as targets by performing CRISPR Knock Outs and finding which ones do not downregulate Gasdermin E upon YAP1 overexpression.

While YAP1's role in SCLC is still undeciphered, these studies place Gasdermin E as a key player in chemoimmunotherapy response due to its role in inflammatory cell death. Further research elucidating the master regulators of its expression could majorly impact how we treat this disease and, more importantly, improve the survival of the patients.



# Conclusion

The work carried out in this thesis had a major focus on understanding how to better treat SCLC. First, we found that Dinaciclib and CDK9 inhibition proved to be effective tools for the treatment of this cancer, with great synergy potential with first-line chemoimmunotherapy and capable of overcoming one of SCLCs' deadliest hallmark, its acquired resistance to chemotherapy. Second, we identified Gasdermin E as a potentially targetable vulnerability that modulates the response to treatment. Although we are yet to fully understand the underlying mechanism of its regulation, harnessing Gasdermin E's expression would prove crucial to enhancing current and future therapies. This thesis follows the work of many scientists and clinicians calling for a more personalized approach to SCLC treatment. Technological advances have gained us a deeper understanding of the molecular dependencies of this disease, bringing with it novel and targeted drugs and treatments. It is time for the clinic to start reflecting this by taking into account all the recent advances in clinical trials. It is also worth mentioning that SCLC is strongly linked to heavy smoking (249-252) (with only 16% of diagnoses arising from never-smokers (250)), and the most effective course of action is prevention. Nonetheless, were the disease to develop, the science carried out in this work, and the work of many other scientists, will lead to the improvement of the survival of the patients and, hopefully one day, to the complete cure of this recalcitrant disease.

# Materials and Methods

## 1.10.2 Cell Lines and Cell Culture

Cells were grown in their required media. The mouse non-small cell lung cancer (NSCLC) cell lines KP-1, KP-2, KP-3, and KP-5 were generously provided by A. Montinaro. The small cell lung cancer (SCLC) cell lines 404.2, 424.3, 424.2G, and 428.1 were derived directly from lung tumours of the RP mouse model for SCLC, characterized by the loss of Trp53 and Rb1. The 1380 cell line was similarly derived from the RP model but was further developed by injecting it into the lungs of a C57BL/6J recipient mouse and re-isolating it after successful *in vivo* growth. All cell lines, except for 1380, were maintained in DMEM (Gibco | Thermo Fisher Scientific, Billings, MT, USA, cat# 10566016) with 10% Fetal Bovine Serum (FBS) (Gibco, cat# 10270106). The 1380 cell line was cultured in RPMI 1640 (Gibco, cat# 21875034) with 10% FBS. The H526, H2171, H1975, PC-9, HEK, H358, and H1694 cell lines were cultured according to the supplier's specifications. All media were supplemented with the antibiotic Primocin (Invivogen, San Diego, CA, USA, cat# ant-pm-1) (174).

Cells were grown in T25, T75 and T175 sterile flasks (Sarstedt, ref# 83.3910.002, 83.3911.002, 83.3912.002, respectively), using autoclaved 2 ml, 5 ml, 10 ml and 25 ml discardable pipets (Greiner Bio-One, ref# 710180, 606180, 607180, 760180, respectively), 10 µl, 200 µl and 1 000 µl tips (Starlab, ref# S1110-3000, S1111-0000, S1111-6001, respectively) and 1.5 ml and 2 ml Eppendorf tubes (Eppendorf, ref# 0030 120.086, 0030 120.094, respectively) as required.

## 1.10.3 Buffers

Buffer	Composition
Phosphate-buffered saline (PBS)	137 mM NaCl, 2.7 mM KCl, 10 mM Na <sub>2</sub> HPO <sub>4</sub> , and 1.8 mM KH <sub>2</sub> PO <sub>4</sub>
Radioimmunoprecipitation assay buffer (RIPA)	Sodium Chloride 150mM, Tris-HCl 50mM pH 8.0, NP-40 1%, Sodium deoxycholate 0.5%, SDS 0.1%

Membrane Extraction Buffer (MEB)	150 mM mannitol, 10 mM Hepes-KOH pH 7.5, 150 mM KCl, 1 mM EGTA, 1 mM EDTA, 0.1% BSA, 5 mM succinate
SDS running buffer	25 mM Tris HCl, 0.192 M Glycine and 0.1% (w/v) Sodium Dodecyl Sulfate (SDS); pH 8.3
Tris-buffered saline Tween (TBS-T)	20 mM Tris, 150 NaCl mM, 0.1% (w/v) Tween® 20, pH 7.4
Super Optimal Broth (SOB)	2% tryptone, 0.5% yeast extract, 0.05% NaCl, 250 µM KCl, pH 7.0
Lysogeny Broth (LB)	10g/L Tryptone, 5g/L Yeast extract, 5g/L NaCl, pH 7.0 (Carl Roth, ref# X964.1)

Table 3. Buffers and their compositions.

## 1.10.4 Drugs

Target	Company	Catalogue number
Dinaciclib	Selleck-Chemicals	S2768
NVP-2	Selleck-Chemicals	S8981
Cisplatin	Selleck-Chemicals	S1166
z-VAD-FMK	Selleck-Chemicals	S8102
Etoposide	Absource Diagnostic	S1225-0100
Propidium Iodide	Sigma-Aldrich	P4864

Table 4. Drugs used and their suppliers.

Recombinant iz-huTRAIL was generously provided by H. Walczak. VC-1 was generated and provided by Vichem Chemie Research Ltd. (Budapest, Hungary) (174).

### Antibodies

Target	Company	Catalogue number
RNA pol II RBP1 p-Ser2	Biologend	920204
RNA pol II	Biologend	904001

MCL-1	Cell Signaling	5453
cFLIP	Cell Signaling	56343
C-MYC	Cell Signaling	5605
PARP	BD Biosciences	556362
Caspase 9	Abcam	ab202068
Caspase 8	Cell Signaling	9746
Cleaved Caspase 3	Cell Signaling	9664
Gasdermin E	Abcam	ab215191
$\beta$ -Actin	Sigma-Aldrich	A1978
Tubulin	Sigma-Aldrich	T9026
GAPDH	Sigma-Aldrich	G8795
Rabbit IgG	SouthernBiotech	4050-05
Mouse IgG	SouthernBiotech	1031-05

Table 5. Antibodies used and their suppliers.

### 1.10.5 Cell viability and cell death assays

Adherent cells were plated the day before the experiment at a density of 6,000 cells per well in a black 96-well plate (Nunc MicroWell 96 Wells, Thermo Scientific, Ref# 137101). The next day, cells were treated with the specified drugs for 30 hours. For suspension cells, 10,000 cells per well were plated and treated concurrently in a 96-well plate (Nunc MicroWell 96-Well, Thermo Scientific, Ref# 167008) for 30 hours. Cell viability was measured using the CellTiter-Glo assay (Promega, Madison, WI, USA, Cat# G7571) following the manufacturer's instructions. Luminescence was recorded using a Tecan Infinite M-plex (Tecan, Männedorf, Switzerland). For IC<sub>50</sub> determination of VC-1, the compound was pre-printed using the D300e Digital Dispenser (Tecan). Viability was assessed after 72 hours using CellTiter-Glo. The cell lines tested included: NSCLC: A549, HCC827, HCC4006, H2172, H1568, H1299, H2110, HCC15,

PC9, H23, H522; SCLC: H196, H69, GLC2, H82, H1092, H2029, H526, H524, GLC8, H1048, H841, GLC1 (174).

The IncuCyte™ Live-Cell Imaging system was employed to monitor cytotoxicity through PI uptake. A 96-well plate (Nunc MicroWell 96-Well, Thermo Scientific, Rwf# 167008) was seeded with 20,000 (human SCLC cell lines), or 8,000 (mouse cell lines) cells per well, with treatments specified in each figure. Images were captured every 3 hours, and the percentage of dead cells was determined by quantifying PI-positive cells using the Cell-by-Cell function of the IncuCyte analysis software.

### 1.10.6 LDH release assay

Released LDH was assessed using the Cytotoxicity Detection Kit (LDH) (Roche, Ref# 11644793001). Cells were seeded at a density of 8,000 cells per well in a 96-well plate (Nunc MicroWell 96-Well, Thermo Scientific, Rwf# 167008) and were seeded a day prior to treatment with the drugs indicated in the figure or figure legend for 24 hours. The 100% LDH release was induced with the “lysis solution” from the LDH-Glo Cytotoxicity Assay kit (Promega, ref# J2380). After 24 hours of treatment, plates were centrifuged at 300 g for 5 minutes to sediment all cells and debris, and the supernatant was collected. Next, instructions for the kit were followed as per the manufacturer's instructions, reading absorbance using a Tecan Infinite M-plex (Tecan, Männedorf, Switzerland) at 492 nm with 610 nm as the reference wavelength.

### 1.10.7 IL-1 $\beta$ ELISA

The ELISA was carried out using the Mouse IL-1 beta/IL-1F2 DuoSet ELISA (R&D Systems, ref# DY401) supplemented with the DuoSet ELISA Ancillary Reagent Kit 2 (R&D Systems, ref# DY008B). Plates were coated and prepared according to the manufacturer's instructions and stored at -20 °C until used. For the ELISA assay, the coated plates were placed at room temperature for 30 minutes prior to the start of the procedure, which was carried out following the manufacturer's instructions. The positive control consisted of supernatant from *mycobacterium tuberculosis-infected*

macrophages, which was kindly provided by Dr. Hamid Kashkar. Absorbance was measured using a Tecan Infinite M-plex (Tecan, Männedorf, Switzerland) at 450 nm with 540 nm as the reference wavelength.

### 1.10.8 Dynamic BH3 profiling

Dynamic BH3 profiling was performed as previously described (169, 174). Briefly,  $3 \times 10^5$  cells were incubated with targeted therapies (or DMSO for the control condition) for 16 hours at 37°C. After incubation, cells were stained with the viability marker Zombie Violet (423113, BioLegend, Koblenz, Germany) for 10 minutes at room temperature, then washed with PBS and resuspended in 330  $\mu$ l of MEB buffer. Meanwhile, 12 different peptide solutions were prepared in MEB with 0.002% digitonin (D141, Sigma-Aldrich). The final concentrations of the peptide solutions were: 10, 3, 1, 0.3, 0.1, 0.03, and 0.01  $\mu$ M of BIM BH3 peptide; 10  $\mu$ M of BAD BH3 peptide; 100  $\mu$ M of HRK BH3 peptide; 10  $\mu$ M of MS1 BH3 peptide; 25  $\mu$ M of alamethicin (BML-A 150-0005, Enzo Life Sciences, Lörrach, Germany); and DMSO as the control.

Subsequently, 25  $\mu$ l of the cell suspensions were incubated with 25  $\mu$ l of each peptide solution in a 96-well plate (3795, Corning, Madrid, Spain) for 1 hour at room temperature, followed by fixation with formaldehyde and staining with cytochrome c antibody (Alexa Fluor® 647—6H2.B4, 612310, BioLegend). Individual DBP analyses were performed 16 hours after dinaciclib treatment (25 nM) in triplicates for DMSO, alamethicin, various concentrations of BIM BH3, and BAD, HRK, and MS1 BH3 peptides. The analyses were conducted using a high-throughput Cytex® Aurora Spectral Flow cytometer (Cytex Bioscience, Fremont, CA, USA). The % priming represents the maximum percentage of cytochrome c released following BH3 peptide exposure, and  $\Delta$ % priming indicates the maximum difference between treated and untreated cells (174).

### 1.10.9 Cell cycle analysis

$1.25 \times 10^6$  (H526, H1694, and H2171) or  $3 \times 10^5$  (H526 and H1975) cells were treated with dinaciclib (50 nM). After 24 hours, the cells were collected, centrifuged for 5 minutes at 500 g, washed with PBS, fixed and permeabilized by transferring the cells to 70% ethanol, and stained with Propidium Iodide (PI) for 20 minutes at room temperature. The fluorescence intensity was measured with BD FACSymphony A3 Flow Cytometer (BD Biosciences, Germany), and cell cycle distribution was assessed by analyzing DNA content using FlowJo v10.10 software (BD Biosciences) (174).

### 1.10.10 Western blot analysis

Suspension cells were treated as specified, placed in ice, and centrifuged at 500 g for 5 minutes. The supernatant was discarded, and the cells were then lysed in RIPA lysis buffer containing 1x cOmplete Protease Inhibitor Cocktail (Sigma-Aldrich, cat# 11697498001) and 1x PhosSTOP (Roche, Basel, Switzerland, cat# 4906837001). Adherent cells were treated as specified and placed in ice, and their media and PBS used to wash the remaining unattached cells were collected. The collected media and PBS were centrifuged at 500 g to separate the media from the dead/dying cells. The attached cells were lysed with RIPA buffer as described before being scraped with Cell Scrappers (Sarstedt, cat# 83.3951). Lysates were incubated for 30 minutes with 0.4  $\mu$ l of Pierce™ Universal Nuclease at 37 °C (Thermo Scientific, ref # 88700) to rid the viscosity brought by free DNA from the lysed cells. After the incubation, lysates were centrifuged at 4 °C for 10 minutes at 20,000 g and transferred to new tubes without the pelleted debris and undissolved particles. Following the manufacturer's instructions, protein concentration was assessed using a Pierce™ BCA Protein Assay Kit (Thermo Scientific, ref# 23227).

Proteins were separated on 4–15% Mini- or Midi-PROTEAN® TGX™ gels (Bio-Rad, Hercules, CA, USA, cat# 4561086, cat# 5671085) using SDS running buffer. The separated proteins were transferred onto Mini- or Midi- 0.2  $\mu$ m nitrocellulose membranes (Bio-Rad, cat# 1704158, cat# 1704159) with the Trans-Blot® Turbo™ Transfer System (Bio-Rad). Membranes were blocked with 5% BSA (Bovine Serum

Albumin Fraction V, heat shock, fatty acid-free; Roche, ref# 03117057001) TBS-T solution for one hour before washing with fresh TBS-T and incubating overnight at 4 degrees in a rotating tube with the primary antibody at the recommended dilution by the manufacturer. Primary antibodies were diluted in TBST-T with 2.5% BSA, and 0.02 % NaN<sub>3</sub>. After the overnight incubation, membranes were washed 3 times with TBS-T prior to incubation with secondary antibody (anti-Mouse or anti-Rabbit, as required), diluted 1:10,000 in TBST with a spoonful of dissolved Non-fat dried milk powder (ITW Reagents, ref# A0830).

### 1.10.11 siRNA mediated silencing

For small interfering RNA (siRNA)-mediated knockdowns, 5,000 cells were seeded in a 96-well plate in 100 µl of antibiotic-free media the day before transfection. 9.5 µl of Opti-MEM (Thermo Scientific, 31985070) and 0.5 µl of Dharmafect Reagent I (Dharmacon, T-2001-02) were mixed on one side for each well of the 96-well plate, and 0.5 µl of siRNA (stock 20 µM) was mixed with 9.5 µl of Opti-MEM on the other. Both solutions were incubated for 5 minutes at Room Temperature (RT). Both solutions were mixed carefully by pipetting and incubated at RT for 20 more minutes. After the incubation period, 80 µl of antibiotic-free Opti-MEM was added to the 20 µl mix to make the Transfection mix.

Media was removed from the cells and replaced with 100 µl of the Transfection mix. The knocked-down cells were incubated for 48 hours before being used in experiments.

### 1.10.12 siRNA sequences

Target	Sequences	Catalogue number
<i>DFNA5</i>	GGGCAAUUCAGUGCGUUC; GGUCAGCGCACUAGCAGAA;	L-041196-01-0020 Dfna5 (54722) ON-TARGETplus



	GCUUCGAGCAUGAGAGGAA; UCUUGCAGCUGGUGGGAUA	siRNA – SMARTpool, Dharmacon
Non-targeting (scramble/scrRNA)	UAAGGCUAUGAAGAGAUAC	D-001210-02-20 siGENOME Non-Targeting siRNA #2, Dharmacon

Table 6. siRNA sequences and suppliers.

### 1.10.13 Plasmid construction for CRISPR gRNA

Lyophilized oligonucleotides were purchased from Eurofins Genomics.

Gasdermin E gRNA oligonucleotide Forward:

CACCGGCAGATAAAATCTGGTACT

Gasdermin E gRNA oligonucleotide Reverse:

AAACAGTACCAGATTTTATCTGCC

The lyophilized oligonucleotides were reconstituted in autoclaved, distilled water to a concentration of 100  $\mu$ M. Primers were incubated with T4 ligation buffer (NEB, ref# B0202S) and T4 PNK (NEB, ref# M0201S). The mixture was incubated for 30 minutes at 37°C, followed by a 5-minute incubation at 95°C, and then allowed to slowly cool down to room temperature at a rate of 5°C per minute.

The cloning of the gRNA to the backbone plasmid lentiCRISPRv2 (Addgene, ref# 52961) was done using the Golden Gate method (253, 254) and the restriction enzyme BsmB1-v2 (NEB, ref# R0580). The gRNA was cloned to the plasmids using a T4 DNA Ligase (Thermo Scientific, ref# EL0011) following the manufacturer's instructions.

### 1.10.14 *E. coli* competence preparation and transformation

To prepare chemo-competent cells, *E. coli stb13* (kindly provided by Dr. Alessandro Annibaldi) were first streaked on an antibiotic-free LB agar plate and allowed to grow

overnight at 37°C. The next day, a single clone was picked and cultured overnight in 5 mL of SOB medium with freshly added 25 mM MgCl<sub>2</sub> at 37°C with shaking at 150 RPM. The following day, 240 mL of SOB medium were inoculated with 1 mL of the overnight culture and grown at 18°C until the OD<sub>600</sub> reached 0.6.

The culture was then cooled on ice for 10 minutes, centrifuged at 3,000 RPM for 10 minutes at 4°C, and the pellet was resuspended in 10 mL of cold transformation buffer (10 mM PIPES, 15 mM CaCl<sub>2</sub>, 250 mM KCl, pH 6.7, 55 mM MnCl<sub>2</sub>). After adding 7% DMSO, the bacteria were aliquoted into 100 µL portions in 1.5 mL tubes and stored at -80 °C.

After thawing the competent *E. coli* DH5α cells on ice, 1 µL of plasmid DNA was added to 50 µL of the cells. The mixture was incubated on ice for 5 minutes. Following the incubation, the transformed cells were plated onto prewarmed LB agar plates containing ampicillin (100 µg/ml) and incubated overnight at 37 °C.

### 1.10.15 Transfection of HEK cells for viral production

4.85 µg of the transfer plasmid (lentiCRISPRv2 with or without gRNA), 3.65 µg of pSPAX and 1.5 µg of pMD2.G plasmids were combined with 500 µL of Opti-MEM. 30 µL polyethylenimine (PEI) was mixed on a second tube with 470 µL of Opti-MEM. After 5 minutes, both solutions were mixed and incubated for 15 minutes before adding dropwise to the plate. The cells were left under normal culture conditions after shaking to properly distribute the mix in the dish. Media was changed after 24 hours, and collected and filtered after 72 hours.

### 1.10.16 Infection of target cells

424.3 cells were infected using sterile filtered virus-containing supernatant from transfected HEK cells. Cells were plated at approximately 30% confluence, and the virus-containing supernatant was added for three consecutive days. To enhance transduction efficiency by reducing the repulsion between cell surface charges and

virions, 8 µg/ml polybrene (Hexadimethrine bromide) was added to the virus suspension (255).

Positive cells were sorted using the INFLUX cell sorter (BD Biosciences), using the green channel to identify infected cells by the expression of the eGFP-tagged Cas9. Single cells were sorted into a 96-well plate for clonal amplification and confirmed by Immunoblotting. Cells were then used for the stated experiments.

### 1.10.17 In vivo toxicity assessment of VC-1

To evaluate the safety of VC-1, both acute and chronic toxicity were assessed. A single injection of 40 mg/kg (n = 3) for the acute toxicity study was administered intraperitoneally (i.p). For the chronic toxicity study, animals received three injections per week for two weeks (n = 3). Control animals (n = 1) were injected with the vehicle. The animals were monitored three times per week for general conditions, including body weight and behaviour. On day 14, the mice were sacrificed by cervical dislocation, and liver weight was measured (174).

### 1.10.18 In vivo tumour studies

Adult C57BL/6 mice (6–8 weeks old) were housed in individually ventilated cages (IVC) systems with ad libitum access to food and water. The animal facility maintained a temperature of 23°C with a 12-hour light/dark cycle. Three models of small cell lung cancer (SCLC) were used, as described below:

#### 1.10.18.1 Autochthonous mouse model:

Mice harbouring LoxP sites flanking the Rb1 Trp53 (RP model) were used to induce small cell lung cancer (SCLC). In Chapter 2, RP mice were crossed with Gasdermin E KO mice to generate the RP Gasdermin E<sup>wt/wt</sup> and RP Gasdermin E<sup>KO/KO</sup> used in the experiments. For induction of lung tumours, 8–12-week-old mice were anaesthetized with Ketamine (100 mg/kg) and Xylazine (10 mg/kg) by intraperitoneal injection, followed by intratracheal inhalation of replication-deficient adenovirus expressing Cre (Ad5-CMV-Cre, 2.5 × 10<sup>7</sup> PFU, University of Iowa). Tumor formation was monitored bi-weekly using magnetic resonance imaging (MRI) five months (RP, Chapter 1) or 7

months (RP GsdmE, Chapter 2) after inhalation. MRI was performed using a 3.0 T Philips Achieva clinical MRI system (Philips Best, the Netherlands) with a dedicated mouse solenoid coil (Philips Hamburg, Germany). T2-weighted MR images were acquired in the axial plane using a turbo-spin echo (TSE) sequence (repetition time (TR) = 3819 ms, echo time (TE) = 60 ms, field of view (FOV) = 40 × 40 × 20 mm<sup>3</sup>, reconstructed voxel size = 0.13 × 0.13 × 1.0 mm<sup>3</sup>, number of averages = 1) under 2.5% isoflurane anaesthesia. MR images (DICOM files) were analyzed blindly by determining and calculating regions of interest (ROIs) using Horos software (174).

Chapter 1: Once tumours reached a minimum volume >1 mm<sup>3</sup>, mice were randomized into two groups and treated twice per week, every 2 weeks, with either the vehicle HP-β-CD 10% (Hydroxypropyl Beta Cyclodextrin; Sigma, #C0926-5G) or dinaciclib at 30 mg/kg (MedChemExpress, #HY-10492, Lot#120243). Treatment continued until tumours reached a size of 800 mm<sup>3</sup>, at which point mice were sacrificed (174).

Chapter 2: Tumour volumes were monitored until they reached a size of 1,500 cm<sup>3</sup>, at which point the mice were sacrificed. Tumour growth speed and survival were assessed.

#### 1.10.18.2 Syngeneic mouse model by subcutaneous injection of mouse SCLC cells:

The 424.3 cell line was used to generate tumours by injecting 5 × 10<sup>6</sup> cells in 100 μl PBS subcutaneously into the flanks of 8-week-old female C57BL/6N mice (Charles River, Wilmington, MA, USA). Mice were randomized into either vehicle or treatment groups once tumours reached a minimum size of 2 × 2 mm. Tumour dimensions were measured blindly using callipers, and volume was calculated using the formula  $\pi/6 \times \text{length} \times \text{width}^2$ , where length is measured perpendicular to the width and length > width. Treatment was administered twice a week, every other week, until endpoint criteria were met. The treatment regimen consisted of dinaciclib (Insight Biotechnology, #HY-10492, Lot#14761 and Lot#120243) at a dose of 20 mg/kg, formulated in 10% HP-β-CD (Hydroxypropyl Beta Cyclodextrin; Sigma, #C0926-5G) (174).

The 1380 cell line was used to generate tumours by injecting  $3 \times 10^6$  cells in 100  $\mu$ l of Matrigel (Corning, Corning, NY, USA, cat# 354234) subcutaneously into the flanks of either 8-week-old female C57BL/6N mice obtained from the core facility of the CECAD research centre (Fig. 17c, d, f), or 16-week-old female C57BL/6 mice (Fig. 19) obtained from a specific-pathogen-free (SPF) colony of the Department of Experimental Pharmacology, National Institute of Oncology (Budapest, Hungary) (174).

Mice were randomly assigned to vehicle or treatment groups 10 days after cell injection when the average tumour size reached 50-100 mm<sup>3</sup>. Treatment and tumour measurement were carried out as previously described for dinaciclib (MedChemExpress, #HY-10492, Lot#14761, and Lot#120243) at a dose of 30 mg/kg, formulated in 10% HP- $\beta$ -CD (Hydroxypropyl Beta Cyclodextrin; Sigma, #C0926-5G) (174).

For VC-1, treatment consisted of three intraperitoneal (i.p.) injections per week at a 20 mg/kg dose. VC-1 was resuspended in MilliQ water along with 10% HP- $\beta$ -CD (Hydroxypropyl Beta Cyclodextrin; Cyclolab, Budapest, Hungary, #CY2005.2) (174).

### 1.10.18.3 Xenografts of human SCLC cells in immunocompromised mice

$1 \times 10^6$  H526 cell was inoculated in 100  $\mu$ l solution (M199 medium:Matrigel 1:1 mixture) (Corning, #356234) in the right flank of 16-week-old NOD-SCID females. Mice were randomly assigned to vehicle or treatment groups 10 days after the cell injection when the average tumour size reached 50-100 mm<sup>3</sup>. Treatment and tumour measurement were carried out as mentioned before for dinaciclib and VC-1.

NOD-SCID mice are characterized for having an absence of functional T cells and B cells, hypogammaglobulinemia, a normal hematopoietic microenvironment, and lymphopenia. *Prkdc<sup>scid</sup>* mice (DNA-dependent protein kinase catalytic subunit), known as SCID (severe combined immunodeficiency), exhibit a DNA repair defect and impaired rearrangement of genes responsible for antigen-specific receptor formation on lymphocytes. The majority of homozygous SCID mice lack detectable levels of IgM,

IgG1, IgG2a, IgG2b, IgG3, or IgA antibodies. Their thymus, lymph nodes, and splenic follicles also typically lack lymphocytes. Some SCID mice spontaneously develop partial immune reactivity with age and are considered “leaky”. NOD (non-obese diabetic) mice have been used extensively for type 1 diabetes research, however, when crossed with SCID mice, the diabetic phenotype from the NOD background is lost, as is the spontaneous immune activity from the “leaky” SCID background. As such, NOD-SCID mice are a favourable environment for xenografts.

### 1.10.19 Ethical approval

Animal experiments from Fig. 17, 18 and 27 were approved by the local authorities (LANUV, North-Rhine-Westphalia, Germany) and performed under licence numbers 81-02.04.2019.A491 (Fig. 17, 18) and 81-02.04.2021.A102 (Fig. 27). Animal experiments from Fig. 20 were conducted at the Department of Experimental Pharmacology, National Institute of Oncology (Budapest, Hungary). The animals involved in these studies were cared for in accordance with the "Guiding Principles for the Care and Use of Animals" based on the Helsinki Declaration, and all protocols were approved by the local ethical committee. Animal housing density adhered to regulations and recommendations outlined in directive 2010/63/EU of the European Parliament and of the Council of the European Union concerning the protection of animals used for scientific purposes. The studies were conducted under the following permission licenses for breeding and performing experiments with laboratory animals: PEI/001/1738-3/2015 and PE/EA/1461–7/2020. Personnel involved in animal experiments received prior training and have obtained the necessary personal licensing course (FELASA-B). All animal experiments were performed in compliance with international and institutional ethical guidelines on animal

## 1.10.20 Statistical analyses

Statistical analyses were carried out using GraphPad Prism 8 v8.0.2. (GraphPad Software Inc., San Diego, CA, USA) IC50s were calculated by non-linear regression comparing normalised response (null hypothesis) vs. normalised response – variable slope and choosing the better model in each case. Log-Rank (Mantel-Cox) analysis was used to compare survival.

# Reference list

1. Galluzzi L, Vitale I, Aaronson SA, Abrams JM, Adam D, Agostinis P, et al. Molecular mechanisms of cell death: recommendations of the Nomenclature Committee on Cell Death 2018. *Cell Death Differ*. 2018;25(3):486-541.
2. Peltzer N, Walczak H. Cell Death and Inflammation - A Vital but Dangerous Liaison. *Trends Immunol*. 2019;40(5):387-402.
3. de Vasconcelos NM, Lamkanfi M. Recent Insights on Inflammasomes, Gasdermin Pores, and Pyroptosis. *Cold Spring Harb Perspect Biol*. 2020;12(5).
4. Schwarzer R, Jiao H, Wachsmuth L, Tresch A, Pasparakis M. FADD and Caspase-8 Regulate Gut Homeostasis and Inflammation by Controlling MLKL- and GSDMD-Mediated Death of Intestinal Epithelial Cells. *Immunity*. 2020;52(6):978-93 e6.
5. Holze C, Michaudel C, Mackowiak C, Haas DA, Benda C, Hubel P, et al. Oxeiptosis, a ROS-induced caspase-independent apoptosis-like cell-death pathway. *Nat Immunol*. 2018;19(2):130-40.
6. Dixon SJ, Lemberg KM, Lamprecht MR, Skouta R, Zaitsev EM, Gleason CE, et al. Ferroptosis: an iron-dependent form of nonapoptotic cell death. *Cell*. 2012;149(5):1060-72.
7. Kroemer G, Levine B. Autophagic cell death: the story of a misnomer. *Nat Rev Mol Cell Biol*. 2008;9(12):1004-10.
8. Brinkmann V, Reichard U, Goosmann C, Fauler B, Uhlemann Y, Weiss DS, et al. Neutrophil extracellular traps kill bacteria. *Science*. 2004;303(5663):1532-5.
9. Strasser A, O'Connor L, Dixit VM. Apoptosis signaling. *Annu Rev Biochem*. 2000;69:217-45.
10. Murphy JM, Czabotar PE, Hildebrand JM, Lucet IS, Zhang JG, Alvarez-Diaz S, et al. The pseudokinase MLKL mediates necroptosis via a molecular switch mechanism. *Immunity*. 2013;39(3):443-53.
11. Kayagaki N, Stowe IB, Lee BL, O'Rourke K, Anderson K, Warming S, et al. Caspase-11 cleaves gasdermin D for non-canonical inflammasome signalling. *Nature*. 2015;526(7575):666-71.
12. Taddei ML, Giannoni E, Fiaschi T, Chiarugi P. Anoikis: an emerging hallmark in health and diseases. *J Pathol*. 2012;226(2):380-93.
13. Tsvetkov P, Coy S, Petrova B, Dreishpoon M, Verma A, Abdusamad M, et al. Copper induces cell death by targeting lipoylated TCA cycle proteins. *Science*. 2022;375(6586):1254-61.
14. David KK, Andrabi SA, Dawson TM, Dawson VL. Parthanatos, a messenger of death. *Front Biosci (Landmark Ed)*. 2009;14(3):1116-28.
15. Kerr JF, Wyllie AH, Currie AR. Apoptosis: a basic biological phenomenon with wide-ranging implications in tissue kinetics. *Br J Cancer*. 1972;26(4):239-57.
16. Gunther SD, Fritsch M, Seeger JM, Schiffmann LM, Snipas SJ, Coutelle M, et al. Cytosolic Gram-negative bacteria prevent apoptosis by inhibition of effector caspases through lipopolysaccharide. *Nat Microbiol*. 2020;5(2):354-67.
17. Van Opdenbosch N, Lamkanfi M. Caspases in Cell Death, Inflammation, and Disease. *Immunity*. 2019;50(6):1352-64.
18. Julien O, Wells JA. Caspases and their substrates. *Cell Death Differ*. 2017;24(8):1380-9.
19. Kawane K, Motani K, Nagata S. DNA degradation and its defects. *Cold Spring Harb Perspect Biol*. 2014;6(6).
20. Chaitanya GV, Steven AJ, Babu PP. PARP-1 cleavage fragments: signatures of cell-death proteases in neurodegeneration. *Cell Commun Signal*. 2010;8:31.
21. Elmore S. Apoptosis: a review of programmed cell death. *Toxicol Pathol*. 2007;35(4):495-516.
22. Kothakota S, Azuma T, Reinhard C, Klippel A, Tang J, Chu K, et al. Caspase-3-generated fragment of gelsolin: effector of morphological change in apoptosis. *Science*. 1997;278(5336):294-8.
23. Nagata S. Apoptosis and Clearance of Apoptotic Cells. *Annu Rev Immunol*. 2018;36:489-517.
24. Kallenberger SM, Beaudouin J, Claus J, Fischer C, Sorger PK, Legewie S, et al. Intra- and interdimeric caspase-8 self-cleavage controls strength and timing of CD95-induced apoptosis. *Sci Signal*. 2014;7(316):ra23.
25. Li P, Zhou L, Zhao T, Liu X, Zhang P, Liu Y, et al. Caspase-9: structure, mechanisms and clinical application. *Oncotarget*. 2017;8(14):23996-4008.
26. Mesner PW, Jr., Budihardjo, II, Kaufmann SH. Chemotherapy-induced apoptosis. *Adv Pharmacol*. 1997;41:461-99.



27. Corazzari M, Gagliardi M, Fimia GM, Piacentini M. Endoplasmic Reticulum Stress, Unfolded Protein Response, and Cancer Cell Fate. *Front Oncol.* 2017;7:78.
28. Li P, Nijhawan D, Budihardjo I, Srinivasula SM, Ahmad M, Alnemri ES, et al. Cytochrome c and dATP-dependent formation of Apaf-1/caspase-9 complex initiates an apoptotic protease cascade. *Cell.* 1997;91(4):479-89.
29. Newton K, Strasser A, Kayagaki N, Dixit VM. Cell death. *Cell.* 2024;187(2):235-56.
30. Czabotar PE, Garcia-Saez AJ. Mechanisms of BCL-2 family proteins in mitochondrial apoptosis. *Nat Rev Mol Cell Biol.* 2023;24(10):732-48.
31. Dadsena S, Jenner A, Garcia-Saez AJ. Mitochondrial outer membrane permeabilization at the single molecule level. *Cell Mol Life Sci.* 2021;78(8):3777-90.
32. Montero J, Haq R. Adapted to Survive: Targeting Cancer Cells with BH3 Mimetics. *Cancer Discov.* 2022;12(5):1217-32.
33. Montero J, Letai A. Why do BCL-2 inhibitors work and where should we use them in the clinic? *Cell Death Differ.* 2018;25(1):56-64.
34. Tait SW, Green DR. Mitochondrial regulation of cell death. *Cold Spring Harb Perspect Biol.* 2013;5(9).
35. Ke FFS, Vanyai HK, Cowan AD, Delbridge ARD, Whitehead L, Grabow S, et al. Embryogenesis and Adult Life in the Absence of Intrinsic Apoptosis Effectors BAX, BAK, and BOK. *Cell.* 2018;173(5):1217-30 e17.
36. Shalaby R, Diwan A, Flores-Romero H, Hertlein V, Garcia-Saez AJ. Visualization of BOK pores independent of BAX and BAK reveals a similar mechanism with differing regulation. *Cell Death Differ.* 2023;30(3):731-41.
37. Llambi F, Wang YM, Victor B, Yang M, Schneider DM, Gingras S, et al. BOK Is a Non-canonical BCL-2 Family Effector of Apoptosis Regulated by ER-Associated Degradation. *Cell.* 2016;165(2):421-33.
38. Wei MC, Lindsten T, Mootha VK, Weiler S, Gross A, Ashiya M, et al. tBID, a membrane-targeted death ligand, oligomerizes BAK to release cytochrome c. *Genes & Development.* 2000;14(16):2060-71.
39. Gavathiotis E, Suzuki M, Davis ML, Pitter K, Bird GH, Katz SG, et al. BAX activation is initiated at a novel interaction site. *Nature.* 2008;455(7216):1076-81.
40. Sarosiek KA, Chi X, Bachman JA, Sims JJ, Montero J, Patel L, et al. BID preferentially activates BAK while BIM preferentially activates BAX, affecting chemotherapy response. *Mol Cell.* 2013;51(6):751-65.
41. Cheng EH, Wei MC, Weiler S, Flavell RA, Mak TW, Lindsten T, et al. BCL-2, BCL-X(L) sequester BH3 domain-only molecules preventing BAX- and BAK-mediated mitochondrial apoptosis. *Mol Cell.* 2001;8(3):705-11.
42. O'Neill KL, Huang K, Zhang J, Chen Y, Luo X. Inactivation of prosurvival Bcl-2 proteins activates Bax/Bak through the outer mitochondrial membrane. *Genes & Development.* 2016;30(8):973-88.
43. Letai A, Bassik MC, Walensky LD, Sorcinelli MD, Weiler S, Korsmeyer SJ. Distinct BH3 domains either sensitize or activate mitochondrial apoptosis, serving as prototype cancer therapeutics. *Cancer Cell.* 2002;2(3):183-92.
44. Chen L, Willis SN, Wei A, Smith BJ, Fletcher JI, Hinds MG, et al. Differential targeting of prosurvival Bcl-2 proteins by their BH3-only ligands allows complementary apoptotic function. *Mol Cell.* 2005;17(3):393-403.
45. Haupt Y, Maya R, Kazaz A, Oren M. Mdm2 promotes the rapid degradation of p53. *Nature.* 1997;387(6630):296-9.
46. Kubbutat MH, Jones SN, Vousden KH. Regulation of p53 stability by Mdm2. *Nature.* 1997;387(6630):299-303.
47. Aubrey BJ, Kelly GL, Janic A, Herold MJ, Strasser A. How does p53 induce apoptosis and how does this relate to p53-mediated tumour suppression? *Cell Death Differ.* 2018;25(1):104-13.
48. Riley T, Sontag E, Chen P, Levine A. Transcriptional control of human p53-regulated genes. *Nat Rev Mol Cell Biol.* 2008;9(5):402-12.
49. Kamada R, Toguchi Y, Nomura T, Imagawa T, Sakaguchi K. Tetramer formation of tumor suppressor protein p53: Structure, function, and applications. *Biopolymers.* 2016;106(4):598-612.
50. Laptenko O, Prives C. Transcriptional regulation by p53: one protein, many possibilities. *Cell Death Differ.* 2006;13(6):951-61.
51. Menendez D, Inga A, Resnick MA. The expanding universe of p53 targets. *Nat Rev Cancer.* 2009;9(10):724-37.

52. Cho Y, Gorina S, Jeffrey PD, Pavletich NP. Crystal structure of a p53 tumor suppressor-DNA complex: understanding tumorigenic mutations. *Science*. 1994;265(5170):346-55.
53. Wiederschain D, Kawai H, Shilatifard A, Yuan ZM. Multiple mixed lineage leukemia (MLL) fusion proteins suppress p53-mediated response to DNA damage. *J Biol Chem*. 2005;280(26):24315-21.
54. de Polo A, Luo Z, Gerarduzzi C, Chen X, Little JB, Yuan ZM. AXL receptor signalling suppresses p53 in melanoma through stabilization of the MDMX-MDM2 complex. *J Mol Cell Biol*. 2017;9(2):154-65.
55. Yang A, Kaghad M, Wang Y, Gillett E, Fleming MD, Dotsch V, et al. p63, a p53 homolog at 3q27-29, encodes multiple products with transactivating, death-inducing, and dominant-negative activities. *Mol Cell*. 1998;2(3):305-16.
56. Jost CA, Marin MC, Kaelin WG, Jr. p73 is a simian [correction of human] p53-related protein that can induce apoptosis. *Nature*. 1997;389(6647):191-4.
57. Kerr JB, Hutt KJ, Michalak EM, Cook M, Vandenberg CJ, Liew SH, et al. DNA damage-induced primordial follicle oocyte apoptosis and loss of fertility require TAp63-mediated induction of Puma and Noxa. *Mol Cell*. 2012;48(3):343-52.
58. Walczak H, Degli-Esposti MA, Johnson RS, Smolak PJ, Waugh JY, Boiani N, et al. TRAIL-R2: a novel apoptosis-mediating receptor for TRAIL. *EMBO J*. 1997;16(17):5386-97.
59. von Karstedt S, Montinaro A, Walczak H. Exploring the TRAILs less travelled: TRAIL in cancer biology and therapy. *Nat Rev Cancer*. 2017;17(6):352-66.
60. Dickens LS, Boyd RS, Jukes-Jones R, Hughes MA, Robinson GL, Fairall L, et al. A death effector domain chain DISC model reveals a crucial role for caspase-8 chain assembly in mediating apoptotic cell death. *Mol Cell*. 2012;47(2):291-305.
61. Hinz M, Scheidereit C. The I $\kappa$ B kinase complex in NF- $\kappa$ B regulation and beyond. *EMBO Rep*. 2014;15(1):46-61.
62. Lafont E, Kantari-Mimoun C, Draber P, De Miguel D, Hartwig T, Reichert M, et al. The linear ubiquitin chain assembly complex regulates TRAIL-induced gene activation and cell death. *EMBO J*. 2017;36(9):1147-66.
63. Peltzer N, Darding M, Montinaro A, Draber P, Draberova H, Kupka S, et al. LUBAC is essential for embryogenesis by preventing cell death and enabling haematopoiesis. *Nature*. 2018;557(7703):112-7.
64. Ofengeim D, Yuan J. Regulation of RIP1 kinase signalling at the crossroads of inflammation and cell death. *Nat Rev Mol Cell Biol*. 2013;14(11):727-36.
65. Degterev A, Hitomi J, Gemscheid M, Ch'en IL, Korkina O, Teng X, et al. Identification of RIP1 kinase as a specific cellular target of necrostatins. *Nat Chem Biol*. 2008;4(5):313-21.
66. Van Herreweghe F, Festjens N, Declercq W, Vandenameele P. Tumor necrosis factor-mediated cell death: to break or to burst, that's the question. *Cell Mol Life Sci*. 2010;67(10):1567-79.
67. Laurien L, Nagata M, Schunke H, Delanghe T, Wiederstein JL, Kumari S, et al. Autophosphorylation at serine 166 regulates RIP kinase 1-mediated cell death and inflammation. *Nat Commun*. 2020;11(1):1747.
68. Sun L, Wang H, Wang Z, He S, Chen S, Liao D, et al. Mixed lineage kinase domain-like protein mediates necrosis signaling downstream of RIP3 kinase. *Cell*. 2012;148(1-2):213-27.
69. Zhao J, Jitkaew S, Cai Z, Choksi S, Li Q, Luo J, et al. Mixed lineage kinase domain-like is a key receptor interacting protein 3 downstream component of TNF-induced necrosis. *Proc Natl Acad Sci U S A*. 2012;109(14):5322-7.
70. Samson AL, Zhang Y, Geoghegan ND, Gavin XJ, Davies KA, Mlodzianoski MJ, et al. MLKL trafficking and accumulation at the plasma membrane control the kinetics and threshold for necroptosis. *Nat Commun*. 2020;11(1):3151.
71. Ros U, Pena-Blanco A, Hanggi K, Kunzendorf U, Krautwald S, Wong WW, et al. Necroptosis Execution Is Mediated by Plasma Membrane Nanopores Independent of Calcium. *Cell Rep*. 2017;19(1):175-87.
72. Vercammen D, Brouckaert G, Denecker G, Van de Craen M, Declercq W, Fiers W, et al. Dual signaling of the Fas receptor: initiation of both apoptotic and necrotic cell death pathways. *J Exp Med*. 1998;188(5):919-30.
73. Pasparakis M, Vandenameele P. Necroptosis and its role in inflammation. *Nature*. 2015;517(7534):311-20.
74. Martinon F, Burns K, Tschopp J. The inflammasome: a molecular platform triggering activation of inflammatory caspases and processing of proIL- $\beta$ . *Mol Cell*. 2002;10(2):417-26.

75. Zheng D, Liwinski T, Elinav E. Inflammasome activation and regulation: toward a better understanding of complex mechanisms. *Cell Discov.* 2020;6:36.
76. Fernandes-Alnemri T, Yu JW, Juliana C, Solorzano L, Kang S, Wu J, et al. The AIM2 inflammasome is critical for innate immunity to *Francisella tularensis*. *Nat Immunol.* 2010;11(5):385-93.
77. Munoz-Planillo R, Kuffa P, Martinez-Colon G, Smith BL, Rajendiran TM, Nunez G. K(+) efflux is the common trigger of NLRP3 inflammasome activation by bacterial toxins and particulate matter. *Immunity.* 2013;38(6):1142-53.
78. Zhao Y, Yang J, Shi J, Gong YN, Lu Q, Xu H, et al. The NLR4 inflammasome receptors for bacterial flagellin and type III secretion apparatus. *Nature.* 2011;477(7366):596-600.
79. Hara H, Seregin SS, Yang D, Fukase K, Chamaillard M, Alnemri ES, et al. The NLRP6 Inflammasome Recognizes Lipoteichoic Acid and Regulates Gram-Positive Pathogen Infection. *Cell.* 2018;175(6):1651-64 e14.
80. Khare S, Dorfleutner A, Bryan NB, Yun C, Radian AD, de Almeida L, et al. An NLRP7-containing inflammasome mediates recognition of microbial lipopeptides in human macrophages. *Immunity.* 2012;36(3):464-76.
81. Shi J, Zhao Y, Wang Y, Gao W, Ding J, Li P, et al. Inflammatory caspases are innate immune receptors for intracellular LPS. *Nature.* 2014;514(7521):187-92.
82. Shi J, Zhao Y, Wang K, Shi X, Wang Y, Huang H, et al. Cleavage of GSDMD by inflammatory caspases determines pyroptotic cell death. *Nature.* 2015;526(7575):660-5.
83. Wang K, Sun Q, Zhong X, Zeng M, Zeng H, Shi X, et al. Structural Mechanism for GSDMD Targeting by Autoprocessed Caspases in Pyroptosis. *Cell.* 2020;180(5):941-55 e20.
84. Bauernfeind FG, Horvath G, Stutz A, Alnemri ES, MacDonald K, Speert D, et al. Cutting edge: NF-kappaB activating pattern recognition and cytokine receptors license NLRP3 inflammasome activation by regulating NLRP3 expression. *J Immunol.* 2009;183(2):787-91.
85. Swanson KV, Deng M, Ting JP. The NLRP3 inflammasome: molecular activation and regulation to therapeutics. *Nat Rev Immunol.* 2019;19(8):477-89.
86. Song N, Liu ZS, Xue W, Bai ZF, Wang QY, Dai J, et al. NLRP3 Phosphorylation Is an Essential Priming Event for Inflammasome Activation. *Mol Cell.* 2017;68(1):185-97 e6.
87. De Schutter E, Roelandt R, Riquet FB, Van Camp G, Wullaert A, Vandenabeele P. Punching Holes in Cellular Membranes: Biology and Evolution of Gasdermins. *Trends Cell Biol.* 2021;31(6):500-13.
88. Saeki N, Kuwahara Y, Sasaki H, Satoh H, Shiroishi T. Gasdermin (Gsdm) localizing to mouse Chromosome 11 is predominantly expressed in upper gastrointestinal tract but significantly suppressed in human gastric cancer cells. *Mamm Genome.* 2000;11(9):718-24.
89. Rogers C, Erkes DA, Nardone A, Aplin AE, Fernandes-Alnemri T, Alnemri ES. Gasdermin pores permeabilize mitochondria to augment caspase-3 activation during apoptosis and inflammasome activation. *Nat Commun.* 2019;10(1):1689.
90. Ruan J, Xia S, Liu X, Lieberman J, Wu H. Cryo-EM structure of the gasdermin A3 membrane pore. *Nature.* 2018;557(7703):62-7.
91. Liu X, Zhang Z, Ruan J, Pan Y, Magupalli VG, Wu H, et al. Inflammasome-activated gasdermin D causes pyroptosis by forming membrane pores. *Nature.* 2016;535(7610):153-8.
92. Symmank J, Jacobs C, Schulze-Spate U. Suicide signaling by GSDMA: a single-molecule mechanism for recognition and defense against SpeB-expressing GAS. *Signal Transduct Target Ther.* 2022;7(1):153.
93. Zhou Z, He H, Wang K, Shi X, Wang Y, Su Y, et al. Granzyme A from cytotoxic lymphocytes cleaves GSDMB to trigger pyroptosis in target cells. *Science.* 2020;368(6494).
94. Wang S, Chang CW, Huang J, Zeng S, Zhang X, Hung MC, et al. Gasdermin C sensitizes tumor cells to PARP inhibitor therapy in cancer models. *J Clin Invest.* 2024;134(1).
95. Burgener SS, Leborgne NGF, Snipas SJ, Salvesen GS, Bird PI, Benarafa C. Cathepsin G Inhibition by Serpinb1 and Serpinb6 Prevents Programmed Necrosis in Neutrophils and Monocytes and Reduces GSDMD-Driven Inflammation. *Cell Rep.* 2019;27(12):3646-56 e5.
96. Rogers C, Fernandes-Alnemri T, Mayes L, Alnemri D, Cingolani G, Alnemri ES. Cleavage of DFNA5 by caspase-3 during apoptosis mediates progression to secondary necrotic/pyroptotic cell death. *Nat Commun.* 2017;8:14128.
97. Miao R, Jiang C, Chang WY, Zhang H, An J, Ho F, et al. Gasdermin D permeabilization of mitochondrial inner and outer membranes accelerates and enhances pyroptosis. *Immunity.* 2023;56(11):2523-41 e8.
98. Hanahan D, Weinberg RA. Hallmarks of cancer: the next generation. *Cell.* 2011;144(5):646-74.

99. Hanahan D. Hallmarks of Cancer: New Dimensions. *Cancer Discov.* 2022;12(1):31-46.
100. Vaddavalli PL, Schumacher B. The p53 network: cellular and systemic DNA damage responses in cancer and aging. *Trends Genet.* 2022;38(6):598-612.
101. DeVita VT, Jr., Chu E. A history of cancer chemotherapy. *Cancer Res.* 2008;68(21):8643-53.
102. Strasser A, Vaux DL. Cell Death in the Origin and Treatment of Cancer. *Mol Cell.* 2020;78(6):1045-54.
103. Tsujimoto Y. Stress-resistance conferred by high level of bcl-2 alpha protein in human B lymphoblastoid cell. *Oncogene.* 1989;4(11):1331-6.
104. McDonnell TJ, Deane N, Platt FM, Nunez G, Jaeger U, McKearn JP, et al. bcl-2-immunoglobulin transgenic mice demonstrate extended B cell survival and follicular lymphoproliferation. *Cell.* 1989;57(1):79-88.
105. Villunger A, Michalak EM, Coultas L, Mullauer F, Bock G, Ausserlechner MJ, et al. p53- and drug-induced apoptotic responses mediated by BH3-only proteins puma and noxa. *Science.* 2003;302(5647):1036-8.
106. Bouillet P, Metcalf D, Huang DC, Tarlinton DM, Kay TW, Kontgen F, et al. Proapoptotic Bcl-2 relative Bim required for certain apoptotic responses, leukocyte homeostasis, and to preclude autoimmunity. *Science.* 1999;286(5445):1735-8.
107. Turajlic S, Sottoriva A, Graham T, Swanton C. Resolving genetic heterogeneity in cancer. *Nat Rev Genet.* 2019;20(7):404-16.
108. Aggarwal BB. Signalling pathways of the TNF superfamily: a double-edged sword. *Nat Rev Immunol.* 2003;3(9):745-56.
109. Kinkhabwala M, Sehajpal P, Skolnik E, Smith D, Sharma VK, Vlassara H, et al. A novel addition to the T cell repertory. Cell surface expression of tumor necrosis factor/cachectin by activated normal human T cells. *J Exp Med.* 1990;171(3):941-6.
110. Lowin B, Hahne M, Mattmann C, Tschopp J. Cytolytic T-cell cytotoxicity is mediated through perforin and Fas lytic pathways. *Nature.* 1994;370(6491):650-2.
111. Voskoboinik I, Whisstock JC, Trapani JA. Perforin and granzymes: function, dysfunction and human pathology. *Nat Rev Immunol.* 2015;15(6):388-400.
112. Zhang Z, Zhang Y, Xia S, Kong Q, Li S, Liu X, et al. Gasdermin E suppresses tumour growth by activating anti-tumour immunity. *Nature.* 2020;579(7799):415-20.
113. de Souza Fernandez Pereira M, Carr DR, Gatti-Mays ME, Olsen MR, Setty BA, Shahwan KT, et al. Natural Killer Cell Recognition and Control of Epithelial Cancers. *Cancer J.* 2022;28(4):263-9.
114. Arasanz H, Gato-Canas M, Zuazo M, Ibanez-Vea M, Breckpot K, Kochan G, et al. PD1 signal transduction pathways in T cells. *Oncotarget.* 2017;8(31):51936-45.
115. Estimated age-standardized mortality rates (World) 2020. 2020.
116. Harbour JW, Lai SL, Whang-Peng J, Gazdar AF, Minna JD, Kaye FJ. Abnormalities in structure and expression of the human retinoblastoma gene in SCLC. *Science.* 1988;241(4863):353-7.
117. Rudin CM, Brambilla E, Faivre-Finn C, Sage J. Small-cell lung cancer. *Nat Rev Dis Primers.* 2021;7(1):3.
118. Johnson DG, Schneider-Broussard R. Role of E2F in cell cycle control and cancer. *Front Biosci.* 1998;3:d447-8.
119. Weinberg RA. The retinoblastoma protein and cell cycle control. *Cell.* 1995;81(3):323-30.
120. Henley SA, Dick FA. The retinoblastoma family of proteins and their regulatory functions in the mammalian cell division cycle. *Cell Div.* 2012;7(1):10.
121. George J, Lim JS, Jang SJ, Cun Y, Ozretic L, Kong G, et al. Comprehensive genomic profiles of small cell lung cancer. *Nature.* 2015;524(7563):47-53.
122. Jackman DM, Yeap BY, Sequist LV, Lindeman N, Holmes AJ, Joshi VA, et al. Exon 19 deletion mutations of epidermal growth factor receptor are associated with prolonged survival in non-small cell lung cancer patients treated with gefitinib or erlotinib. *Clin Cancer Res.* 2006;12(13):3908-14.
123. Rosell R, Moran T, Queralt C, Porta R, Cardenal F, Camps C, et al. Screening for epidermal growth factor receptor mutations in lung cancer. *N Engl J Med.* 2009;361(10):958-67.
124. Yarden Y, Sliwkowski MX. Untangling the ErbB signalling network. *Nat Rev Mol Cell Biol.* 2001;2(2):127-37.
125. Dogan S, Shen R, Ang DC, Johnson ML, D'Angelo SP, Paik PK, et al. Molecular epidemiology of EGFR and KRAS mutations in 3,026 lung adenocarcinomas: higher susceptibility of women to smoking-related KRAS-mutant cancers. *Clin Cancer Res.* 2012;18(22):6169-77.
126. Tomasini P, Walia P, Labbe C, Jao K, Leighl NB. Targeting the KRAS Pathway in Non-Small Cell Lung Cancer. *Oncologist.* 2016;21(12):1450-60.

127. Cascetta P, Marinello A, Lazzari C, Gregorc V, Planchard D, Bianco R, et al. KRAS in NSCLC: State of the Art and Future Perspectives. *Cancers (Basel)*. 2022;14(21).
128. Wu YL, Cheng Y, Zhou X, Lee KH, Nakagawa K, Niho S, et al. Dacomitinib versus gefitinib as first-line treatment for patients with EGFR-mutation-positive non-small-cell lung cancer (ARCHER 1050): a randomised, open-label, phase 3 trial. *Lancet Oncol*. 2017;18(11):1454-66.
129. Janne PA, Riely GJ, Gadgeel SM, Heist RS, Ou SI, Pacheco JM, et al. Adagrasib in Non-Small-Cell Lung Cancer Harboring a KRAS(G12C) Mutation. *N Engl J Med*. 2022;387(2):120-31.
130. Nakajima EC, Drezner N, Li X, Mishra-Kalyani PS, Liu Y, Zhao H, et al. FDA Approval Summary: Sotorasib for KRAS G12C-Mutated Metastatic NSCLC. *Clin Cancer Res*. 2022;28(8):1482-6.
131. Meuwissen R, Linn SC, Linnoila RI, Zevenhoven J, Mooi WJ, Berns A. Induction of small cell lung cancer by somatic inactivation of both Trp53 and Rb1 in a conditional mouse model. *Cancer Cell*. 2003;4(3):181-9.
132. Ferone G, Lee MC, Sage J, Berns A. Cells of origin of lung cancers: lessons from mouse studies. *Genes Dev*. 2020;34(15-16):1017-32.
133. Park KS, Liang MC, Raiser DM, Zamponi R, Roach RR, Curtis SJ, et al. Characterization of the cell of origin for small cell lung cancer. *Cell Cycle*. 2011;10(16):2806-15.
134. Sutherland KD, Proost N, Brouns I, Adriaensen D, Song JY, Berns A. Cell of origin of small cell lung cancer: inactivation of Trp53 and Rb1 in distinct cell types of adult mouse lung. *Cancer Cell*. 2011;19(6):754-64.
135. Yang D, Denny SK, Greenside PG, Chaikovsky AC, Brady JJ, Ouadah Y, et al. Intertumoral Heterogeneity in SCLC Is Influenced by the Cell Type of Origin. *Cancer Discov*. 2018;8(10):1316-31.
136. Xu J, Yu H, Sun X. Less Is More: Rare Pulmonary Neuroendocrine Cells Function as Critical Sensors in Lung. *Dev Cell*. 2020;55(2):123-32.
137. Ireland AS, Micinski AM, Kastner DW, Guo B, Wait SJ, Spainhower KB, et al. MYC Drives Temporal Evolution of Small Cell Lung Cancer Subtypes by Reprogramming Neuroendocrine Fate. *Cancer Cell*. 2020;38(1):60-78 e12.
138. George J, Maas L, Abedpour N, Cartolano M, Kaiser L, Fischer RN, et al. Evolutionary trajectories of small cell lung cancer under therapy. *Nature*. 2024;627(8005):880-9.
139. Gay CM, Stewart CA, Park EM, Diao L, Groves SM, Heeke S, et al. Patterns of transcription factor programs and immune pathway activation define four major subtypes of SCLC with distinct therapeutic vulnerabilities. *Cancer Cell*. 2021;39(3):346-60 e7.
140. Pearsall SM, Humphrey S, Revill M, Morgan D, Frese KK, Galvin M, et al. The Rare YAP1 Subtype of SCLC Revisited in a Biobank of 39 Circulating Tumor Cell Patient Derived Explant Models: A Brief Report. *J Thorac Oncol*. 2020;15(12):1836-43.
141. Qu S, Fetsch P, Thomas A, Pommier Y, Schrupp DS, Miettinen MM, et al. Molecular Subtypes of Primary SCLC Tumors and Their Associations With Neuroendocrine and Therapeutic Markers. *J Thorac Oncol*. 2022;17(1):141-53.
142. Baine MK, Hsieh MS, Lai WV, Egger JV, Jungbluth AA, Daneshbod Y, et al. SCLC Subtypes Defined by ASCL1, NEUROD1, POU2F3, and YAP1: A Comprehensive Immunohistochemical and Histopathologic Characterization. *J Thorac Oncol*. 2020;15(12):1823-35.
143. Szeitz B, Megyesfalvi Z, Woldmar N, Valko Z, Schwendenwein A, Barany N, et al. In-depth proteomic analysis reveals unique subtype-specific signatures in human small-cell lung cancer. *Clin Transl Med*. 2022;12(9):e1060.
144. Ng J, Cai L, Girard L, Prall OWJ, Rajan N, Khoo C, et al. Molecular and Pathologic Characterization of YAP1-Expressing Small Cell Lung Cancer Cell Lines Leads to Reclassification as SMARCA4-Deficient Malignancies. *Clin Cancer Res*. 2024;30(9):1846-58.
145. Steffens CC, Elender C, Hutzschenreuter U, Dille S, Binnering A, Spring L, et al. Treatment and outcome of 432 patients with extensive-stage small cell lung cancer in first, second and third line - Results from the prospective German TLK cohort study. *Lung Cancer*. 2019;130:216-25.
146. Meriggi F. Second-Line Treatment Options for Small-Cell Lung Cancer: A Light at the End of the Tunnel. *Cancers (Basel)*. 2024;16(2).
147. Shi H, Guo N, Zhao Z, Liu L, Ni T, Zhang J, et al. Comparison of the second-line treatments for patients with small cell lung cancer sensitive to previous platinum-based chemotherapy: A systematic review and Bayesian network analysis. *Front Oncol*. 2023;13:1154685.
148. Boon NJ, Oliveira RA, Korner PR, Kochavi A, Mertens S, Malka Y, et al. DNA damage induces p53-independent apoptosis through ribosome stalling. *Science*. 2024;384(6697):785-92.

149. Liu SV, Reck M, Mansfield AS, Mok T, Scherpereel A, Reinmuth N, et al. Updated Overall Survival and PD-L1 Subgroup Analysis of Patients With Extensive-Stage Small-Cell Lung Cancer Treated With Atezolizumab, Carboplatin, and Etoposide (IMpower133). *J Clin Oncol*. 2021;39(6):619-30.
150. Malumbres M. Cyclin-dependent kinases. *Genome Biol*. 2014;15(6):122.
151. Ding L, Cao J, Lin W, Chen H, Xiong X, Ao H, et al. The Roles of Cyclin-Dependent Kinases in Cell-Cycle Progression and Therapeutic Strategies in Human Breast Cancer. *Int J Mol Sci*. 2020;21(6).
152. Fujinaga K, Huang F, Peterlin BM. P-TEFb: The master regulator of transcription elongation. *Mol Cell*. 2023;83(3):393-403.
153. Cramer P. Eukaryotic Transcription Turns 50. *Cell*. 2019;179(4):808-12.
154. Egloff S. CDK9 keeps RNA polymerase II on track. *Cell Mol Life Sci*. 2021;78(14):5543-67.
155. Yamaguchi Y, Inukai N, Narita T, Wada T, Handa H. Evidence that negative elongation factor represses transcription elongation through binding to a DRB sensitivity-inducing factor/RNA polymerase II complex and RNA. *Mol Cell Biol*. 2002;22(9):2918-27.
156. Huang KL, Jee D, Stein CB, Elrod ND, Henriques T, Mascibroda LG, et al. Integrator Recruits Protein Phosphatase 2A to Prevent Pause Release and Facilitate Transcription Termination. *Mol Cell*. 2020;80(2):345-58 e9.
157. Barboric M, Nissen RM, Kanazawa S, Jabrane-Ferrat N, Peterlin BM. NF-kappaB binds P-TEFb to stimulate transcriptional elongation by RNA polymerase II. *Mol Cell*. 2001;8(2):327-37.
158. Kanazawa S, Soucek L, Evan G, Okamoto T, Peterlin BM. c-Myc recruits P-TEFb for transcription, cellular proliferation and apoptosis. *Oncogene*. 2003;22(36):5707-11.
159. Eberhardy SR, Farnham PJ. Myc recruits P-TEFb to mediate the final step in the transcriptional activation of the cad promoter. *J Biol Chem*. 2002;277(42):40156-62.
160. Chao SH, Fujinaga K, Marion JE, Taube R, Sausville EA, Senderowicz AM, et al. Flavopiridol inhibits P-TEFb and blocks HIV-1 replication. *J Biol Chem*. 2000;275(37):28345-8.
161. Lemke J, von Karstedt S, Abd El Hay M, Conti A, Arce F, Montinaro A, et al. Selective CDK9 inhibition overcomes TRAIL resistance by concomitant suppression of cFlip and Mcl-1. *Cell Death Differ*. 2014;21(3):491-502.
162. Montinaro A, Areso Zubiaur I, Saggau J, Kretz AL, Ferreira RMM, Hassan O, et al. Potent pro-apoptotic combination therapy is highly effective in a broad range of cancers. *Cell Death Differ*. 2022;29(3):492-503.
163. Ghia P, Scarfo L, Perez S, Pathiraja K, Derosier M, Small K, et al. Efficacy and safety of dinaciclib vs ofatumumab in patients with relapsed/refractory chronic lymphocytic leukemia. *Blood*. 2017;129(13):1876-8.
164. Olson CM, Jiang B, Erb MA, Liang Y, Doctor ZM, Zhang Z, et al. Pharmacological perturbation of CDK9 using selective CDK9 inhibition or degradation. *Nat Chem Biol*. 2018;14(2):163-70.
165. Hossain DMS, Javaid S, Cai M, Zhang C, Sawant A, Hinton M, et al. Dinaciclib induces immunogenic cell death and enhances anti-PD1-mediated tumor suppression. *J Clin Invest*. 2018;128(2):644-54.
166. Booher RN, Hatch H, Dolinski BM, Nguyen T, Harmonay L, Al-Assaad AS, et al. MCL1 and BCL-xL levels in solid tumors are predictive of dinaciclib-induced apoptosis. *PLoS One*. 2014;9(10):e108371.
167. Galli GG, Carrara M, Yuan WC, Valdes-Quezada C, Gurung B, Pepe-Mooney B, et al. YAP Drives Growth by Controlling Transcriptional Pause Release from Dynamic Enhancers. *Mol Cell*. 2015;60(2):328-37.
168. DuPage M, Dooley AL, Jacks T. Conditional mouse lung cancer models using adenoviral or lentiviral delivery of Cre recombinase. *Nat Protoc*. 2009;4(7):1064-72.
169. Alcon C, Martin F, Prada E, Mora J, Soriano A, Guillen G, et al. MEK and MCL-1 sequential inhibition synergize to enhance rhabdomyosarcoma treatment. *Cell Death Discov*. 2022;8(1):172.
170. Lovell JF, Billen LP, Bindner S, Shamas-Din A, Fradin C, Leber B, et al. Membrane binding by tBid initiates an ordered series of events culminating in membrane permeabilization by Bax. *Cell*. 2008;135(6):1074-84.
171. Ke C, Hou H, Su K, Huang C, Yuan Q, Li S, et al. Extracellular vesicle-mediated co-delivery of TRAIL and dinaciclib for targeted therapy of resistant tumors. *Biomater Sci*. 2022;10(6):1498-514.
172. Bebbler CM, Thomas ES, Stroh J, Chen Z, Androulidaki A, Schmitt A, et al. Ferroptosis response segregates small cell lung cancer (SCLC) neuroendocrine subtypes. *Nat Commun*. 2021;12(1):2048.

173. Hopkins-Donaldson S, Ziegler A, Kurtz S, Bigosch C, Kandioler D, Ludwig C, et al. Silencing of death receptor and caspase-8 expression in small cell lung carcinoma cell lines and tumors by DNA methylation. *Cell Death Differ.* 2003;10(3):356-64.
174. Valdez Capuccino L, Kleitke T, Szokol B, Svajda L, Martin F, Bonechi F, et al. CDK9 inhibition as an effective therapy for small cell lung cancer. *Cell Death Dis.* 2024;15(5):345.
175. Mita MM, Joy AA, Mita A, Sankhala K, Jou YM, Zhang D, et al. Randomized phase II trial of the cyclin-dependent kinase inhibitor dinaciclib (MK-7965) versus capecitabine in patients with advanced breast cancer. *Clin Breast Cancer.* 2014;14(3):169-76.
176. Kumar SK, LaPlant B, Chng WJ, Zonder J, Callander N, Fonseca R, et al. Dinaciclib, a novel CDK inhibitor, demonstrates encouraging single-agent activity in patients with relapsed multiple myeloma. *Blood.* 2015;125(3):443-8.
177. Flynn J, Jones J, Johnson AJ, Andritsos L, Maddocks K, Jaglowski S, et al. Dinaciclib is a novel cyclin-dependent kinase inhibitor with significant clinical activity in relapsed and refractory chronic lymphocytic leukemia. *Leukemia.* 2015;29(7):1524-9.
178. Gregory GP, Kumar S, Wang D, Mahadevan D, Walker P, Wagner-Johnston N, et al. Pembrolizumab plus dinaciclib in patients with hematologic malignancies: the phase 1b KEYNOTE-155 study. *Blood Adv.* 2022;6(4):1232-42.
179. van der Loo JC, Hanenberg H, Cooper RJ, Luo FY, Lazaridis EN, Williams DA. Nonobese diabetic/severe combined immunodeficiency (NOD/SCID) mouse as a model system to study the engraftment and mobilization of human peripheral blood stem cells. *Blood.* 1998;92(7):2556-70.
180. Gregory GP, Hogg SJ, Kats LM, Vidacs E, Baker AJ, Gilan O, et al. CDK9 inhibition by dinaciclib potently suppresses Mcl-1 to induce durable apoptotic responses in aggressive MYC-driven B-cell lymphoma in vivo. *Leukemia.* 2015;29(6):1437-41.
181. Inoue-Yamauchi A, Jeng PS, Kim K, Chen HC, Han S, Ganesan YT, et al. Targeting the differential addiction to anti-apoptotic BCL-2 family for cancer therapy. *Nat Commun.* 2017;8:16078.
182. Varadarajan S, Poornima P, Milani M, Gowda K, Amin S, Wang HG, et al. Maritocloxacin and dinaciclib inhibit MCL-1 activity and induce apoptosis in both a MCL-1-dependent and -independent manner. *Oncotarget.* 2015;6(14):12668-81.
183. Belyanskaya LL, Ziogas A, Hopkins-Donaldson S, Kurtz S, Simon HU, Stahel R, et al. TRAIL-induced survival and proliferation of SCLC cells is mediated by ERK and dependent on TRAIL-R2/DR5 expression in the absence of caspase-8. *Lung Cancer.* 2008;60(3):355-65.
184. Horn L, Mansfield AS, Szczesna A, Havel L, Krzakowski M, Hochmair MJ, et al. First-Line Atezolizumab plus Chemotherapy in Extensive-Stage Small-Cell Lung Cancer. *N Engl J Med.* 2018;379(23):2220-9.
185. Nemunaitis JJ, Small KA, Kirschmeier P, Zhang D, Zhu Y, Jou YM, et al. A first-in-human, phase 1, dose-escalation study of dinaciclib, a novel cyclin-dependent kinase inhibitor, administered weekly in subjects with advanced malignancies. *J Transl Med.* 2013;11:259.
186. Xu T, Wang Z, Liu J, Wang G, Zhou D, Du Y, et al. Cyclin-Dependent Kinase Inhibitors Function as Potential Immune Regulators via Inducing Pyroptosis in Triple Negative Breast Cancer. *Front Oncol.* 2022;12:820696.
187. Mansfield AS, Kazarnowicz A, Karaseva N, Sanchez A, De Boer R, Andric Z, et al. Safety and patient-reported outcomes of atezolizumab, carboplatin, and etoposide in extensive-stage small-cell lung cancer (IMpower133): a randomized phase I/III trial. *Ann Oncol.* 2020;31(2):310-7.
188. Sharma SV, Lee DY, Li B, Quinlan MP, Takahashi F, Maheswaran S, et al. A chromatin-mediated reversible drug-tolerant state in cancer cell subpopulations. *Cell.* 2010;141(1):69-80.
189. Yashiro-Ohtani Y, Wang H, Zang C, Arnett KL, Bailis W, Ho Y, et al. Long-range enhancer activity determines Myc sensitivity to Notch inhibitors in T cell leukemia. *Proc Natl Acad Sci U S A.* 2014;111(46):E4946-53.
190. Lu H, Xue Y, Yu GK, Arias C, Lin J, Fong S, et al. Compensatory induction of MYC expression by sustained CDK9 inhibition via a BRD4-dependent mechanism. *Elife.* 2015;4:e06535.
191. Kubickova A, De Sanctis JB, Hajduch M. Isoform-Directed Control of c-Myc Functions: Understanding the Balance from Proliferation to Growth Arrest. *Int J Mol Sci.* 2023;24(24).
192. Sato K, Masuda T, Hu Q, Tobo T, Gillaspie S, Niida A, et al. Novel oncogene 5MP1 reprograms c-Myc translation initiation to drive malignant phenotypes in colorectal cancer. *EBioMedicine.* 2019;44:387-402.
193. Hann SR, King MW, Bentley DL, Anderson CW, Eisenman RN. A non-AUG translational initiation in c-myc exon 1 generates an N-terminally distinct protein whose synthesis is disrupted in Burkitt's lymphomas. *Cell.* 1988;52(2):185-95.

194. Hann SR, Dixit M, Sears RC, Sealy L. The alternatively initiated c-Myc proteins differentially regulate transcription through a noncanonical DNA-binding site. *Genes Dev.* 1994;8(20):2441-52.
195. Vita M, Henriksson M. The Myc oncoprotein as a therapeutic target for human cancer. *Semin Cancer Biol.* 2006;16(4):318-30.
196. Mossafa H, Damotte D, Jenabian A, Delarue R, Vincenneau A, Amouroux I, et al. Non-Hodgkin's lymphomas with Burkitt-like cells are associated with c-Myc amplification and poor prognosis. *Leuk Lymphoma.* 2006;47(9):1885-93.
197. Pelengaris S, Khan M, Evan G. c-MYC: more than just a matter of life and death. *Nat Rev Cancer.* 2002;2(10):764-76.
198. Wang C, Zhang J, Yin J, Gan Y, Xu S, Gu Y, et al. Alternative approaches to target Myc for cancer treatment. *Signal Transduct Target Ther.* 2021;6(1):117.
199. Bottger F, Semenova EA, Song JY, Ferone G, van der Vliet J, Cozijnsen M, et al. Tumor Heterogeneity Underlies Differential Cisplatin Sensitivity in Mouse Models of Small-Cell Lung Cancer. *Cell Rep.* 2019;27(11):3345-58 e4.
200. Rudin CM, Poirier JT, Byers LA, Dive C, Dowlati A, George J, et al. Molecular subtypes of small cell lung cancer: a synthesis of human and mouse model data. *Nature Reviews Cancer.* 2019;19(5):289-97.
201. Zhang H, Christensen CL, Dries R, Oser MG, Deng J, Diskin B, et al. CDK7 Inhibition Potentiates Genome Instability Triggering Anti-tumor Immunity in Small Cell Lung Cancer. *Cancer Cell.* 2020;37(1):37-54 e9.
202. Sun Y, Zhang Y, Schultz CW, Pommier Y, Thomas A. CDK7 Inhibition Synergizes with Topoisomerase I Inhibition in Small Cell Lung Cancer Cells by Inducing Ubiquitin-Mediated Proteolysis of RNA Polymerase II. *Mol Cancer Ther.* 2022;21(9):1430-8.
203. Christensen CL, Kwiatkowski N, Abraham BJ, Carretero J, Al-Shahrour F, Zhang T, et al. Targeting transcriptional addictions in small cell lung cancer with a covalent CDK7 inhibitor. *Cancer Cell.* 2014;26(6):909-22.
204. Heath EI, Bible K, Martell RE, Adelman DC, Lorusso PM. A phase 1 study of SNS-032 (formerly BMS-387032), a potent inhibitor of cyclin-dependent kinases 2, 7 and 9 administered as a single oral dose and weekly infusion in patients with metastatic refractory solid tumors. *Invest New Drugs.* 2008;26(1):59-65.
205. Stephenson JJ, Nemunaitis J, Joy AA, Martin JC, Jou YM, Zhang D, et al. Randomized phase 2 study of the cyclin-dependent kinase inhibitor dinaciclib (MK-7965) versus erlotinib in patients with non-small cell lung cancer. *Lung Cancer.* 2014;83(2):219-23.
206. Gojo I, Sadowska M, Walker A, Feldman EJ, Iyer SP, Baer MR, et al. Clinical and laboratory studies of the novel cyclin-dependent kinase inhibitor dinaciclib (SCH 727965) in acute leukemias. *Cancer Chemother Pharmacol.* 2013;72(4):897-908.
207. Hu C, Shen L, Zou F, Wu Y, Wang B, Wang A, et al. Predicting and overcoming resistance to CDK9 inhibitors for cancer therapy. *Acta Pharm Sin B.* 2023;13(9):3694-707.
208. Lu H, Zhang S, Wu J, Chen M, Cai MC, Fu Y, et al. Molecular Targeted Therapies Elicit Concurrent Apoptotic and GSDME-Dependent Pyroptotic Tumor Cell Death. *Clin Cancer Res.* 2018;24(23):6066-77.
209. Wang CJ, Tang L, Shen DW, Wang C, Yuan QY, Gao W, et al. The expression and regulation of DFNA5 in human hepatocellular carcinoma DFNA5 in hepatocellular carcinoma. *Mol Biol Rep.* 2013;40(12):6525-31.
210. Lage H, Helmbach H, Grottko C, Dietel M, Schadendorf D. DFNA5 (ICERE-1) contributes to acquired etoposide resistance in melanoma cells. *FEBS Lett.* 2001;494(1-2):54-9.
211. Peng LS, Duan SL, Li RQ, Wang D, Han YY, Huang T, et al. Prognostic value and immune infiltration of the gasdermin family in lung adenocarcinoma. *Front Oncol.* 2022;12:1043862.
212. Liu Z, Liu H, Dong Q, Li H, Zhang B, Liu Y, et al. Prognostic role of DFNA5 in head and neck squamous cell carcinoma revealed by systematic expression analysis. *BMC Cancer.* 2021;21(1):951.
213. Guo J, Yu J, Mu M, Chen Z, Xu Z, Zhao C, et al. DFNA5 inhibits colorectal cancer proliferation by suppressing the mTORC1/2 signaling pathways via upregulation of DEPTOR. *Cell Cycle.* 2022;21(20):2165-78.
214. Xu L, Shi F, Wu Y, Yao S, Wang Y, Jiang X, et al. Gasdermin E regulates the stability and activation of EGFR in human non-small cell lung cancer cells. *Cell Commun Signal.* 2023;21(1):83.
215. Akino K, Toyota M, Suzuki H, Imai T, Maruyama R, Kusano M, et al. Identification of DFNA5 as a target of epigenetic inactivation in gastric cancer. *Cancer Sci.* 2007;98(1):88-95.



216. Kim MS, Chang X, Yamashita K, Nagpal JK, Baek JH, Wu G, et al. Aberrant promoter methylation and tumor suppressive activity of the DFNA5 gene in colorectal carcinoma. *Oncogene*. 2008;27(25):3624-34.
217. Fujikane T, Nishikawa N, Toyota M, Suzuki H, Nojima M, Maruyama R, et al. Genomic screening for genes upregulated by demethylation revealed novel targets of epigenetic silencing in breast cancer. *Breast Cancer Res Treat*. 2010;122(3):699-710.
218. Croes L, Beyens M, Franssen E, Ibrahim J, Vanden Berghe W, Suls A, et al. Large-scale analysis of DFNA5 methylation reveals its potential as biomarker for breast cancer. *Clin Epigenetics*. 2018;10:51.
219. Huo CL, Deng Y, Sun ZG. A comprehensive analysis of gasdermin family gene as therapeutic targets in pan-cancer. *Sci Rep*. 2022;12(1):13329.
220. Zhou B, Abbott DW. Gasdermin E permits interleukin-1 beta release in distinct sublytic and pyroptotic phases. *Cell Rep*. 2021;35(2):108998.
221. Wang Y, Gao W, Shi X, Ding J, Liu W, He H, et al. Chemotherapy drugs induce pyroptosis through caspase-3 cleavage of a gasdermin. *Nature*. 2017;547(7661):99-103.
222. Xuzhang W, Lu T, Jin W, Yu Y, Li Z, Shen L, et al. Cisplatin-induced Pyroptosis Enhances the Efficacy of PD-L1 Inhibitor in Small-Cell Lung Cancer via GSDME/IL12/CD4Tem Axis. *Int J Biol Sci*. 2024;20(2):537-53.
223. Ebner S, Ratzinger G, Krosbacher B, Schmutz M, Weiss A, Reider D, et al. Production of IL-12 by human monocyte-derived dendritic cells is optimal when the stimulus is given at the onset of maturation, and is further enhanced by IL-4. *J Immunol*. 2001;166(1):633-41.
224. Airoidi I, Guglielmino R, Carra G, Corcione A, Gerosa F, Taborelli G, et al. The interleukin-12 and interleukin-12 receptor system in normal and transformed human B lymphocytes. *Haematologica*. 2002;87(4):434-42.
225. Liu J, Cao S, Kim S, Chung EY, Homma Y, Guan X, et al. Interleukin-12: an update on its immunological activities, signaling and regulation of gene expression. *Curr Immunol Rev*. 2005;1(2):119-37.
226. Trinchieri G. Interleukin-12 and the regulation of innate resistance and adaptive immunity. *Nat Rev Immunol*. 2003;3(2):133-46.
227. Tait Wojno ED, Hunter CA, Stumhofer JS. The Immunobiology of the Interleukin-12 Family: Room for Discovery. *Immunity*. 2019;50(4):851-70.
228. Rudin CM, Poirier JT, Byers LA, Dive C, Dowlati A, George J, et al. Molecular subtypes of small cell lung cancer: a synthesis of human and mouse model data. *Nat Rev Cancer*. 2019;19(5):289-97.
229. Dammert MA, Bragelmann J, Olsen RR, Bohm S, Monhasery N, Whitney CP, et al. MYC paralog-dependent apoptotic priming orchestrates a spectrum of vulnerabilities in small cell lung cancer. *Nat Commun*. 2019;10(1):3485.
230. Chalishazar MD, Wait SJ, Huang F, Ireland AS, Mukhopadhyay A, Lee Y, et al. MYC-Driven Small-Cell Lung Cancer is Metabolically Distinct and Vulnerable to Arginine Depletion. *Clin Cancer Res*. 2019;25(16):5107-21.
231. Cardnell RJ, Li L, Sen T, Bara R, Tong P, Fujimoto J, et al. Protein expression of TTF1 and cMYC define distinct molecular subgroups of small cell lung cancer with unique vulnerabilities to aurora kinase inhibition, DLL3 targeting, and other targeted therapies. *Oncotarget*. 2017;8(43):73419-32.
232. Huang F, Ni M, Chalishazar MD, Huffman KE, Kim J, Cai L, et al. Inosine Monophosphate Dehydrogenase Dependence in a Subset of Small Cell Lung Cancers. *Cell Metab*. 2018;28(3):369-82 e5.
233. Mollaoglu G, Guthrie MR, Bohm S, Bragelmann J, Can I, Ballieu PM, et al. MYC Drives Progression of Small Cell Lung Cancer to a Variant Neuroendocrine Subtype with Vulnerability to Aurora Kinase Inhibition. *Cancer Cell*. 2017;31(2):270-85.
234. Wooten DJ, Groves SM, Tyson DR, Liu Q, Lim JS, Albert R, et al. Systems-level network modeling of Small Cell Lung Cancer subtypes identifies master regulators and destabilizers. *PLoS Comput Biol*. 2019;15(10):e1007343.
235. Kaminskas E, Farrell AT, Wang YC, Sridhara R, Pazdur R. FDA drug approval summary: azacitidine (5-azacytidine, Vidaza) for injectable suspension. *Oncologist*. 2005;10(3):176-82.
236. Schneider BJ, Kalemkerian GP, Bradley D, Smith DC, Egorin MJ, Daignault S, et al. Phase I study of vorinostat (suberoylanilide hydroxamic acid, NSC 701852) in combination with docetaxel in patients with advanced and relapsed solid malignancies. *Invest New Drugs*. 2012;30(1):249-57.
237. Nervi C, De Marinis E, Codacci-Pisanelli G. Epigenetic treatment of solid tumours: a review of clinical trials. *Clin Epigenetics*. 2015;7:127.

238. Nebbioso A, Carafa V, Benedetti R, Altucci L. Trials with 'epigenetic' drugs: an update. *Mol Oncol.* 2012;6(6):657-82.
239. Jia C, Zhang Z, Tang J, Cai MC, Zang J, Shi K, et al. Epithelial-Mesenchymal Transition Induces GSDME Transcriptional Activation for Inflammatory Pyroptosis. *Front Cell Dev Biol.* 2021;9:781365.
240. Wei Y, Lan B, Zheng T, Yang L, Zhang X, Cheng L, et al. GSDME-mediated pyroptosis promotes the progression and associated inflammation of atherosclerosis. *Nat Commun.* 2023;14(1):929.
241. Pan J, Li Y, Gao W, Jiang Q, Geng L, Ding J, et al. Transcription factor Sp1 transcriptionally enhances GSDME expression for pyroptosis. *Cell Death Dis.* 2024;15(1):66.
242. Wu Q, Guo J, Liu Y, Zheng Q, Li X, Wu C, et al. YAP drives fate conversion and chemoresistance of small cell lung cancer. *Sci Adv.* 2021;7(40):eabg1850.
243. Lamar JM, Stern P, Liu H, Schindler JW, Jiang ZG, Hynes RO. The Hippo pathway target, YAP, promotes metastasis through its TEAD-interaction domain. *Proc Natl Acad Sci U S A.* 2012;109(37):E2441-50.
244. Owonikoko TK, Dwivedi B, Chen Z, Zhang C, Barwick B, Ernani V, et al. YAP1 Expression in SCLC Defines a Distinct Subtype With T-cell-Inflamed Phenotype. *J Thorac Oncol.* 2021;16(3):464-76.
245. Chen P, Sun C, Wang H, Zhao W, Wu Y, Guo H, et al. YAP1 expression is associated with survival and immunosuppression in small cell lung cancer. *Cell Death Dis.* 2023;14(9):636.
246. Ott PA, Bang YJ, Piha-Paul SA, Razak ARA, Bennouna J, Soria JC, et al. T-Cell-Inflamed Gene-Expression Profile, Programmed Death Ligand 1 Expression, and Tumor Mutational Burden Predict Efficacy in Patients Treated With Pembrolizumab Across 20 Cancers: KEYNOTE-028. *J Clin Oncol.* 2019;37(4):318-27.
247. Ayers M, Luceford J, Nebozhyn M, Murphy E, Loboda A, Kaufman DR, et al. IFN-gamma-related mRNA profile predicts clinical response to PD-1 blockade. *J Clin Invest.* 2017;127(8):2930-40.
248. Cristescu R, Mogg R, Ayers M, Albright A, Murphy E, Yearley J, et al. Pan-tumor genomic biomarkers for PD-1 checkpoint blockade-based immunotherapy. *Science.* 2018;362(6411).
249. Ban WH, Yeo CD, Han S, Kang HS, Park CK, Kim JS, et al. Impact of smoking amount on clinicopathological features and survival in non-small cell lung cancer. *BMC Cancer.* 2020;20(1):848.
250. Tseng JS, Chiang CJ, Chen KC, Zheng ZR, Yang TY, Lee WC, et al. Association of Smoking With Patient Characteristics and Outcomes in Small Cell Lung Carcinoma, 2011-2018. *JAMA Netw Open.* 2022;5(3):e224830.
251. Pesch B, Kendzia B, Gustavsson P, Jockel KH, Johnen G, Pohlabeln H, et al. Cigarette smoking and lung cancer--relative risk estimates for the major histological types from a pooled analysis of case-control studies. *Int J Cancer.* 2012;131(5):1210-9.
252. Khuder SA, Dayal HH, Mutgi AB, Willey JC, Dayal G. Effect of cigarette smoking on major histological types of lung cancer in men. *Lung Cancer.* 1998;22(1):15-21.
253. Engler C, Marillonnet S. Golden Gate cloning. *Methods Mol Biol.* 2014;1116:119-31.
254. Weber E, Engler C, Gruetzner R, Werner S, Marillonnet S. A modular cloning system for standardized assembly of multigene constructs. *PLoS One.* 2011;6(2):e16765.
255. Davis HE, Rosinski M, Morgan JR, Yarmush ML. Charged polymers modulate retrovirus transduction via membrane charge neutralization and virus aggregation. *Biophys J.* 2004;86(2):1234-42.

# Acknowledgements

First and foremost, I would like to thank Prof. Dr. Nieves Peltzer for her guidance, support, and patience and, most importantly, for granting me this opportunity. I learned a lot from you, and I will forget about it. I would also like to thank The University of Cologne for taking me in, and the SFBs 1403 and 1399 for financing this research project. Lastly, I would like to thank our collaborators on campus and in Budapest, who helped push this project forward.

## Personal thanks

To the lab, for the laughs, the drinks, the gossip and for sticking together and pushing through with everything we had to figure out. Tabea, this work would not have been possible without you, keep up being amazing! Önay, I will miss you and our conversations (keep the tea coming!). Lucy, I will miss bothering you by repeating german expressions and saying you read smut at work (though it's kinda true). Xime, don't back down, one last push and you got this! Yuan, thank you for all the advice and for keeping everyone in check! I wish you the best with the baby, you'll be a fun and amazing mom. Öykü, I know your time in the lab has passed, but you will always deserve a cappuccino. And the latest additions, Hyoubi, Shenglian and Sina, keep your head high and your experiments coming!

To my family, specially to my parents. Ma y Pa, los quiero mucho, el apoyo que me han dado no tiene igual. Estoy acá gracias a ustedes, y me han dado el impulso para llegar más lejos todavía. Y quien sabe, tal vez las almendras tuvieron que ver! Juan, Sofi, gracias por ser un cable a tierra. Ahora que la tesis esta escrita les hare caso y aprenderé alemán jaja!

To Bea, for being there for me, as my girlfriend, as a scientist (an awesome one btw), as a (board)gamer and as my best friend, telling me what I need to hear and helping me to the right path. You've helped me both within and without this thesis. With you, I can really be me. Never lose your fire! Te amo.

A la superbanda, amigos de fierro como ustedes no hay. Piers, Fran, Giorgio, Marcos, los quiero un montón wachos. Por ustedes voy a Mordor ida y vuelta. Stay weird. Really. Otherwise I won't recognize you.

A mis amigos de la Facu. Una locura encontrarlos varios en Alemania. No va a ser la última vez que nos crucemos (también va para quienes no vinieron). La receta de las galletas es: 200g de manteca derretida en el microondas, 3 huevos, taza y media de azúcar, y aprox. 3 tazas colmadas de harina leudante. Importante es la esencia de vainilla, también le ponía un poquito de canela, un chorro de cognac de café y los chips de chocolate. La variedad de limón es un poco de esencia de vainilla con jugo de limón y ralladura de cascara de limón. Después nada raro, mezclar primero la manteca derretida con los huevos y el azúcar, agregar los "condimentos", y por último la harina tamizada mientras mezclas. Después al horno y listo! Ahora sin excusas!

To my DnD group (Curse of Strahd), thanks for helping me stay sane by regularly hallucinating a crazy world as a group. It's been a lot of fun playing with you guys!

A Belu, por ser mi amiga reel-otaku. Sasageyo, sasageyo!

To all my friends that I've picked up, scattered as you are around the world, I cherish you.

And lastly, as self-centred as it may sound, I'd like to thank myself. For celebrating the small victories, finding a reason to laugh even when in deep *bleep*, and keeping my goals in sight. For picking myself up, even when the falls hurt, and keep pushing forward. For not losing myself and allowing myself to just be me. For taking care of myself when I needed it. For always trying my best, and for learning from it when it was not enough. For keeping growing. For my future self: remember, things don't get easier, we get better. You'll make it through whatever crazy thing you've gotten yourself into.

Ich versichere, dass ich die von mir vorgelegte Dissertation selbstständig angefertigt, die benutzten Quellen und Hilfsmittel vollständig angegeben und die Stellen der Arbeit -einschließlich Tabellen, Karten und Abbildungen -, die anderen Werken im Wortlaut oder dem Sinn nach entnommen sind, in jedem Einzelfall als Entlehnung kenntlich gemacht habe; dass diese Dissertation noch keiner anderen Fakultät oder Universität zur Prüfung vorgelegen hat; dass sie - abgesehen von unten angegebenen Teilpublikationen -noch nicht veröffentlicht worden ist sowie, dass ich eine solche Veröffentlichung vor Abschluss des Promotionsverfahrens nicht vornehmen werde. Die Bestimmungen dieser Promotionsordnung sind mir bekannt. Die von mir vorgelegte Dissertation ist von Prof. Dr. Maria de las Nieves Peltzer betreut worden.

Übersicht der Publikationen:

Valdez Capuccino, L., Kleitke, T., Szokol, B. et al. CDK9 inhibition as an effective therapy for small cell lung cancer. Cell Death Dis 15, 345 (2024). <https://doi.org/10.1038/s41419-024-06724-4> (Published)

Ich versichere, dass ich alle Angaben wahrheitsgemäß nach bestem Wissen und Gewissen gemacht habe und verpflichte mich, jedmögliche, die obigen Angaben betreffenden Veränderungen, dem Promotionsausschuss unverzüglich mitzuteilen.

22.10.2024

Datum

*Lucas Valdez Capuccino*  
Unterschrift

✉ l.valcap95@gmail.com  
🏠 Cologne, NRW, Germany  
🎂 29 years old  
🌐 in/lvalcap95  
📍 Open to relocate  
☎ +49 0178 9209893

## Languages

**Spanish**  
Native

**English**  
Bilingual

**German**  
Basic

**Portuguese**  
Basic

## Assets

**Curious, Solution Oriented,  
Fast Learner, Independent,  
Team Player, Adaptive**

## Interests

**Analog Photography**

**Strategy Boardgames**

e.g. Scythe, Terraforming Mars,  
Arborea

## References

**Prof. Dr. Nieves Peltzer**

Professor, Principal investigator,  
University of Cologne (Currently  
University of Stuttgart)  
n.peltzer@ibmg.uni-  
stuttgart.de

# Lucas VALDEZ CAPUCCINO

## Ph.D. in Molecular Medicine

### Work experience

#### Ph.D. in Molecular Medicine

09/2020 - 10/2024 [Uniklinik Köln](#) Köln - Germany

- Preclinically assessed a previously unpublished CDK9 inhibitor (small molecule) for the treatment of Small Cell Lung Cancer (SCLC).
- Managed an international collaboration between 3 academic laboratories and 1 industry partner.
- The collaborative effort led to a first-author publication (see Publications).
- Developed SOPs for the working group, including Western Blot, Genotyping, and *ex vivo* immune cell isolation, among others.
- Trained and supervised students, including 1 Master's and 1 bachelor's thesis.

#### Research Fellowship

09/2019 - 08/2020 [National Institute of Cancer](#) Buenos Aires - Argentina

- Preclinically assessed RAC1 inhibition with an in-house designed small molecule for the treatment of Glioblastoma.
- Optimized and established an SOP for 3D cell culture for the working group.
- Performed anti-tumour drug assessment using *in vitro* and *s.c.* tumour models in immunocompromised mice.

#### Short-term Scientific Visit

01/2018 - 02/2018 [Rutgers University](#) Newark, NJ - USA

- Set up and programmed an Epi-Fluorescence Microscope for simultaneous fluorescence and membrane potential measurements (Patch Clamp).
- Microinjected mRNA into *Xenopus* Oocytes for protein expression.

### Education

#### Ph.D. in Molecular Medicine

09/2020 - 10/2024 [University of Cologne](#) Köln - Germany

- Using *in vitro* and *in vivo* models, as well as NGS techniques, I preclinically assessed the anti-tumour capacity of CDK9 inhibition against SCLC, paving the way for new treatments against this recalcitrant disease.
- For the written and defended thesis, I received *Magna cum laude*.

#### Licentiate in Biotechnology and Molecular Biology

02/2014 - 07/2019 [National University of La Plata](#) La Plata, BA, Argentina

- Grade: 8.88 out of 10

### Extracurricular activity

#### Organization and Managing

I was part of the organizing committee team of my Graduate School (IPMM) from 2022 to 2023 for the annual PhD scientific events "IPMM Days 2022" and "IPMM Days 2023". Here, we:

- Reached out and acquired funding from industry sponsors.
- Secured and managed a budget of ~€3000 yearly for each event.
- Selected and invited Keynote speakers.
- Designed the schedule, moderated sessions and communicated relevant information (registration deadline reminders, etc) to the students.
- Organized the travel and stay of said Keynote speakers, prize money and catering.
- Evaluated and elected the best scientific talks and posters.

#### Leadership

- Completed "Leadership Starter Kit Workshop" by the University of Cologne, 2023
- Attended "Managing Conflict Workshop" by Desiree Dickerson, 2023

#### Programming

Completed workshops and seminars in R and Matlab directed towards data analysis, including:

- Flow Cytometry Analysis with R - Physalia Courses, 2024
- RNA-seq data Analysis with DESeq2 - Physalia Courses, 2023
- Introduction to R package "ggplot2" - University of Cologne, 2023
- Data Analysis with R - Scavetta Academy, 2023
- Introduction to R/Bioconductor - Physalia Courses, 2023
- Machine Learning - Stanford University, 2018

## Technical Skills

### Molecular Biology

3D cell culture, primary cell culture, cytotoxicity assays (FACS, Incucyte, CTG, MTT), Western Blot, Immuno-precipitation (IP), Molecular Cloning, Flow cytometry, IHC, ELISA, Whole-genome Sequencing, RNA-seq, Mass Spectrometry, siRNA transfection, lenti-viral production & infection for stable CRISPR expression.

### In vivo/ex vivo

Felasa B, organ harvesting, cell isolation, mouse handling, s.c. & i.p. Injection, Tumour genetic model generation, Adenoviral (AAV) Inhalation, thoracic MRI, breeding, genotyping.

### Omics: sample preparation, acquisition and analysis

RNA-seq (Illumina), Whole-Genome Sequencing (Illumina) and Proteomics (Orbitrap).

### Data analysis

R (Tidyverse, Bioconductor), Graphpad PRISM, Fiji, QuPath, and eLabjournal & Quartz (organizational softwares).

## Publications and presentations

### Publications

- CDK9 inhibition as an effective therapy for small cell lung cancer. [Valdez Capuccino L. et al.](#) Cell Death and Disease (Nature), 2024.
- Preclinical Efficacy and Toxicology Evaluation of RAC1 Inhibitor 1A-116 in Human Glioblastoma Models. [Cardama G., Maggio J., Valdez Capuccino L. et al.](#) Cancers (Basel), 2022.

### Presentations

- **ECDO & EATI Joint Annual Conference 2023 (Paris)**: Poster presentation.
- **EACR 2023 Turin**: Poster presentation.
- **Institutional "Floor meeting" 2020 - 2024**: I periodically gave scientific presentations to showcase my work.
- **Cologne Spring Meeting 2023** "Cell Death and Mitochondrial Signalling in Health and Disease": Poster presentation.
- **EMBO Workshop 2022** "Dying in self-defence: Cell Death Signalling in Animals and Plants" (Crete): Poster presentation.